FACULTY OF TECHNOLOGY

DEVELOPMENT OF COMMINUTION TEST METHOD FOR SMALL DRILL CORE SAMPLE

Hannu Heiskari

PROCESS ENGINEERING

Master's thesis

September 2017

ABSTRACT
FOR THESIS

University of Oulu Faculty of Technology

Degree Programme (Bachelor's Thesis, Master's Thesis)	Major Subject (Licentiate Thesis)
Process engineering	
Author	**Thesis Supervisor**
Hannu Heiskari	Saija Luukkanen, Professor.

Title of Thesis

Development of comminution test method for small drill core sample

Major Subject	Type of Thesis	Submission Date	Number of Pages
Mineral processing	Master's thesis	September 2017	82 p., 25 App.

Abstract

Grinding circuits are an essential part of a mineral processing plant. Grinding is very energy intensive, and can have major effects on the following separation stages of mineral processing. This sets high requirements for the design and operation of grinding circuits. Early on in the resource evaluation, ore samples used in metallurgical testing tend to be composited samples from drill cores. These composited samples can have broad mineralogical variations in them. Geometallurgy aims to create a predictive model to improve plant operation and design, based on the inherent variability of ore blocks in an ore deposit. Thus to apply geometallurgy, mineralogical information and data about the variability in ore blocks is essential. This creates a need for variability testing, where test methods are fast, inexpensive and require low volumes of sample.

In this thesis the common Bond ball mill grindability test is conducted on three different sample materials. The samples show good variability in terms of mineralogy and grindability. Along with the Bond test, the Mergan ball mill grindability test is also conducted on the same sample materials. The Mergan test is faster than the Bond test, and uses less sample material than the Bond test. The aim of the testwork is to analyze the differences between the two test methods, and see if there is a correlation between them. This correlation can then be used to create a new grindability test method, where the test is done with the Outotec Mergan mill, but the test results can be scaled to estimate Bond work index for the sample.

Results show that there is indeed a correlation between the two grindability test methods. Using a linear model, an experimental model is presented, where the Mergan mill can be used to approximate the Bond work index for an ore with good correlation. To validate and improve the experimental model presented, more testing should be conducted in the future.

Additional Information

TIIVISTELMÄ
OPINNÄYTETYÖSTÄ Oulun yliopisto Teknillinen tiedekunta

Koulutusohjelma (kandidaatintyö, diplomityö) Prosessitekniikka		Pääaineopintojen ala (lisensiaatintyö)	
Tekijä Hannu Heiskari		Työn ohjaaja yliopistolla Saija Luukkanen, professori.	
Työn nimi Development of comminution test method for small drill core sample			
Opintosuunta Rikastustekniikka	Työn laji Diplomityö	Aika Syyskuu 2017	Sivumäärä 82 s., 25 liitettä

Tiivistelmä

Jauhatuspiirit ovat tärkeä osa rikastamoa. Jauhatus vaatii erittäin paljon energiaa, ja sillä voi olla merkittäviä vaikutuksia rikastuksen seuraaviin osaprosesseihin. Tämä asettaa korkeat vaatimukset jauhatuspiirien suunnittelulle ja käytölle. Malmiesiintymän tutkimuksen varhaisissa vaiheissa metallurgiseen tutkimukseen saatavat näytteet ovat yleensä komposiittinäytteitä kairasydämistä, joissa voi olla suuria mineralogisia eroja. Geometallurgian tarkoituksena on luoda ennustava malli, joka perustuu malmiesiintymässä olevien eri malmioiden eroavaisuuksiin. Tätä mallia voidaan käyttää kaivoksien suunnittelun ja toiminnan optimoimiseen. Geometallurgian hyödyntämiseen tieto malmioiden eroavaisuuksista ja mineralogiasta on siis välttämätöntä. Tämä on saanut aikaan tarpeen testimenetelmille, joilla tätä vaihtelevuutta voidaan testata, ja näiden testimenetelmien tulee olla nopeita, halpoja, ja testien käyttämien näytemäärien täytyy olla pieniä.

Tämän työn kokeellisessa osuudessa yleistä Bondin kuulamyllyjauhautuvuustestiä käytetään kolmen eri malminäytteen jauhautuvuuden testaamiseen. Työssä käytettävät malminäytteet eroavat toisistaan paljon niin mineralogian kuin jauhautuvuudenkin puolesta. Samojen näytteiden jauhautuvuutta testataan myös Mergan kuulamyllyjauhautuvuustestillä. Mergan menetelmän etuja ovat Bondin testiin verrattuna se että Mergan on nopeampi tehdä, ja sen näytevaatimus on Bondin testiä pienempi. Koetoiminnan tarkoituksena on verrata näiden kahden jauhautuvuustestien tuloksia ja eroavaisuuksia, ja analysoida löytyykö näiden testimenetelmien väliltä korrelaatiota. Tätä korrelaatiota voidaan sitten käyttää uuden jauhautuvuustestin kehittämiseen, jossa näytteen jauhautuvuuden testaamiseen käytetään Outotecin Merganmyllyä, ja saatu tulos skaalataan Bondin ”työindeksiin”.

Koetulosteen perusteella jauhautuvuustestien väliltä löytyi korrelaatio. Tätä korrelaatiota käytetään kokeellisen lineaarisen mallin luomiseen, jossa malmin jauhautuvuutta voidaan testata Merganmyllyllä ja arvioida siitä Bondin ”työindeksi” hyvällä korrelaatiolla. Kokeellisen mallin toimivuuden vahvistamiseen ja parantamiseen tarvitaan kuitenkin vielä lisää testejä tulevaisuudessa.

Muita tietoja

FOREWORD

This thesis was written as an assignment under the supervision of Outotec Oy and University of Oulu. The testwork and writing of this thesis was done between March and September of 2017, in the city of Pori.

First of all, I would like to express gratitude for Outotec Oy and University of Oulu for allowing me the chance to write this thesis. I would like thank my supervisors from Outotec, Jussi Liipo and Harri Lehto for their help and guidance. From the University of Oulu, I would like to thank my supervisors, Professor Saija Luukkanen and Maria Sinche Gonzales (PhD, Eng.) for their knowledge, advice and support in writing of this thesis. I would also like to express my gratitude to Pekka Kurki from Outotec Research Center Pori, who taught me the all the procedures for this thesis, and for answering all my questions and helping me whenever it was needed. Also thanks to all the people at ORC, who made the great work environment I had the chance to be a part of, and for all their help I got during my time there. I feel that this journey has increased my knowledge immensely, but I still have so much more to learn.

I would also like thank my family and friends for their support during my studies in university. Special thanks to my girlfriend Kaisa for all the support she has given me during this project, which is the single most challenging thing I have ever faced. Without every single one of you, this wouldn’t have been possible.

TABLE OF CONTENTS

TERMS AND ABBREVATIONS

AG	autogenous grinding
b	the representative diameter of the particles [m]
C	constant, which depends on the material and comminution method [kWh/t]
D	diameter [m]
D_{80}	80% passing size [μm]
d	diameter of ball [m]
E	energy
E_0	energy used in Mergan grinding [kWh/t]
e	coefficient of restitution of the material of the balls and mill
F_{80}	80% passing size in the feed [μm]
G_{bp}	ball mill grindability [g/rev]
g	acceleration due to gravity [m/s^2]
h	height [m]
J	volume occupied by charge [m^3]
K	constant chosen to balance the units of the equation
k	constant, used to calculate $W_{i,GCT}$ [kWh/t]
k	grinding rate constant
L	length [m]
M	weight of the mill feed [g]
M_d	dry mass [g]
M_i	index related to the breakage property of the ore [kWh/t]
M-W_i	Mergan work index
Ms	saturated-surface-dry mass [g]
MSO	massive sulphide ore
m	weight of the under-size [g]
N	speed of rotation [m/s], [rev/min]
N	total number of mill revolutions
N_c	total number of mill revolutions giving the (2.5/3.5)M test sieve over-size
n	mill revolutions per minute
n	number of impacts
P	power [W], [Nm/s]

P_1	sieve opening at which test is carried out [μm]
P_{80}	80% passing size in the product [μm]
PLI	point load index
PSI	Protodyakanov's strength index
R	test-sieve over-size [g]
R_0	test-sieve over-size at the beginning of grinding [g]
R_0	proportion of test sieve over-size in the new feed
RGO	refractory gold ore
RHN	rebound hardness number
RQD	rock quality designation
SAG	semi-autogenous grinding
T	measured torque [Nm]
t	grinding time [s]
t_c	grinding time in a standard grinding cycle after which the over-size (R) on the test sieve is (2.5/3.5)M, which corresponds to the 250% circulating load
U	volume of liquid in pulp
U	weight of the new feed [g]
V	volume [m^3]
W	work [J]
W_i	work index, material specific parameter which expresses the resistance of the material to crushing and grinding [kWh/t]
$W_{i,MP}$	Mergan predicted Bond work index [kWh/t]
W_{74}	energy consumption per ton of -74 μm material produced [kWh/t]
x	particle size [μm]
x_f	feed particle size [μm]
x_p	product particle size [μm]
η	mill drive and engine efficiency
ρ	density [t/m^3]
ρ_w	density of water [t/m^3]
υ	kinematic viscosity [m^2/s]
σ	effective density
λ	geometric scaling factor

1 INTRODUCTION

Grinding, the last stage of the comminution process, is the most energy-intensive operation in mineral processing, and can account for more than 50% of the operation cost of a mineral processing plant. The purpose of grinding is the economic degree of liberation of the mineral of interest. (Wills & Finch, 2015) Therefore, knowledge of a given ore's comminution properties are essential when operating a mineral processing plant, or when conducting a feasibility study.

Comminution theory is concerned in the relationship between energy input into comminution and the product particle size distribution made from a given feed size. Grindability tests aim to estimate the energy consumption of grinding and to give parameters for the sizing of the grinding mill using different test methods. The Bond test, although an industry standard, can require up to 10 kg of sample material, and is rather time consuming. (Bond, 1961a)

In the early stage of resource evaluation, when physical access and knowledge of an ore deposit is limited or evolving, only drill core based samples are available for metallurgical testing. Therefore, commonly samples collected for the testing are composite samples representing a broad mineralogical variation within them. This hinders the detailed mapping of ore variability using drill core samples. However, in the geometallurgy context, mineralogical information is essential for creating a proper ore block model that takes into account the inherent variability in the ore. Geometallurgical information is essential in production planning and management, along with process control of the resource's exploitation before and during production. (Walters, 2008)

Geometallurgical approach to metallurgical testing has been under rapid research and development in the recent years. Tests used in geometallurgical mapping must be fast, inexpensive, and required ore sample must be small. Therefore, a fast grindability test method that uses less sample material than the Bond test is required. In this thesis, a new laboratory test method is developed. The aim of this test method is to use the Outotec Mergan mill for the grindability test, and scale the results to the Bond ball mill test. The

Outotec Mergan method is faster than the Bond ball mill test, and requires less sample material. However, the Mergan method gives grinding energy consumption, which can be used to calculate Mergan work index, but this Mergan work index differs from the Bond work index. Therefore, it is needed to analyze if the Mergan work index correlates with Bond work index. All the testwork was conducted using Outotec Mergan and Bond ball mills at Outotec Research Center, located in the city of Pori, Finland.

The literature review of this thesis focuses on basics of grindability, along with geometallurgy, and presents various grindability test methods. In the experimental part of this thesis, Bond ball mill tests and Mergan tests are done for 3 different ore samples, and the results of these tests are analyzed. A new experimental model is represented, where the Mergan test can be used to estimate the Bond work index of a specific ore.

2 GRINDABILITY FUNDAMENTALS

2.1 Basics

Most valuable minerals are often finely disseminated and intimately associated with the gangue minerals, and thus they must be initially liberated before separation can be done. This liberation is achieved by comminution, in which the particle size of the ore is progressively reduced until the clean particles of the valuable mineral can be separated from the gangue minerals by following separation processes. Grinding, the last stage of comminution process, where particles are reduced in size by both impact and abrasion is carried out until the mineral and gangue are produced as separate particles. When an adequate amount of the mineral of interest is separated by comminution from the parent rock, that size is usually known as the liberation size. (Wills & Finch, 2015; Gupta & Yan, 2006)

Grinding is carried out either dry, or more commonly in suspension in water. It is performed in cylindrical steel vessels that contain a charge of loose crushing bodies, called the grinding medium. The grinding medium is free to move inside the mill, thus comminuting the ore particles. Grinding mills are generally classified into two types, tumbling mills and stirred mills. In tumbling mills, the mill shell is rotated and motion is imparted to the charge via the mill shell. This movement is illustrated in Figure 1. The grinding medium may be steel balls, steel rods, or rock itself (AG/SAG). Tumbling mills are typically employed in primary grinding, typically reducing particles in size to between 25 and 300 μm. In stirred mills, the mill shell is stationary mounted either horizontally or vertically, and motion is imparted to the charge by the movement of an internal stirrer. Stirred mills find application in fine (15-40μm) and ultrafine (<15μm) grinding. (Wills & Finch, 2015)

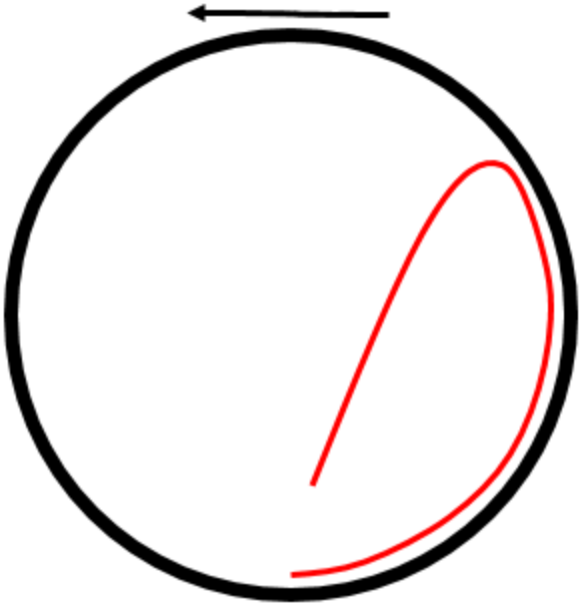

Figure 1. Trajectory of grinding media in tumbling mill. Modified from the source. (Wills & Finch, 2015)

All ores have an economic optimum particle size in respect of following process stages. If the ore is ground to too coarse particle size, insufficient mineral liberation limits recovery in the separation stage. On the other hand, grinding the mineral to too fine particle size increases grinding costs and may reduce final recovery. Thus efficient grinding can be considered a key element to good mineral processing. (Wills & Finch, 2015)

Grinding costs are driven by energy and steel consumption. In some cases extensive grinding may not be a disadvantage, as the increase in energy consumption may be offset in the following processes. Although the economic degree of liberation is the principal purpose of grinding, grinding is sometimes used to increase mineral surface area. As an example of such processes, grinding of an industrial mineral such as talc is aimed at a particle size that meets customer requirements. Another example would be grinding of gold-ore, when extraction is made with hydrometallurgical methods, such as cyanide leaching, where larger surface area improves cyanide leaching rate. (Wills & Finch, 2015)

Grinding is the most energy intensive operation in mineral processing. Although tumbling mills have been developed to a high degree of mechanical efficiency and reliability, their energy efficiency remains an area of debate. The greatest problem in tumbling mills, and all crushing and grinding machines for that matter, is that the majority energy input is absorbed by the machine itself, and only a small fraction of energy input is available for breaking the ore. Wills and Finch (2015) state that *"in a ball mill, for instance, it has been shown that less than 1% of the total energy input is available for actual size reduction, the bulk of the energy being utilized in the production of heat."* Also, plastic material will eat up energy while changing shape, but will then retain this shape without actually creating significant new surface. (Wills & Finch, 2015)

The breakage of the ore is mostly the result of repeated, random impact and abrasion. At the present, there is no way that these impacts can be directed at the interfaces between the mineral grains. Technologies such as microwave heating and high voltage pulsing are currently used as an assisted breakage mechanic in grinding processes, not as the main grinding process. (Wills & Finch, 2015) Another example would be high pressure roller mill that can offer savings in comparison to traditional comminution circuits, while well accepted in the cement industry, hasn't yet seen much use in the mineral processing industry (Mörsky, et al., 1995).

Metal wear is usually the second largest single item of expense in conventional grinding, and in wet grinding installations it may approach or even exceed the power cost. The kilograms of metal worn away and scrapped as worn parts varies with the abrasiveness of the ore and the abrasion resistance of the metal. Metal wear is commonly expressed in kg/ton crushed or ground. However, variations in feed, product sizes and in work index are eliminated by expressing metal consumption as kg/kWh. (Bond, 1961b) This is one area where autogenous and semi-autogenous mills have an advantage over traditional mills that use other grinding media than the ore.

The purpose of mining and following beneficiation processes is to create a saleable product, concentrate. Concentrate is a product, higher in the grade of mineral of interest, than the ore being fed into the mineral processing circuit. Some industrial applications

such as aggregate production aim their comminution process at the size reduction of rock to a specified particle size to create a saleable product. (Lynch, 2015)

The purpose of comminution circuit in mineral processing is to prepare the ore as a suitable feed for separation processes. Separation processes upgrade the material by rejecting the particles that do not contain economic amounts of the target mineral. The implication is that the comminution process changes the ore from a population of particles with a relatively uniform grade to particles with a range of compositions that allow them to be separated into high-grade and low-grade streams. This so called mineral liberation is a phenomenon, where according to Lynch (2015) *"parent particles with a given mineral composition break into progeny particles with a range of mineral compositions"*, is illustrated in Figure 2. (Lynch, 2015)

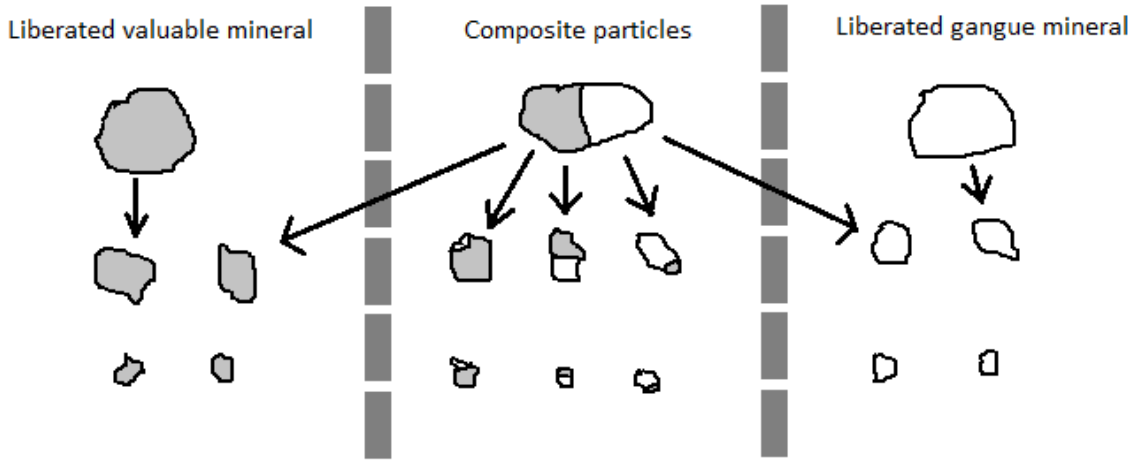

Figure 2. A simple representation of mineral liberation during breakage. Modified from the source. (Lynch, 2015)

2.2 Particle breakage mechanics

Most minerals are crystalline materials in which the atoms are regularly arranged in three-dimensional arrays. The configuration of atoms is determined by the size and types of physical and chemical bonds holding them together. In the crystalline lattice of minerals, these inter-atomic bonds are effective only over small distances, and can be broken if extended by a tensile stress, such generated by tensile or compressive loading. Even when

rocks are uniformly loaded, the internal stresses are not evenly distributed, as the rock consists of a variety of minerals dispersed as grains of various sizes. The distribution of stress depends upon the mechanical properties of the individual minerals, but more importantly upon the presence of cracks and flaws in the matrix, which act as sites for stress concentration. The theories of comminution assume that the material is brittle, however, crystals can store energy without breaking, and release this energy when the stress is removed. Such behavior is known as elastic. (Wills & Finch, 2015)

The physical properties of the rock, e.g. shape and size, mainly determine the breakage characteristics of an ore. According to Norazirah et al. (2015) *"the shape properties are increasingly being recognized as an important parameter influencing the performance particles in mineral processing operations."* The characterization of the breakage process can be done in two basic functions. The first one is the *"selection function that represents the fractional rate of breakage of particles in each size class"* and the second one is *"the breakage function that gives the average size distribution of the daughter fragments resulting from primary breakage event".* (Norazirah, et al., 2016)

When analysis is done to the breakage distribution of particle breakage, single particle breakage characterization test methods are commonly used by researchers. They are commonly grouped into three categories; single impact, double impact and slow compression. The use of these tests is in input energy-size reduction relationships, based on energy utilization. This can be grouped in to two categories. First is a drop weight test. In a drop weight test a particle is resting on a hard surface, and is then struck by a falling weight. The second type, known as a pendulum test, can give additional information on the energy utilization in single particle breakage tests. (Norazirah, et al., 2016)

Even when a single particle is considered, the breakage event cannot be totally predicted because of the large amount of variables that affect the outcome. Thus, to understand particle breakage process, the focal point must be on the strength of the particle, the energy consumed in the particle breakage event and the size distribution of the daughter fragments yielded in the breakage event. When a particle's theoretical strength is considered, the assumption is that the particle is homogenous. In reality, there are always flaws present in particles as lattice faults, grain boundaries and microcracks. These flaws

have much greater stress concentrations than the other parts of the particle. Thus fracture initiates usually from these points, and in reality, the strength of the particle is lower than the theoretical strength due to these flaws. (Fuerstenau & Han, 2003)

Obviously, commercial level comminution processes do not break particles one by one. To process ores at a commercial level, up to thousands of tons of ore per hour, comminution devices must obviously break huge assemblies of particles. In reality, comminution happens in multiparticle breakage event, and these events are more complex and less efficient that single particle breakage events. This is because particles interact with each other during multiparticle breakage. The general belief is that the amount of breakage that occurs is dependent on how energy is dissipated in the process, either useful or wasted. Efficiency of breakage is dependent on the number of particle layers undergoing compression. As particle layers increase in number, the efficiency decreases. (Fuerstenau & Han, 2003) Figure 3 illustrates the differences of a single-particle and multiparticle breakage event in a compression breakage.

Figure 3. Illustration of single-particle and multi-particle breakage event. Modified from the source. (Fuerstenau & Han, 2003)

The process of grinding an ore particle is dependent on the probability of the particle entering an area between the grinding medium, and the probability that some breakage event occurs when the particle is in the area. Size reduction can be achieved by several different mechanisms, such as impact or compression due to some sudden force being applied to the particle surface, chipping or attrition due to steady compressing forces that break the matrix of a particle, and due to abrasion (shear) where forces act parallel to, and

along the surfaces of the particles. These mechanisms cause deformations in the particles, changing their shape beyond certain limits, which then causes them to break. These mechanisms are illustrated in Figure 4. (Wills & Finch, 2015)

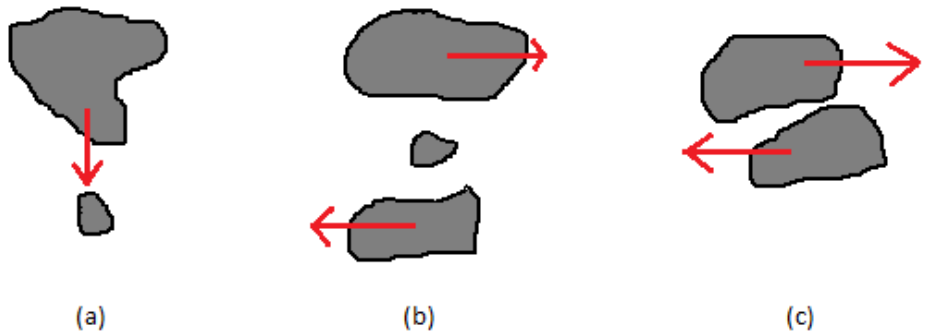

Figure 4. Mechanisms of breakage: (a) Impact or compression, (b) Chipping or attrition, and (c) Abrasion. Modified from the source. (Wills & Finch, 2015)

Modern day comminution uses research methods such as DEM (Discrete Element Method) to predict the flow of the particulates and to simulate the different multiparticle breakage events inside the mill. Since grinding is inherently a process involving collisions between particles and the mill itself, methods to analyze the size reduction happening inside the mill, and their effect on mill performance is a topic of heavy investigation. (Cleary & Morrison, 2016)

2.3 Mill power draw

The power required to drive a tumbling mill depends to some extent on every one of the physical dimensions defining the mill shell and ball charge, and on many of those defining the properties of the ore charge. The power to drive the mill, P, would be expected to depend upon the length of the mill, L, the diameter, D, the diameter of ball, d, the density of the ball, ρ, the volume occupied by the charge (including voids) expressed as a fraction of the total mill volume, J, the speed of rotation, N, the acceleration due to gravity, g, the coefficient of restitution of the material of the balls and mill, e. (Rose & Sullivan, 1958)

The power, P, would also be expected to depend upon the following characteristics of the ore: the representative diameter of the particles, b, the energy necessary to bring about unit increase in the specific surface of the ore, E, and the volume, V, occupied by the ore charge (including voids) expressed as a fraction of the volume between the balls in the mill. Furthermore, the power P would be expected to depends upon the effective kinematic viscosity of the mixture of ore and fluid, υ, the effective density of the mixture, σ, and in the case of wet milling, volume of the liquid in the pulp, U. Finally, when the interior of the mill is fitted with lifters it would be expected that the power, P, would depend on the number of lifters, n, and upon the height of the lifters, h. Thus, the power can be expressed symbolically (1), when ϕ denotes some function of each of the quantities within the bracket. (Rose & Sullivan, 1958)

$$P = \phi(L, D, d, \rho, J, N, g, e, b, E, V, \upsilon, \sigma, U, h, n) \quad (1)$$

Calculations for the power requirements of a mill, from theoretical standpoint, are hard to make. This is due to the fact that even a fairly complete theory on the internal dynamics of a ball mill, where all of the aforementioned variables are given due importance, has not been propounded. Due to the great number of variables, the analysis of the effect of all these variables on the power draw of tumbling mills has been prohibitive for a complete experimental study. (Rose & Sullivan, 1958) It is quite telling that in some cases, things like catastrophe theory have been applied when investigating the inner works of tumbling mills (Zhitie, 1995).

A common practice to estimate the power draw of a mill is as a function of the mill charge motion. The problem of in situ characterization of charge motion is the aggressive internal environment of tumbling mills, and models focus on empirical relationships of the effects of the charge on the power draw, and the charge is usually simplified to a single bulk body. While models have shown good approximation between the mill power draw and the charge motion, they seem to be limited to the scope of their definition. Techniques like PEPT (Positron Emission Particle Tracking) can be used to measure the flow trajectory of radioactive particle in a granular or fluid system such as tumbling mills, allowing for better modeling on the mill power draw as a function of the mill charge movement. (Bbosa, et al., 2011)

2.4 Comminution theory

Comminution theory is interested in the relationship between the energy input in size reduction, and the particle size made from a given feed size. Comminution theory expects that a relationship can be found between the energy required to break the material, and the new surface created in the comminution process. This relationship can only be made manifest if the energy used in the creation of new surface can then be separately measured. Many theories have been presented, but none seem completely satisfactory. All the theories of comminution make the assumption that the material is brittle, and thus no energy is adsorbed in the comminution process which is not finally utilized in ore breakage. (Wills & Finch, 2015) The author of this thesis would like to note that, as mentioned before, no comminution process is even remotely efficient enough that no energy is wasted.

First and oldest theory of comminution was presented by Paul von Rittinger in 1867. According to Rittinger's law, the energy consumed by the comminution process is directly proportional to the new surface area produced which is shown in equation (2). E is the energy used in comminution, x is particle passing size and C is material dependent constant. (Hukki, 1964)

$$E = C\left(\frac{1}{x_p} - \frac{1}{x_f}\right) \tag{2}$$

Friedrich Kick presented his second theory in 1885, represented by equation (3), which can be defined as *"the energy required for producing analogous changes of configuration in geometrically similar bodies of equal technological state varies as the volumes or weights of these bodies"*. According to Kick's law, energy required for transformation is proportional to mass or to volume of the particle. (Hukki, 1964)

$$E = C \ln\left(\frac{x_f}{x_p}\right) \tag{3}$$

The third theory of comminution, presented in 1952 by Fred C. Bond, widely used in the industry, assumes that the energy used in comminution is inversely proportional to the square-root of the diameter of the particle as is shown in equation (4). (Hukki, 1964)

$$E = 2\,C\left(\frac{1}{\sqrt{x}_p} - \frac{1}{\sqrt{x}_f}\right) \tag{4}$$

All of these three theories may be derived from the basic differential equation (5) created by Walker, Lewis, McAdams and Gilliland in 1937. The energy required for comminution grows as the particle size decreases, or in other words, fineness increases. Thus, all three theories of comminution are usable on a specific range of particle size, Kick's law on the coarse size range of particle (crushing), Bond's law on medium particle size (traditional grinding), and Rittinger's in fine grinding range. (Hukki, 1964)

$$dE = -C\frac{dx}{x^n} \tag{5}$$

On the basis of Hukki's evaluation, Morrell proposed in 2004 a modification to Bond's equation that relates specific energy to size reduction and the rock breakage properties are assumed to be constant with respect to particle size. By designating M_i as a comminution index, K as constant to balance the units of the equation, Morrell's equation can be expressed as (6). Morrell concluded that this new equation does not suffer from the same deficiency as Bond's equation, Bond's equation being usable specifically on medium particle size. (Morrell, 2004)

$$W = M_i K(x_2^{f(x_2)} - x_1^{f(x_1)}) \tag{6}$$

3 GEOMETALLURGY CONTEXT

Growing demand for more efficient utilisation of orebodies and proper risk management in mineral processing industry have emerged a new branch called geometallurgy. Lamberg (2011) states that *"geometallurgy combines metallurgical and geological information to create spatially-based predictive model for mineral processing plants."* According to Lamberg, geometallurgy is not a discipline itself, but related to certain ore deposit and certain process, and as such geometallurgy can be called a practical amalgamation of ore geology and mineral processing. A geometallurgical program should go through an 8 step program, illustrated in Figure 5. (Lamberg, 2011)

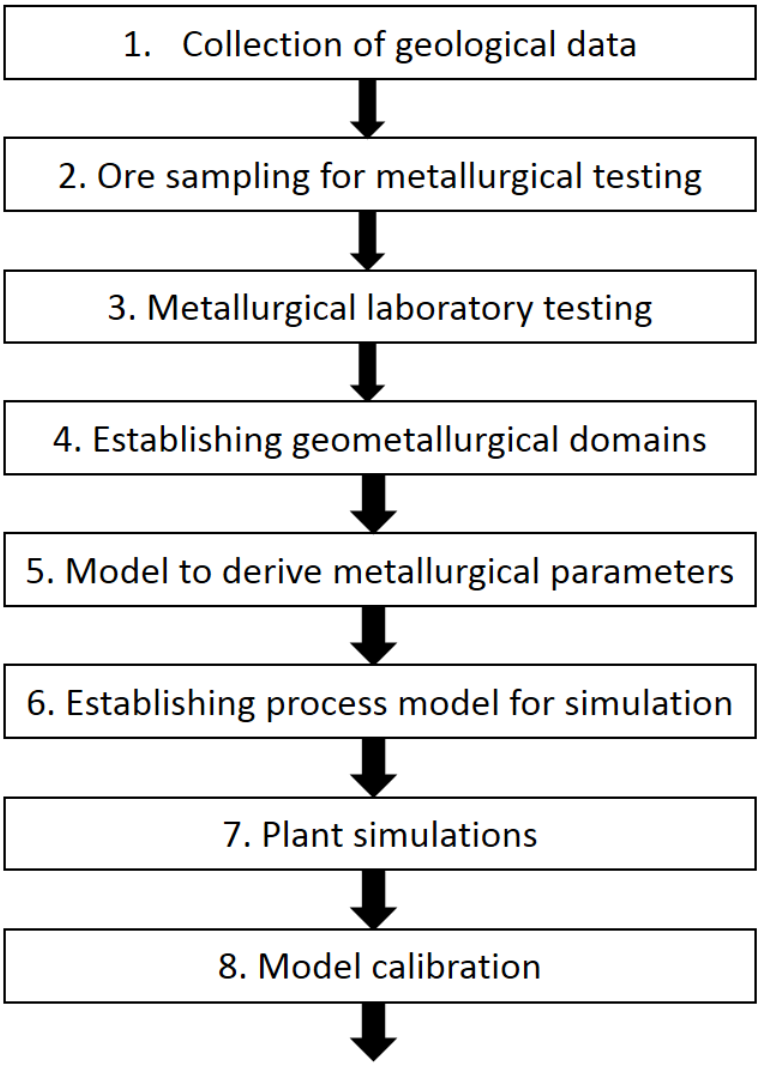

Figure 5. Geometallurgical program in 8 steps. Modified from the source. (Lamberg, 2011)

According to Walters (2008) the discipline of geometallurgy is not new *"but it is becoming increasingly recognized as a discrete and high-value activity that reflects ongoing commercial and cultural trend towards more effective mine site integration and optimization."* The aim of geometallurgy is not replace existing approaches to design and optimization of mining and mineral processing circuits, but rather to complement them. (Walters, 2008)

The idea behind geometallurgy is to provide information that reflects inherent geological variability of the ore, and impact of this variability on the metallurgical performance. To achieve this, ore deposits need to be determined in terms of machine-based process parameters, which include hardness, comminution energy, size reduction, liberation potential and product recovery. These geometallurgical parameters can be used in geostatistics to populate deposit wide block models. Incorporating these geometallurgical parameters into operation of mineral processing plants supplements traditional geology and grade-based attributes, which allows more comprehensive approach to economic optimization of mining and mineral processing. (Walters, 2008)

Geometallurgy requires integration across a wide range of existing operations. Geometallurgy can be described in various ways, including aspects of process mineralogy, mine geology, metallurgy, process control, resource modeling and geostatistics. Geometallurgy can also be called orebody knowledge or ore characterization. (Walters, 2008)

The information about the inherent geological variability of the ore block can be used in geometallurgical models to reduce technical risk when designing and operating mineral processing plants. When considering feasibility before design phase, when physical access to an ore deposit or knowledge about an ore deposit is limited and evolving, geometallurgical approach becomes increasingly important. During design phase of a plant, geometallurgical data can be used to optimize flow sheet design and equipment sizing. Geometallurgical data is also useful when optimizing plant performance and production during the whole life-cycle of the plant. (Walters, 2008)

The linkage of geological information and metallurgical response currently relies on a limited number of samples tested in laboratory conditions. The weakest points in geometallurgical programs are typically small number of test samples used in metallurgical testing, and insufficient information collected from drill cores. In the metallurgical testing samples are quite small both in terms of size and number, and the samples should represent large tonnages of the ore. This sets high requirements for sampling and testing, as samples tested should represent the full variability of the ore block, and the metallurgical response of the ore. (Lamberg, 2011)

One problem with geometallurgical testing is the tendency to composite core-based samples to represent larger scale production or to fulfill the logistical requirements of physical testing procedures. Using composite samples that disguise natural variability and are non-representative and unconstrained can cause significant problems, such as precise test results with uncertain representativity. The ultimate engineering solution to variability in the ore is to homogenize the feed over the life of the mineral processing plant. However, homogenized ore feed might not represent a simple linear combination of the ore, and it might not produce optimal economic outcomes. (Walters, 2008)

Before a final design is chosen, the variability of the ore and its effects on process performance are important knowledge. Thus identifying the variability in the ore deposit through geometallurgical methods allows increase in efficiency and optimization of the mineral processing plant. This is especially true for large scale mining operations, which have increasing potential to exploit ore variability through multiple processing circuits. This can also help with improving overall sustainability and reduce energy costs and environmental footprint of the mineral processing plant. (Walters, 2008)

One of the main drives behind rising application of geometallurgy is the desire to move towards low cost physical testing. This allows using small sample volumes that can be used to define natural variability in the ore. For geometallurgy, defining natural variety with models built from large sets of data with small sample volumes is a much better statistical approach, than building the models with small number of more precise test samples. This approach results in a large number of low cost comparative tests to provide

information about the variability in the ore, and decrease the number of high precision tests. (Walters, 2008)

Even a larger number of more spatially representative tests, when compared to the overall volume of the ore deposit, still represent sparse data. Larger number of data sets does partly overcome some of the problems with current approach, but to effectively use geometallurgical processing information on ore deposit scale, statistical and population modelling techniques are required along with classical geostatistics. (Walters, 2008)

To make the sampling, and also the definition of geometallurgical ore domains more reliable, new measurement and analysis techniques are needed. The challenge is that tests should be done for a very big number of samples, up to thousands, and as such the techniques used must be fast, inexpensive and preferentially fully automated. The tests can be roughly divided into three groups, tests measuring rock properties, tests for quantitative mineralogy and geometallurgical tests. (Lamberg, 2011)

Another problem with using geometallurgy in grinding processes with current grindability test methods is accuracy. The test method should be accurate over the entire range of hardness variability for the entire ore deposit. For geometallurgical analysis, every block in the ore deposit should be represented by a real test. (Starkey & Scinto, 2010)

The development of tests and methods for the geometallurgical modelling of ore blocks has been under a rapid research and development in the recent years, e.g. the Geometallurgical Comminution Test by Mwanga et al. (2017) which will be described in chapter 4.3. The need for rapid, low cost testing of ore properties thus sets a need for improving the Mergan test method (described in chapter 4.2) and topic of this research.

One case where modelling of ore domains lead to better production planning is Batu Hijau, where Metso Mineral Process Technology and PTNNT Batu Hijau worked to develop a model to forecast and optimize SAG mill throughput at the mineral processing plant. Based on the ore characterization and the model created, better mill throughput could be predicted. The ore domains were defined based on ore lithology, rock structure

(RQD) and rock strength (PLI). The model takes the ore through the whole comminution circuit, starting from blasting and ending at grinding circuit. (Burger, et al., 2006)

Outotec's vision on geometallurgical testwork is presented in Figure 6. For this vision the Mergan ball mill test, presented in chapter 4.2, is a better grindability test than Bond test, but the problem with the Mergan test is that it gives grinding energy consumption, which can be used to calculate "Mergan work index" but this work index gives different values than the Bond work index. This causes the need for the testwork in this thesis, to see if there is correlation between the Mergan work index and Bond work index, and to develop the Mergan method so that it can be used to give Bond work index values based on the grinding energy consumption. The product of the Mergan test can also be used in mineralogical and chemical analyses, and beneficiation tests.

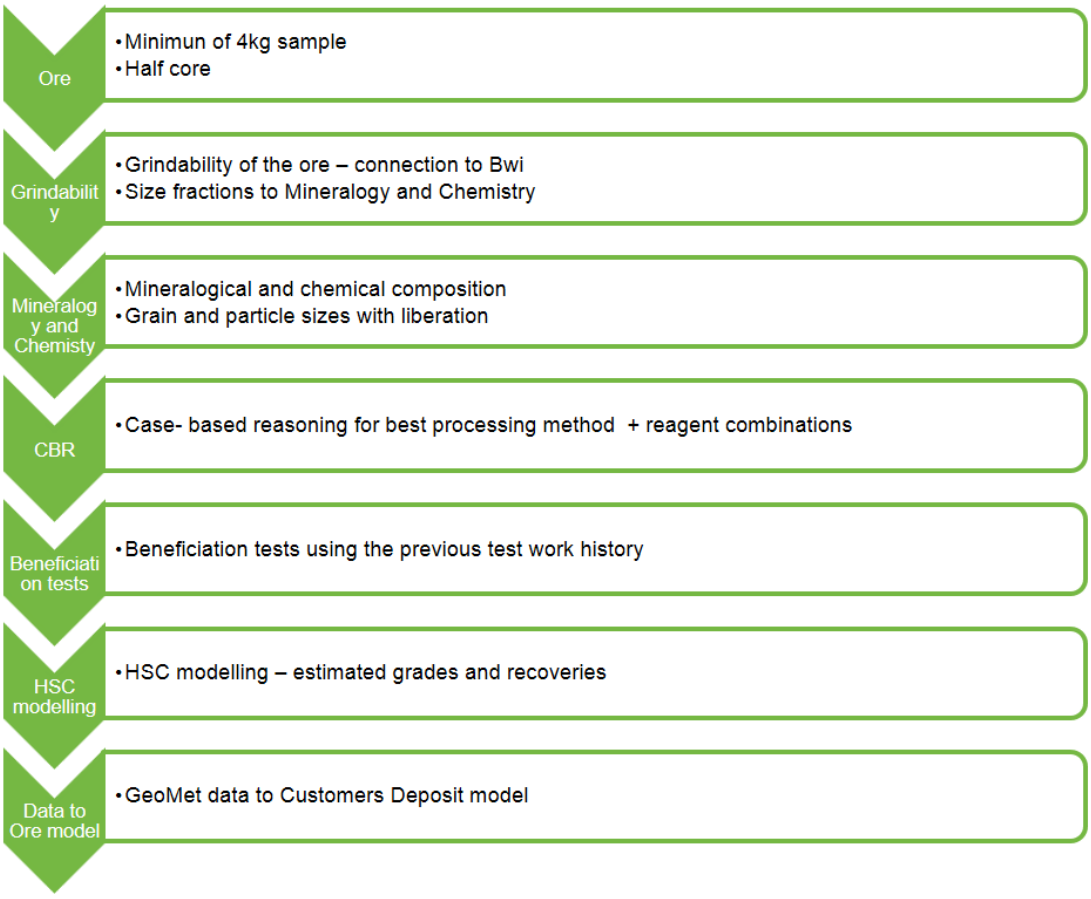

Figure 6. Outotec's geometallurgical testwork vision

4 GRINDABILITY TEST METHODS

Grindability test methods are used for determining the energy requirement when grinding a product to a desired size. These methods vary depending on the mill type and manufacturer. Mill designers typically use the Bond test and tests derived from Bond test for sizing ball mills.

The Bond test, although an industry standard, is not without limitations. The test requires specific preparation work for the sample, and usually can be used to determine grindability to a rather slim range of particle size of the product. A single Bond test can require up to 10 kg of sample material, and is rather time consuming, meaning it can take a skilled technician up to 8 hours or more work for a single test.

Thus, in the geometallurgy context, the standard Bond test can be considered far too demanding in terms of the amount of sample needed, as well as time consumed. This makes the Bond test too expensive and inefficient to be used as a standard test for geometallurgical mapping of ore deposits. Due to this, Bond test is used as a baseline in this thesis, and the other test methods introduced are methods that are either variations of Bond test to overcome the limitations of the Bond test, or can be considered "geometallurgical" tests for ore comminution.

The Mergan test, along with the Bond ball mill test will be used in the experimental part of this thesis. Mergan test can be done faster than the Bond test, and it only uses the weight of 1500 cm^3 of packed sample material. Thus, the Mergan test, if scalable to Bond, is an improvement to Bond test in Outotec's geometallurgy vision.

4.1 Bond test

According to Bond's Third Theory, the work input is proportional to the new crack tip length produced in particle breakage, and equals the work represented by the product minus that represented by the feed. For practical calculations, if we designate the work input in kilowatt hours per short ton as W, P_{80} as 80 percent product passing size in μm,

F_{80} as 80 percent feed passing size (μm) and W_i is designated work index, Bond's basic third theory (4) can be expressed as equation (7). Work index is a material specific comminution parameter which expresses the resistance of the material to crushing and grinding. (Bond, 1961a)

$$W = \frac{10W_i}{\sqrt{P_{80}}} - \frac{10W_i}{\sqrt{F_{80}}} \tag{7}$$

If the material is homogenous to size reduction, its work index (W_i) value will continue constant for all size reduction stages. However, heterogeneous rock structures are common and for instance, certain materials have a natural grain size, and their W_i values will be larger below that size than above it. The efficiency of the reduction machine may also influence the work index. As an example, a ball mill grinding an ore from 80 percent-14 mesh (1410 μm) to 80 percent-100 mesh (150 μm) will have a lower operating work index value with 1.5 in grinding balls than with oversize 3 in balls. Laboratory determinations of the work index show the resistance to breakage at the size range tested, and any variation in the work index values in tests at different product sizes shows that the material is not homogenous to size reduction. As such, laboratory tests should preferably be made at or near the product size required in commercial grinding. (Bond, 1961a)

Bond has derived equations for finding the work index from several types of laboratory crushability and grindability tests. For this thesis, Bond's ball mill grindability test is the most important, which will be described below.

The standard feed is prepared by stage crushing to all feed passing a 6 mesh (3350 μm) sieve, but finer feed can be used when necessary. The feed is screen analyzed and packed by shaking in graduated cylinder, and the weight of 700 cm^3 is placed in the mill and ground dry at 250 percent circulating load. The mill is 12 x 12 in, or 305 x 305 mm in diameter with rounded corners, and a smooth lining except for a 4 x 8 in hand hole door for charging. The mill has a revolution counter and runs at 70 rpm. The grinding charge of the ball mill consists of 285 iron balls weighing 20.125 kg. The ball charge should consist of about 43 1.45 in balls, 67 1.17 in balls, 10 1 in balls, 71 0.75 in balls, and 94

0.61 in balls with a calculated surface area of 842 sq. in. Tests can be made at all sieve sizes below 28 mesh (600 µm). (Bond, 1961a)

The first grinding period is 100 revolutions, after which the mill is dumped, the ball charge is screened out, and the 700 cm^3 of material is screened on sieves of the mesh size tested, with coarser protecting sieves if necessary. The undersize is weighed, and fresh unsegregated feed is added to the oversize material to bring its weight back to that of the original charge. Then the feed is returned to the ball mill and ground for the number of revolutions calculated to produce a 250 percent circulating load, after which the material is again dumped and rescreened. The number of revolutions required is calculated from the results of the previous period to produce sieve undersize equal to 1/3.5 of the total charge in the mill. (Bond, 1961a)

The grinding period cycles are continued until the net grams of sieve undersize produced per mill revolution reaches equilibrium and reverses its direction of increase or decrease. Then the undersize product and circulating load are screen analyzed, and the average of the last three net grams per revolution, G_{bp}, is the ball mill grindability. When P_1 is designated as the opening of the sieve size tested (µm), then the ball mill work index W_i is calculated from equation (8). (Bond, 1961a)

$$W_i = \frac{44.5}{P_1^{0.23} \times G_{bp}^{0.82} \times \left(\frac{10}{\sqrt{P_{80}}} - \frac{10}{\sqrt{F_{80}}}\right)} \tag{8}$$

It should be noted that the work index calculated in equation (8) is specific to short ton. For calculating the work index in kWh/t, equation (9) should be used.

$$W_i = \frac{49.1}{P_1^{0.23} \times G_{bp}^{0.82} \times \left(\frac{10}{\sqrt{P_{80}}} - \frac{10}{\sqrt{F_{80}}}\right)} \tag{9}$$

The work index value from equation (8) should conform with the motor output power to an average overflow ball mill of 8 ft. interior diameter in grinding wet closed circuit. Bond also introduces correction multipliers, such as in dry grinding work input should be multiplied by 1.30 and when D is mill diameter inside the lining in ft., the work input should be multiplied by $(8/D)^{0.2}$. (Bond, 1961a)

4.2 Mergan method

In 1970 Niitti developed a batch type grindability test method, which he named Mergan, milling energy analyzer. According to Niitti, basic demands for a dependable grindability test are:

- The energy consumption has to be measurable.
- The test must be performed either wet or dry corresponding with the industrial grinding process.
- The test must be carried out to the same final fineness as the industrial grinding process.
- The procedure of a test must be simple and rapid.

The measurements of the mill are 268 × 268 mm, corresponding to a 1/100 of a *"base mill"*. The speed of the mill can be regulated within wide limits. The net energy consumption of the mill is continuously determined by a simple but sensitive pendulum type torque measurement from the mill axis. For ease of operation the mill is equipped with a revolution counter switch, along with necessary aids for emptying the mill and separation of the sample from the grinding media. (Niitti, 1970)

Niitti conducted a large series of tests to study the effect of various factors on the grindability of the material, and to determine the optimal conditions for operating the Mergan mill. The main material tested was the Outokumpu ore containing about 50 percent sulphides and 50 percent silicates. At first the optimum working conditions of the mill were investigated by changing various factors so that the minimum energy consumption per ton of new -74 μm material produced, W_{74}, was found. (Niitti, 1970)

The optimum amount of grinding media, steel balls, is 22 kg, which fills almost half of the mill. Figure 7 illustrates the effects of the amount of grinding media on optimum working conditions. With a smaller ball charge the aforementioned energy consumption, W_{74}, increases rapidly. With a heavier ball charge the increase is quite small. Balls of different sizes were also tested. Niitti found that a natural ball charge consisting of balls between 15 and 40 mm was the most efficient, and was chosen as a standard. The

optimum amount of material is 1500 cm^3, which in practice fills the interstitial spaces between the balls. (Niitti, 1970)

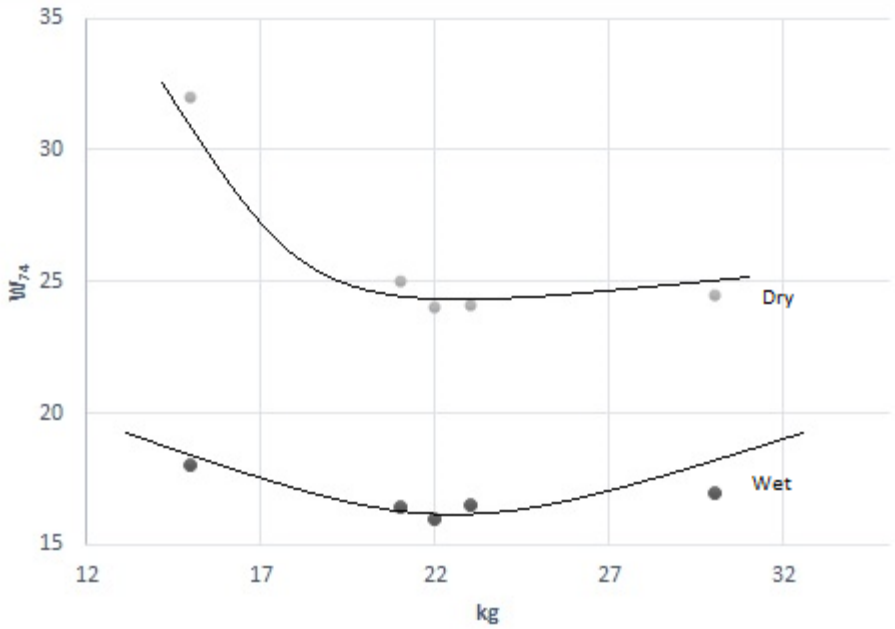

Figure 7. Effects of the amount of grinding media on the batch mill optimum working conditions. Modified from the source. (Niitti, 1970)

The optimum speed of the mill is 70 % of the critical speed of the mill shell. The optimal pulp density in wet grinding 50 to 60 percent solids by weight. Both in case of the pulp density and the mill speed, the increase in energy consumption is quite slow near optimum values, as demonstrated in Figures 8 and 9. (Niitti, 1970)

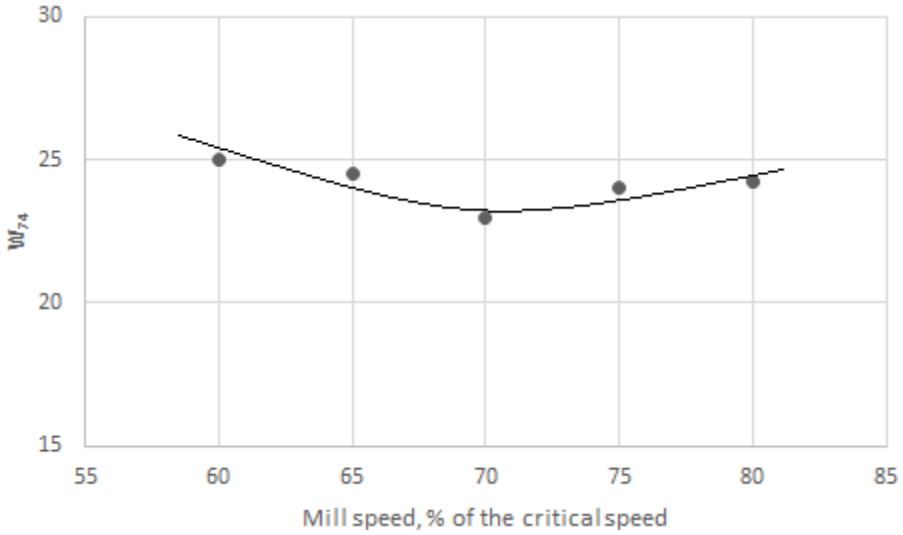

Figure 8. Effects of the mill speed on the optimum working conditions. Modified from the source. (Niitti, 1970)

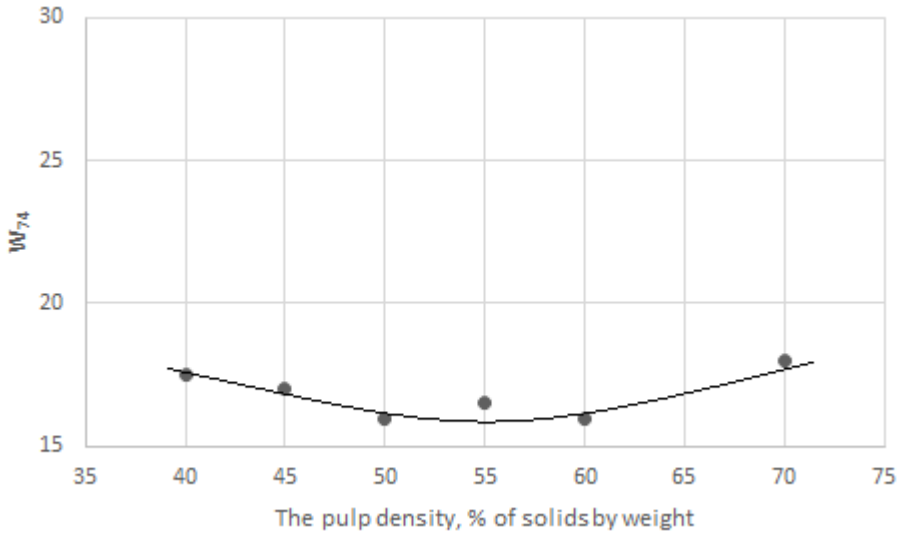

Figure 9. Effects of pulp density on the batch mill optimum working conditions. Modified from the source. (Niitti, 1970)

Accurate measurements of the energy consumption showed that the consumption of this type of batch mill is not constant, but actually changes during the experiment. Initially the energy requirement shows a slight increase of about 5 to 10 percent from the original value. After a few hundred revolutions it starts to decrease and after about 2500 revolutions it levels to a value about 20-35 percent lower than the original value. Niitti

assumed that this decrease happened because of the change in the friction conditions in the mill due to the decrease in grain size. Investigators tried to eliminate this phenomenon by installing lifter bars in the mill, however, experiments indicated that this measure does not eliminate the phenomenon. The aforementioned phenomenon is illustrated in Figure 10. (Niitti, 1970)

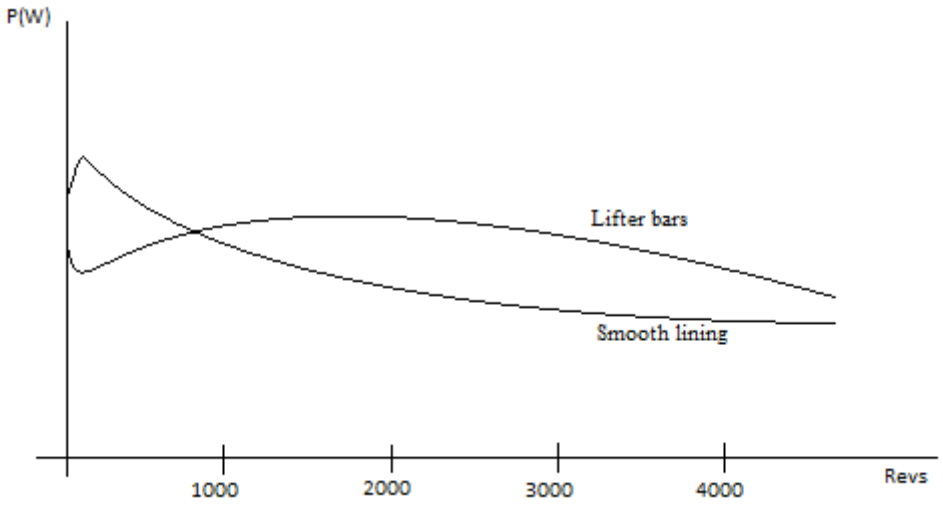

Figure 10. An illustration of net power alteration during grindability test. Modified from the source. (Niitti, 1970)

The material ground also clearly affects the energy consumption of the mill. The energy requirement for dry and wet grinding is quite different. In general, wet grinding is distinctly more efficient than dry grinding, the difference being frequently 30-50 percent. On basis of the facts mentioned above, Niitti concluded that it is not possible to determine accurately the grindability of wet industrial process on the basis of a dry grinding test. The determination must be carried out with the same medium as that with which the grinding process will take place. (Niitti, 1970)

The finer the grinding product is the more difficult the grinding tends to become. This difficulty varies with the material, thus, it is not feasible to describe the grindability with a single figure or index, which would cover the whole range of grain sizes. For a test of the grindability to be reliable, it must be carried out to the same fineness as the actual process of grinding done. (Niitti, 1970)

When conducting a grindability test using the Mergan mill, the sample is to be crushed to about -4 mm size. The fineness of the material is determined by a sieve and surface area of the material by a rapid permeability analysis. Based on the data measured (E_0) as described, the grindability of the material tested can be calculated directly as energy consumption in kWh/t when ground from a given initial fineness to a desired final fineness. The grindability (W_{74}) may be expressed as kWh/t of the new -74 µm material produced, or as kWh/t per 1000 cm^2/cm^3 of the new specific surface area produced. The grinding energy consumption (E_0) can also be used to calculate M-W_i, or "Mergan work index) according to equation (10). (Niitti, 1970; Kurki, 2006)

$$M - W_i = E_0 \left(\frac{\sqrt{F_{80}}}{\sqrt{F_{80}} - \sqrt{P_{80}}} \right) \sqrt{\frac{P_{80}}{100}} \tag{10}$$

where M-W_i is Mergan work index [kWh/t]
E_0 is energy consumption [kWh/t]

It should be also noted, that even though E_0, W_{74} and W_i are all expressed as kWh/t, they mean different things, and can cause some confusion. It is clear that when talking about these grinding parameters, it has to be very specific that what the value stands for.

4.3 Geometallurgical Comminution Test (GCT)

Geometallurgical Comminution Test program, developed at Luleå University of Technology, aims to provide a test method that is usable in analyzing even small drill core samples. The program consists of crushability and grindability test work, along with mineralogical analyses for entire samples as well as selected sieve fractions. Results from the test program include modal mineralogy, particle size distributions, work indices and mineral liberation analysis. (Mwanga, et al., 2017)

As a part of the test program, a small scale batch grindability test method has been created as a shortcut for estimating Bond ball mill work index for the ore. This small scale grindability test method uses a small laboratory ball mill, with a volume of 1400 cm^3. The

mill rotates on the same critical speed as the original Bond mill to fulfill the criteria of kinematic similarity as defined by Steiner (1996). The volume fraction that the ball charge occupies in the mill has been kept at a similar level with the Bond ball mill test. The size of the balls is kept at the same level as the Bond test, but the ball amount has been adjusted according to the mill size. (Mwanga, et al., 2017)

Sample preparation is done by preparing 220 g sample material, pre-crushed in a laboratory jaw crusher to 100% passing 3.35 mm. Dry batch grinding test of the sample is done using cumulatively 2, 5, 10, 17 and 25 min grinding times. After each grinding period, the sample is dry sieved for particle size analysis and returned to the mill for further grinding. The particle size distributions are numerically evaluated to calculate 80% passing size. Additionally the sample amount below the target product size is determined corresponding to the grindability analysis within the Bond procedure. (Mwanga, et al., 2017)

The mill uses a conventional energy meter to record the gross power draw during the grinding test. Due to the limited precision of the energy meter, an energy-time relation has been established for the test. The mechanical power used by the mill is back-calculated using efficiency data for the electrical engine and the mill mechanical drive. The fact that the mill runs at a reduced speed and load is taken into consideration in the calculation. The energy provided to the mill per unit time is assumed to be a constant, because the test runs at a constant sample weight and constant mill parameters. (Mwanga, et al., 2017)

The evaluation of the grinding test results is the based on the bond formula for calculating the specific energy for grinding W, as given in equation (7). Potential differences in the shape of the product particle size distribution compared to a locked-cycle test with screen are neglected in the calculation of the P_{80} value. Further, for a given feed size the change in specific grinding energy is proportional to the reciprocal of the square root of the P_{80} value, shown in equation (11). (Mwanga, et al., 2017)

$$W = k\left(\frac{10}{\sqrt{P_{80}}}\right) \leftrightarrow k = W\left(\frac{P_{80}}{10}\right) \quad (11)$$

where k is a constant [kWh/t].

The proportionality constant k divided by 10 is designated as the GCT work index and can be determined using the several data pairs of W and P_{80} for the different grinding times. Like the Bond work index, the GCT work index is a material dependent parameter. (Mwanga, et al., 2017)

To validate the small scale grindability test procedure and for the development of a correlation between the GCT work index and the standard Bond work index, grinding tests were done with fifteen samples from different types of deposits in the Nordic countries. The sample materials used had wide mineralogical variations. For each sample the full Bond ball mill grindability test was conducted according to the Bond standard procedure and results from that were compared with the GCT grindability test. The target product size in all the tests was kept constant at 106 µm. (Mwanga, et al., 2017)

The small scale grindability test was performed using a Capco jar mill, type 337SS, with a steel ball charge of 1.3 kg and an average ball diameter of 28 mm. The inner mill diameter was 115 mm and the mill speed was set to 91% of critical speed, or 114 rpm, using voltage control. (Mwanga, et al., 2017)

Comparison of the results from the two grindability tests revealed that there is a linear connection between the two work indices. When taking into consideration the geometric scaling factor between Capco jar mill and the Bond mill and a correction of the GCT work indices for mill drive and engine efficiency, a remaining linear correlation factor of 4.0 was derived from the experimental data. Equation (12) gives the model for estimating the Bond work index from GCT work index. (Mwanga, et al., 2017)

$$W_{i,estimated\ Bond} = W_{i,GCT}\left(\frac{1}{\sqrt{\lambda}} \times \eta \times \frac{1}{4}\right) \quad (12)$$

where λ is geometric scaling factor, $\lambda = 2.65$

η is mill drive and engine efficiency, $\eta = 0.64$

The estimated Bond work indices from the GCT model showed a linear correlation with the measured Bond work indices. For metal ore samples the relative error between the two values was on average 5.1%, with a maximum of 8.8%. It should be noted that the experimental variation of the full Bond test is denoted with ± 3.5%. Three samples of industrial minerals that were used, however, showed larger deviations. The authors of the article also point out that the GCT method is not meant to replace standard Bond test, but rather to be a complementary approach when working with small scale samples as in the geometallurgical context. (Mwanga, et al., 2017)

4.4 Wet Bond mill test

Tüzün (2001) states that *"the range of test activities involved in the Bond test procedure means that errors can easily slip into the results due to a lack of understanding of the scope and limits of the test procedure"*. As an example, it was found that when a fine limiting screen size such as 53 µm was used, the Bond work index was higher than expected. Work index values were affected by difficulties present in dry screening, especially when finer closing screens are were, when fluidity is decreasing rapidly. (Tüzün, 2001)

The dry screening procedure can also cause rapid blinding of screens and poor reproducibility when fine closing screens are used. Some materials might be screened successfully through a fine screen when dry, but softer materials such as dolomite and limestone, and notably samples containing clay give inconsistent results. Thus, wet screening should always be used for the finest sieve. As a result, an attempt was made by Tüzün (2001), to overcome some of the limitations of the Bond test procedure and to

provide better estimates of grindability and extrapolations from laboratory scale to production scale. (Tüzün, 2001)

The wet Bond ball mill test procedure follows the Bond ball mill test, however, 1 kg of water is added to the ore charge during grinding, and the sieving is done wet on a Rhologon sieve with the given limiting sieve size for 10 minutes. The oversize sample is then filtered. The moisture content of the oversize is determined from the first test by drying and re-weighing, and the dry weight of the subsequent products can be calculated by subtracting the moisture content from the wet weight. Based on the weight of the oversize, the production of undersize in terms of net grams per mill revolution can be calculated. (Tüzün, 2001)

When the test is finished (undersize produced per revolution reaches and equilibrium and reverses its direction of increase or decrease), the undersize of the last three net grams per revolution is wet screen analyzed to calculate the work index. When the Bond work index obtained from the wet procedure is used in the estimation of the standard Bond index, it should be multiplied by a correction factor of 1.3, established by Bond. (Tüzün, 2001)

The test was performed on quartz, and three different sieve closing sizes was used, 53 µm, 75 µm and 150 µm. Table 1 shows the results obtained from the Wet Bond ball mill test, and Bond index obtained from dry process is used as a comparison. The test shows correlation with Work indices obtained from the normal Bond test. (Tüzün, 2001)

Table 1. The Bond work indices obtained from wet and dry bond tests at various limiting screen sized. Modified from the source. (Tüzün, 2001)

Limiting screen size (µm)	**Bond work index obtained from wet process**		**Bond work index obtained from dry process**
	$W_{i,\ wet}$	$W_{i,\ wet} \times 1{,}3$	W_i
212	-	-	14,5
150	11,7	15,2	15,5
106	-	-	16,8
75	13,5	17,6	17,7
53	15,7	20,4	19,3

4.5 New Size Ball Mill (NSBM)

The test is conducted in a special ball mill. The mill is scaled down with a coefficient of two-thirds of the standard Bond ball mill and its diameters are 200 x 200 mm inside. It is operated at the same speed as the Bond ball mill, as it rotates at 91 % of critical speed, in this case 86 rpm. The ball charge consists of 85 steel balls weighing 5.9 kg, range of diameter being 16-38 mm. (Nematollahi, 1994)

The ore is packed to 207 cm^3 volume instead of 700 cm^3 that is standard in Bond test. The test is conducted to produce a circulating load of 250%. After reaching equilibrium, the grindabilities of the last three cycles are averaged. Equation (13) was derived from the results. The results obtained by this method are compared with the results of the same samples obtained by the Bond ball mill in Table 2. (Nematollahi, 1994)

$$W_i = \frac{11.76}{P_1^{0.23}} \times \frac{1}{G_{bp}^{0.75}} \times \frac{1}{\frac{10}{\sqrt{P_{80}}} - \frac{10}{\sqrt{F_{80}}}} \tag{13}$$

Table 2. Comparison of work indices obtained by Bond ball mill and NSBM. Modified from the source. (Nematollahi, 1994)

Sample	Bond Ball Mill	New Size Ball Mill	Relative error %
	Wi	Wi	
Barite	6,12	6,21	1,47
Feldspar	11,75	11,12	-5,36
Hematite	13,89	14,31	3,02
Calcite	8,36	8,5	1,67
Chromite	14,98	15,7	4,81
Dolomite	21,77	19,18	-11,9
Coke	30,43	28,75	-5,52
Coal	12,99	12,33	-5,08
Silica	11,93	11,49	-3,69
Fluorite	7,4	7,28	-1,62
Magnetite	9,33	9,54	2,25

4.6 Rapid determination of the Bond Work Index

Magdalinović (1989) studied grinding kinetics defined by means of the Bond ball mill to find a simplified procedure for a rapid determination of the work index by just two grinding tests. Tests of grinding kinetics in the Bond ball mill have shown that over a shorter grinding period follows the law of first order kinetics shown in equation (14). (Magdalinović, 1989)

$$R = R_0 e^{-kt} \tag{14}$$

where R is test-sieve over-size at the time (t)
R_0 is test-sieve over-size at the beginning of grinding (t=0)
k is grinding rate constant
t is grinding time

By simulating the closed-circuit grinding in the standard Bond test, Magdalinović derived equations (15) and (16) at a standard 250% circulating load.

$$\frac{R}{U} = 2.5 \tag{15}$$

$$U + R = M \tag{16}$$

where R is weight of the test sieve over-size [g]
U is weight of the new feed [g]
M is weight of the mill feed [g]

From equations (15) and (16) equations (17) and (18) can be derived.

$$R = \frac{2.5}{3.5} M \tag{17}$$

$$U = \frac{1}{3.5}M \tag{18}$$

In a standard grinding cycle R_0 can be calculated from equation (19).

$$R_0 = \frac{2.5}{3.5}M + \frac{1}{3.5}Mr_0 \tag{19}$$

where r_0 is the proportion of test sieve over-size in the new feed

From equation (14) which gives the grinding kinetics in the Bond ball mill, equation (20) can now be derived.

$$t_c = \frac{\ln(1+0.4r_0)}{k} \tag{20}$$

where t_c is grinding time in a standard grinding cycle after which the over-size (R) on the test sieve is (2.5/3.5)M, which corresponds to the 250% circulating load

With the Bond ball mill, the total number of mill revolutions is taken into account rather than grind time. Since grind time can be derived from equation (21), it can then be substituted from equation (14) to form equations (22) and (23).

$$t = \frac{N}{n} \tag{21}$$

where N is total number of mill revolutions
n is mill revolutions per minute

$$k = \frac{n(\ln R_0 - \ln R)}{N} \tag{22}$$

$$N_c = n\frac{\ln(1+0.4r_0)}{k} \quad (23)$$

where N_c is total number of mill revolutions giving the (2.5/3.5)M test sieve over-size, which corresponds to the 250% circulating load

The derived equations (19), (22) and (23) make it possible to abbreviate the Bond test to only two grinding tests. The procedure starts like standard Bond test. After a 700 cm^3 sample (M) is collected and weighed, the value of R is calculated. From the original feed and adequate sample is taken and screened on a test sieve. The under-size is discarded and the over-size is retained. At least R over-size has to be prepared for the two grinding tests. (Magdalinović, 1989)

Two separate samples, weighing (1/3.5)M each are collected from the original feed. Two samples are formed for the two grinding tests by mixing test sieve over-size weighing (2.5/3.5)M with the sample weighing (1/3.5). The proportion of the coarse size (R_0) in the samples is then calculated. Then the first sample is fed into the Bond mill and is ground for a chosen number of mill revolutions, N=50, 100 or 150 revolutions. (Magdalinović, 1989)

After grinding, the entire sample is screened on a test sieve and the over-size (R) is weighed. The over-size grinding rate constant k is calculated from equation (22), along with the total number of mill revolutions N_c for the second grinding test that can be calculated from equation (23). Then the second sample is fed to the Bond mill and is ground for N_c revolutions. (Magdalinović, 1989)

After grinding, the entire sample is screened on the test sieve. Both the over-size and under-size are weighed. The weight of the over-size should be approximately equal to (2.5/3.5)M, while the weight of the under-size m should be (1/3.5)M. Size distribution of the under-size from the second test is determined by means of screen analysis and the value P_{80} is determined graphically. The G_{bp} in the second test is calculated from equation (24). The work index can then be calculated from equation (9). (Magdalinović, 1989)

$$G_{bp} = \frac{m - \frac{1}{3.5}M(1-r_0)}{N_c} \quad (24)$$

The abbreviated procedure for the determination of the work index is based on the assumptions that the grinding rate constant for the coarse size product grinding in the standard Bond test at 250% circulating load is equal to the grinding rate constant for the coarse size product grinding in the abbreviated test procedure, and that at the same time the size distributions of the test sieve under-size are nearly equal to each other. The work indices have been established for the samples of copper ore, andesite and limestone following both the standard Bond procedure and the abbreviated procedure, given in Table 3. (Magdalinović, 1989)

Table 3. Work indices obtained from the standard Bond test and the abbreviated test procedures. Modified from the source. (Magdalinović, 1989)

Sample	Closing sieve size (µm)	Work index (kWh/t)		Difference (%)
		Bond test	Abbreviated test	
Copper ore	500	15,4	14,57	5,4
	315	13,79	12,83	7
	160	11,84	11,46	3,2
	80	12,9	13,07	-1,3
Andesite	500	25,05	24,42	2,5
	315	19,9	21,25	-6,8
	160	22,7	21,31	6,1
	80	22,38	22	1,7
Limestone	500	14,26	13,33	6,5
	315	13,57	12,78	5,8
	160	11,04	10,48	5,1
	80	11,7	11,41	2,5

4.7 Work index from field measurable rock properties

Karra et al. (2016) attempted to determine Bond work index using simple properties of rocks like density, Protodyakonov's strength index and rebound hardness number. These properties can be determined on site as there is no need to carry the blocks to the

laboratory to prepare the samples. Investigations were carried out on three different rock types, basalt, slate and granite. Eight samples of each kind were collected from different quarries. Also during sample collection, each sample was inspected for macroscopic defects so that the test specimens were free from fractures and joints. (Karra, et al., 2016)

For determining the Bond work index, the samples were prepared by crushing large lumps of basalt, slate and granite in a dodge type jaw crusher to -3.35 mm. A gap of 4.8mm and 3.6mm was used to avoid extra fine particles. 2-3 pieces of sample lumps close to cubical shape weighing cumulatively nearly 50 g were used to determine the Protodyakonov's strength index. The rebound hardness test was done on a block of 30 x 30 x 15 cm of nearly regular shape samples using L-type Schmidt hammer. (Karra, et al., 2016)

The Bond work index was determined by doing standard Bond ball mill test with a closing sieve size of 250 µm. The density of the rock samples was found by using 10 lumps of each rock test sample of irregular size, each weighing approximately 50 g. The surface of the samples was cleaned properly and the samples were submerged into an immersion bath for a minimum time of one hour. The weight of surface dried saturated sample was taken at an accuracy of 0.01% and was later dried at a temperature of 105 ºC to constant mass. The sample was cooled for 30 minutes and after its weight was taken. Density was then calculated according to equations (25) and (26). (Karra, et al., 2016)

$$V = \frac{(M_s - M_d)}{\rho_w} \tag{25}$$

$$\rho = \frac{M_s}{V} \tag{26}$$

where M_s is saturated-surface-dry mass of the samples
M_d is dry mass of the sample
ρ_w is density of water

Protodyakonov's strength index test was performed according to standard procedure. A vertical cylinder apparatus which is 78 cm in height, 76 mm in diameter and has a steel plunger of 2.4 kg of drop weight was used. A sample of 50 g, containing 2 lumps of nearly

cylindrical shape in the size range of 2 to 4 cm was taken. 5 sets of these lumps were used for one test sample, total weight of the sample for test being 250 g. The plunger was dropped from a height of 76 cm into the cylinder. Five impacts were imparted to each set and same procedure was repeated for rest of the sets. After 5 impacts, the crushed material of each set was collected, and finally, all the crushed material of the 5 sample sets was sieved through a 500 µm sieve. The sieve under-size was filled into a volume meter and its height was taken for further calculation. Then the Protodyakonov's Strength Index of the sample can be calculated using equation (27). (Karra, et al., 2016)

$$PSI = 20\left(\frac{n}{h}\right) \tag{27}$$

where PSI is Protodyakanov's Strength Index
n is the number of impacts
h is the measured particles height in volume meter

The rebound hardness test was performed on blocks of the sample of size 30 x 30 x 15 cm. The test was performed on each sample block in a grid manner with a portable, pre-calibrated L-type Schmidt hammer. A Schmidt hammer is a portable instrument that can be used for testing rebound hardness number, either in laboratory or in the field. The plunger of the hammer was placed against the specimen orthogonally within ± 5^{o} and was pressed by pushing the hammer against the sample block. The resulting reading was obtained and recorded and 20 recordings were made on each sample. The 20 records were arranged in ascending order. 10 lower values were discarded and the average of the higher 10 was taken as rebound hardness number (RHN). (Karra, et al., 2016)

Two approaches were used to analyze the laboratory experiments, Artificial Neural Networks (ANNs) and regression analysis. The ANN approach was used to validate the authenticity of the data obtained from experiments and the regression analysis was used to find correlating mathematical factors. ANN is known to be more accurate in data prediction based on effectiveness of training of network. The problem is, a mathematical model cannot be developed from ANN. ANN approach was used to ensure that the data obtained from laboratory experiments is error free. The percentage of error between the

actual values from laboratory experiments and ANN predicted values of Bond Work Index was found to be between maximum deviation of 5.44% and minimum deviation of 0.05%. (Karra, et al., 2016)

Regression analysis is a statistical process to find the relationship between a dependent variable and one or more independent variables. The coefficient of correlation was determined for individual relation for density, Protodyakonov's strength index and rebound hardness number with the Bond work index. Combined relationship between Bond work index and all other parameters was also determined. According to the analysis, second order polynomial correlation was giving the best result for individual relationships and a linear correlation was best for combined relationships. Statistical analysis was also conducted. (Karra, et al., 2016)

The models acquired from regression analysis are presented in equations (28), (29), and (30). A comparison of actual values for Bond work index and predicted values from developed equations is shown in Table 4. The values of the predicted work indices are rather close to the ones determined by the standard Bond test. Work to validate the experimental equations was also done by doing more laboratory experiments on a fourth material, limestone. The estimated work indices also correlated decently with the actual Bond work index. (Karra, et al., 2016)

$$W_i = 8.85\rho - 12.58 \tag{28}$$

$$W_i = 4.32(PSI) - 2.2 \tag{29}$$

$$W_i = 0.34(RHN) - 6.61 \tag{30}$$

Table 4. Actual values and predicted values of Bond work indices from developed equations. Modified from the source. (Karra, et al., 2016)

Sample	Bond's work index (kWh/sh. Ton						
	Actual	Predicted					
		Eq. (24)	Error %	Eq. (25)	Error%	Eq. (26)	Error%
Basalt1	12,089	11,62	3,84	11,74	2,92	12,02	0,57
Basalt2	11,018	11,14	-1,09	11,3	-2,56	11,61	-5,34
Basalt3	11,568	11,49	0,66	11,74	-1,46	11,74	-1,52
Basalt4	12,604	11,7	7,14	12,2	3,22	12,23	2,99
Basalt5	11,421	11,46	-0,31	12,2	-6,81	11,68	-2,22
Basalt6	11,805	11,39	3,55	11,74	0,58	11,88	-0,65
Basalt7	11,984	11,24	6,25	11,3	5,71	12,09	-0,88
Basalt8	12,214	11,84	3,09	12,7	-3,94	12,16	0,46
Slate1	8,524	7,99	6,3	8,34	2,2	8,57	-0,54
Slate2	8,564	8,14	4,98	8,88	-3,65	8,64	-0,88
Slate3	8,129	8,4	-3,37	8,6	-5,79	8,16	-0,33
Slate4	8,625	8,52	1,24	8,09	6,25	8,78	-1,76
Slate5	8,748	8,67	0,9	9,17	-4,83	8,78	-0,33
Slate6	7,941	8,28	-4,26	8,34	-4,98	8,02	-0,97
Slate7	8,434	8,38	0,68	8,88	-5,25	8,43	0,02
Slate8	8,439	8,32	1,37	8,6	-1,91	8,43	0,08
Granite1	10,22	10,96	-7,25	9,8	4,1	10,23	-0,06
Granite2	10,133	10,85	-7,12	10,14	-0,09	10,09	0,44
Granite3	10,094	10,55	-4,47	10,51	-4,07	9,95	1,43
Granite4	10,595	10,67	-0,7	10,89	-2,78	10,64	-0,42
Granite5	10,357	11,13	-7,46	10,14	2,07	10,09	2,6
Granite6	11,018	11,15	-1,17	10,51	4,65	10,71	2,8
Granite7	10,879	10,91	-0,27	9,8	9,91	10,57	2,83
Granite8	10,521	10,81	-2,75	10,14	3,6	10,5	0,18

5 TESTWORK, METHODS AND EQUIPMENT

5.1 Samples used

For the testwork carried out in this thesis, three different ore samples were used. The first ore used was a refractory gold ore (RGO), which consisted mainly of dolomite, quartz, albite and muscovite. The second ore was a massive sulphide ore (MSO) which consisted mainly of pyrite, quartz and chalcocite. The third ore was a limestone that consisted mainly of calcite and quartz. All these ores went through mineralogical analysis, further information on this can be found in the appendices. Figures 11, 12 and 13 show pictures taken with an optical microscope from the ore samples.

Based on the mineralogy, the Mohs hardness values for the ores were also approximated. The results of these approximations were that the RGO had a hardness value of 4.4, MSO had a hardness value of 6.0 and the limestone sample had a hardness value of 3.3.

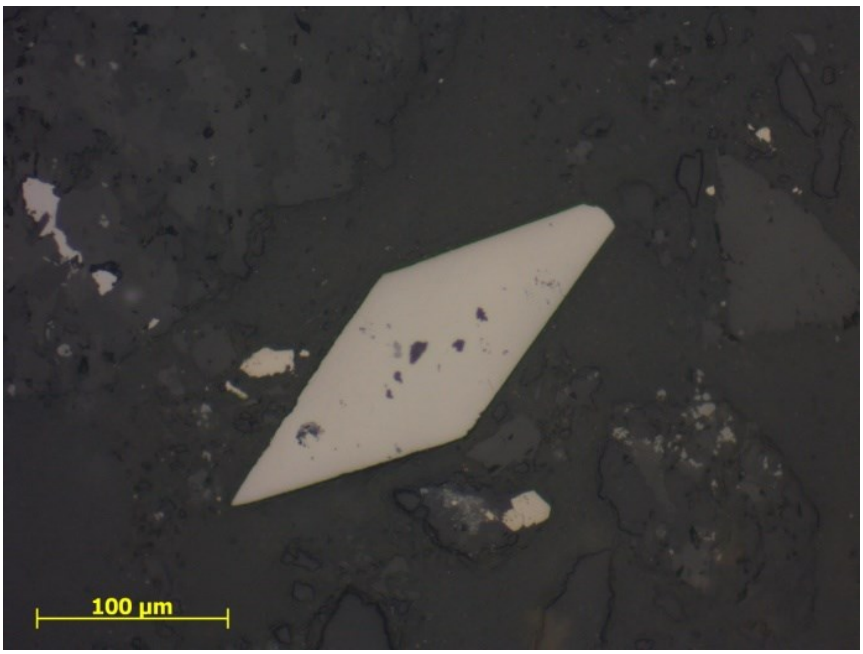

Figure 11. RGO: liberated anhedral arsenopyrite grain

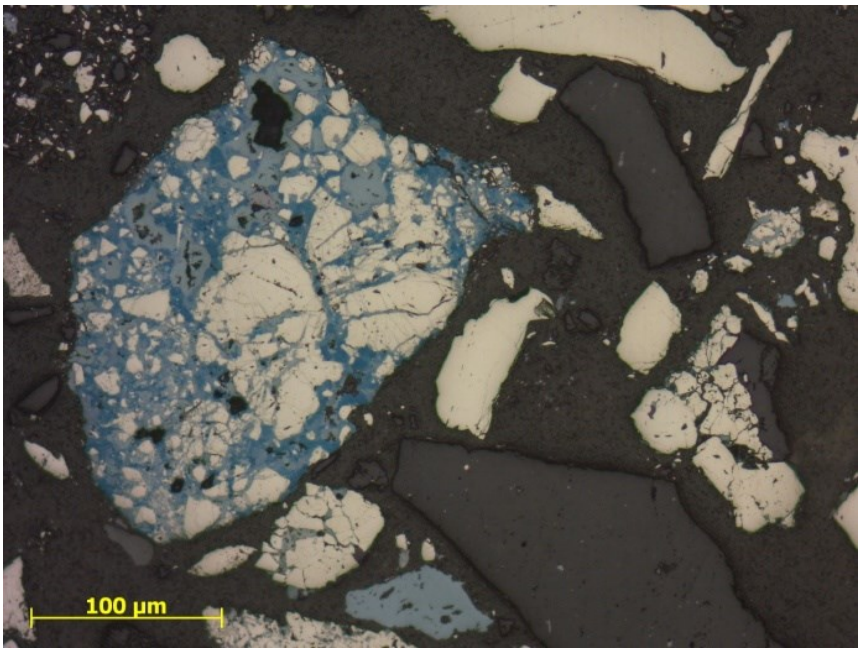

Figure 12. MSO: chalcocite and covellite fill the interstices of pyrite grains

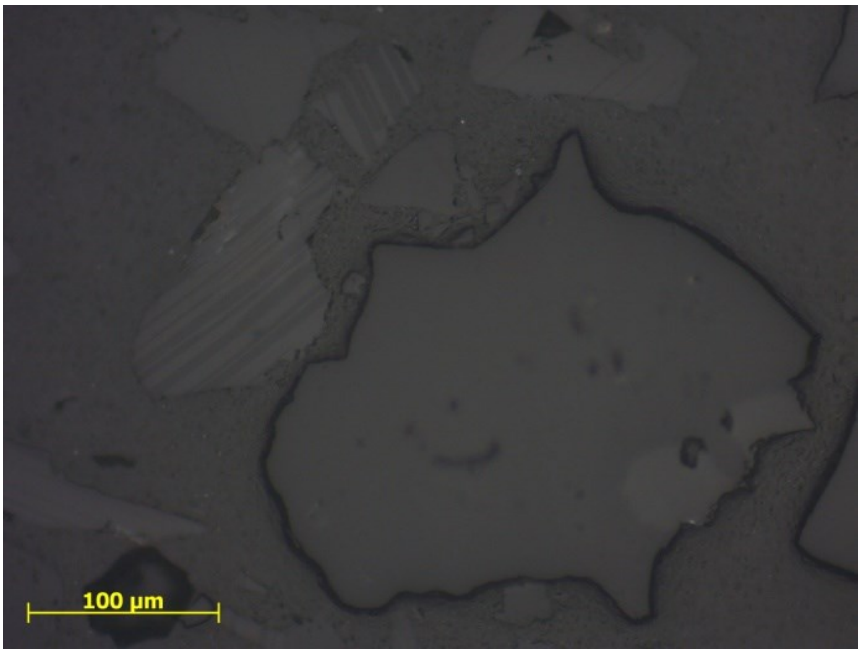

Figure 13. Limestone: calcite and quartz grains

5.2 Sample preparation

Each sample material was in a particle size that can be considered mill feed, or product of crushing circuit, meaning that the diameter of largest particles was approximately 5 cm. The total amount of each sample material was approximately 150-200 kg. All 3 sample materials were first air dried by spreading the material on a plastic sheet and letting it dry there for two days. Then the dried material was crushed with a laboratory scale jaw crusher in the grindability and mineral processing laboratories of Outotec Research center, shown in Figure 14.

Figure 14. Laboratory scale jaw crusher used.

The crushed material was then sieved with a Sweco sieve to pass 3350 µm. The Sweco sieve used is shown in Figure 15.

Figure 15. Sweco sieve used in sample preparation.

The sieve over-size was then crushed again in a laboratory scale roll crusher and then sieved again. This was repeated until all the material of the sample passed the 3350 µm sieve. The laboratory scale roll crusher is shown in Figure 16. Flowsheet of this preparation work process is shown in Figure 17.

Figure 16. Laboratory scale roll crusher

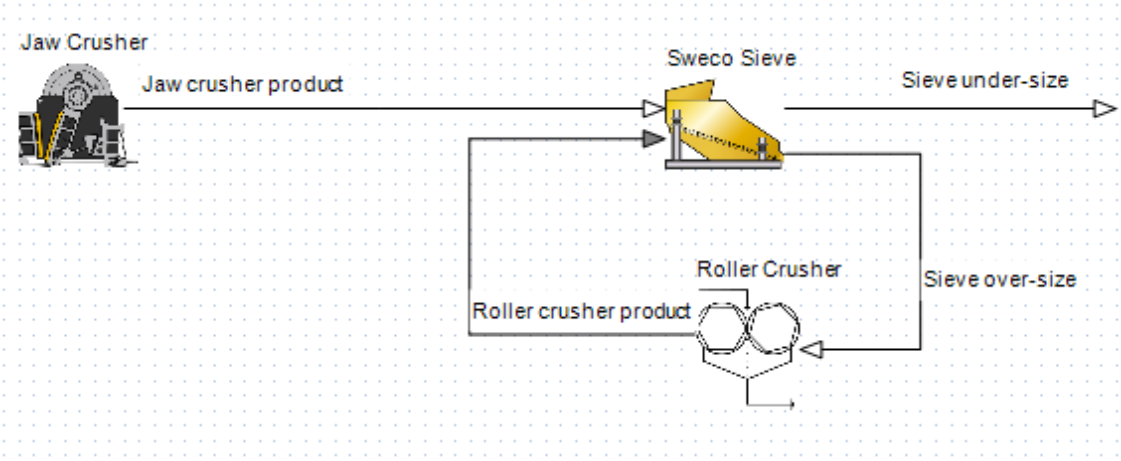

Figure 17. A flowsheet of the sample preparation process.

When all of the sample material passed 3350 µm, the aim was to homogenize the sample material. This was done by dividing each sample into equally representative sample sets by using three different spinning rifflers. The first spinning riffler was a large pilot-scale riffler (Figure 18), which divided the sample into 6 equal portions.

Figure 18. Pilot scale spinning riffler.

Then a portion was divided into 24 different portions on another laboratory scale riffler (Figure 19). Each of these 24 portions weighed approximately 500-700 g.

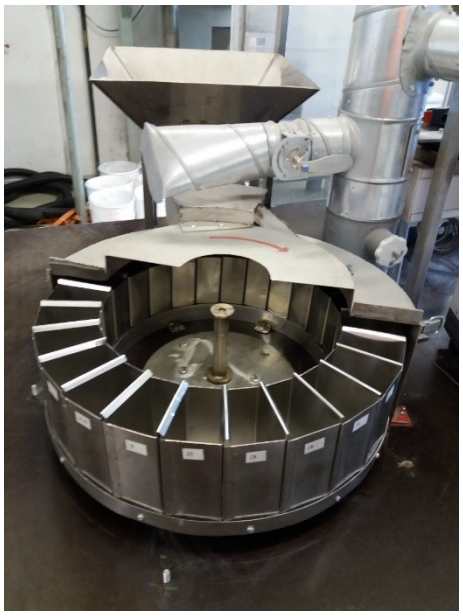

Figure 19. Laboratory scale spinning riffler.

Finally a bottle riffler was used to divide the sample into ten portions, which could then be repeated to get a sample weighing approximately 5 g. Additions weighing less than 5 g were made with a small spoon. The bottle riffler used is shown in Figure 20.

Figure 20. Bottle spinning riffler used.

From each sample material, a representative sample of approximately 500 g was used to determine the F_{80} of the sample. This was done by using a Retsch vibratory sieve (Figure 21). The sieve sizes used to determine the F_{80} started from 2360 µm and the smallest sieve used was a 106 µm sieve.

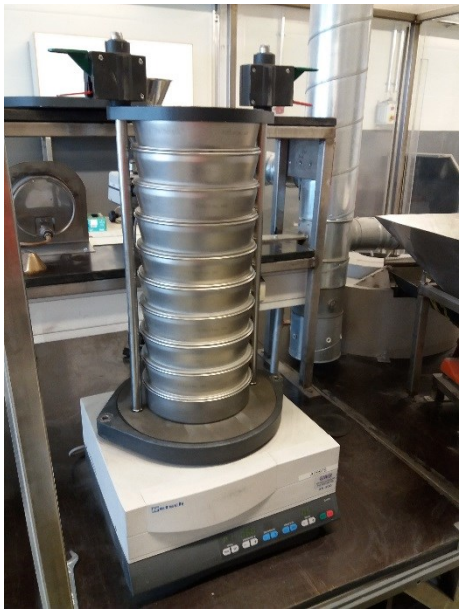

Figure 21. Retsch vibratory sieve used in the testwork, in use with 5x106 µm sieves and 5 containers for sieve under-size.

Finally, the -106 µm material left in the bottom container was first divided in the bottle spinning riffler, and approximately 20 g of the material was sieved with Alpine air jet sieve (Figure 22). When using Alpine air jet sieve, less than 25 g of sample should always be sieved. The full flowsheet for preparing the sample materials for the grindability tests and particle size analysis is shown in Figure 23.

Figure 22. Alpine air jet sieve used in the testwork.

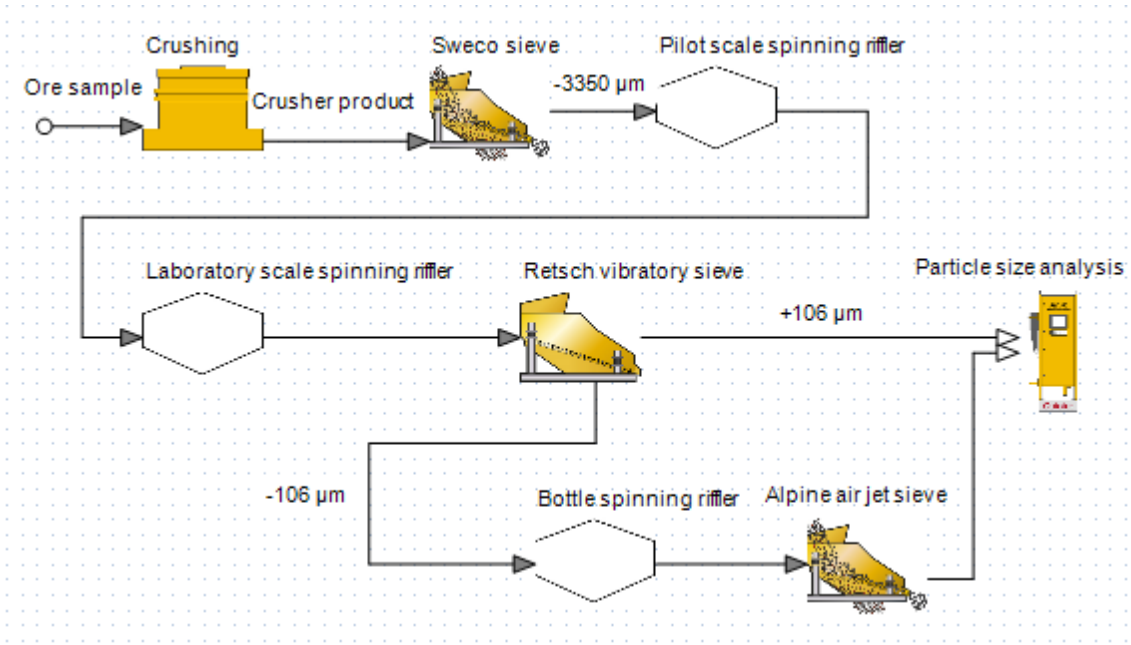

Figure 23. Flowsheet of preparation work and particle size analysis.

Once the F_{80} had been determined for each material, the amount of material used in the Bond and Mergan tests were determined by packing the sample into 700 cm^3 container with the vibratory sieve, and then weighed. The weighed 700 cm^3 material was the Bond

test feed, and from this the weight of 1500 cm^3 material required for the Mergan test could be calculated. The information gained from sample preparation is shown in Table 5. It should be noted that even though the initial feed in the Bond mill is smaller than the Mergan mill, due to the locked cycle nature of the Bond test, the Bond test requires more sample material, based on the circulating load produced during the test. As an example, one single Bond test for the refractory gold ore required in total 4512.7 g of sample material.

Table 5. Information acquired from sample preparation

Sample	F80 (µm)	Bond feed (g)	Mergan feed (g)
Refractory gold ore	2304	1283,3	2750
Massive sulphide ore	2243	1704,2	3652
Limestone	2018	1244,1	2666

5.3 Bond tests

A total of 15 Bond ball mill grindability tests were done for testwork, 5 tests for each ore sample. For each ore sample, one test was done with a sieve closing size of 150 µm, three with 106 µm to ensure that the tests were done properly and could be reproduced, and finally one with a sieve closing size of 75 µm. The ball mill used (Figure 24) is a replica of Bond ball mill described in chapter 4.1. The mill is equipped with a revolution counter, which is used to operate the mill. The mill can be rotated to ease emptying and filling the mill.

Figure 24. Bond ball mill used, positioned for filling.

The mill ball charge used consisted of 277 balls weighing 20.21 kg. The balls were chosen so that the mass of the ball charge would be as close as possible to the original ball charge determined by Bond. Information on the ball charge used is given in Table 6.

Table 6. Bond mill ball charge used

	Diameter (mm)	Mass (kg)	Ball amount
	37	8,92	40
	30	7,34	57
	25	0,67	10
	19	1,98	71
	15	1,3	99
Σ		20,21	277

The Bond test was started by preparing 700 cm^3 of fresh feed and loading it into the Bond mill. The first grinding cycle was always 100 revolutions. After that, the mill was emptied, and the sample material was separated from the ball charge. The material was then divided into 10 portions with the bottle riffler. This was done to ease the load on the sieves used. The material was then sieved in the vibratory sieve in two sets, using 5 sieves

a time. The sieving time was 5 minutes for a set of 5 sieves, so ten minutes in total. Using this method caused some losses of the material, mostly as dust losses. This was taken into account by calculating the losses as sieve-undersize. The materials lost during each cycle was used as an indicator of how well the sieving was done. A loss of 0.5% was set as a limit for a well done sieve cycle, and in almost all cases losses lower than 0.5% were achieved.

However, in the tests where 75 µm sieve closing size was used, the sieving was done with the Sweco sieve. The losses with this method were significantly larger than with the normal sieving method. The losses in almost all grinding cycles went over the 0.5% limit that was set. The Sweco was chosen to be the sieving method as it offers larger sieving area than the Retsch, and wet sieving would have been far too time consuming due to the time it would take to oven-dry the sample after each cycle. The material was passed once through the Sweco sieve screen, and the over-size was passed once more to ensure that all the -75 µm material passed the screen. When the screen showed noticeable signs that the openings became obstructed, the screen was removed and washed.

Both the sieve over-size and under-size were then weighed, the under-size removed and fresh unsegregated feed was added to the sieve over-size to bring the weight back to the original. Then calculations were done to calculate the G_{bp}, and it was used to calculate the amount of revolutions in the next cycle to produce a circulating load of 250%. The sample was then returned into the mill and ground for the amount of revolutions calculated. Flowsheet of the Bond test is shown in Figure 25.

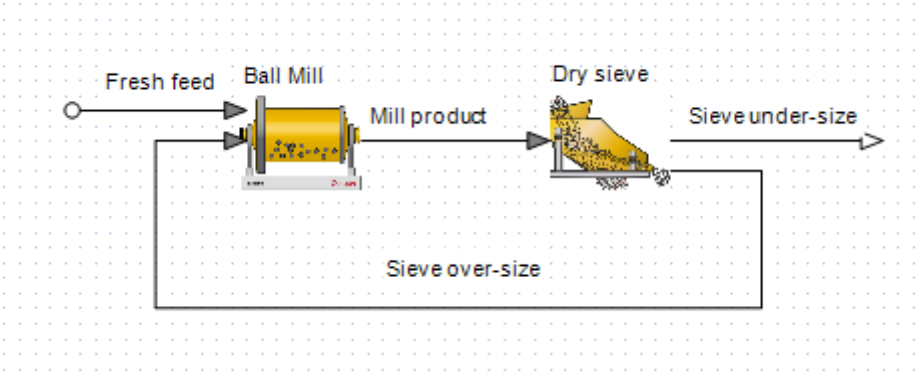

Figure 25. Bond test flowsheet.

The test was considered finished when three different parameters were fulfilled:

- Minimum of 6 grinding cycles were done
- G_{bp} had reached and equilibrium and changed its direction of increase or decrease
- Standard deviation of G_{bp} was less than 3% of the average G_{bp} of the last three cycles

Once the test was finished, the sieve under-size of the last three grinding cycles was mixed, divided in the bottle rotator, and sieved with the Alpine air jet sieve to determine the P_{80} of the material. Once this was done, the work index, W_i, could be calculated.

5.4 Mergan tests

A total of nine Mergan ball mill grindability tests were done during this thesis, three for each ore sample. The goal of the tests was to grind the material to a minimum P_{80} < 150µm, with the goal being as close as possible to 106 µm. The Mergan mill used in the testwork (Figure 26) is a replica of the mill developed by Outokumpu Oy, described in chapter 4.2. The mill measurements are 268 x 268 mm, and the mill has smooth inner lining. The speed of the mill was kept at a constant 60 rpm. The mill was equipped with a HBM T20WN torque transducer to measure the torque of the mill. The mill was also equipped with a revolution counter to operate the mill. The mill can also be operated by grinding time and be rotated to ease filling and emptying the mill.

Figure 26. The Mergan mill used in tests, positioned for filling

The mill ball charge used in the Mergan tests consisted of 318 steel balls. The weight of the ball charge was 22.23 kg, and the ball charge was an "expanded" Bond ball mill charge, meaning that the total weight of each ball size class was expanded until the total mass of the ball charge reached about 22 kg. Information on the ball charge used is shown in Table 7.

Table 7. Mergan mill ball charge used testwork

	Diameter (mm)	Mass (kg)	Ball amount
	39	8,34	37
	31	9,19	74
	26	0,93	12
	19	2,24	83
	15	1,53	112
Σ		22,23	318

At the beginning of the Mergan test 1500 cm^3 of packed material was added to the mill, along with water so that the pulp density of the slurry would be 55 weight% solids. All the grindability tests were done wet. The material was then ground for an arbitrary amount

of revolutions, while the torque transducer was used to record the mill torque at a 1 second interval. After grinding, the mill was emptied, the material was separated from the ball charge, and particle size analysis for the material was done.

When the slurry was separated from the ball charge, it was divided to 12 portions with a laboratory scale slurry divider (spinning riffler) shown in Figure 27. Then 2/12 of the slurry was taken and divided to 12 portions again, and 2/12 of that, or 1/36 of the original slurry was used for particle size analysis. The particle size analysis was then done using a sieve series ranging from 2360 µm to 45 µm, and sieving was done in an ultrasonic bath. The -45 µm material was then filtered in a pressure filtration device, shown in Figure 28. Finally the material was then oven-dried overnight and then weighed so that the particle size distribution could be determined. The material not used in particle size analysis was also pressure filtered.

Figure 27. Laboratory scale slurry divider.

Figure 28. Pressure filtrator.

Once the particle size analysis was done and P_{80} for the ground material was acquired, the 106 µm passing % of the ground material and feed was compared to approximate the mill revolutions needed for the next grinding cycle. The material was then weighed, and water was added to bring the pulp density back to 55 weight% solids and the test was continued until the material was ground to $P_{80} < 150$ µm. For the following Mergan tests this data could be used to grind the material to desired P_{80} in just one grinding cycle.

The mill power draw was then obtained from the torque measurements. Momentary power draw can be calculated from equation (31):

$$P = \frac{2\pi TN}{60} \tag{31}$$

where P is power [Nm/s], [W]
T is measured torque [Nm]
N is mill rotation speed [rev/min]

Momentary power draw could be summed over the grinding time to gain the energy consumption (E_0) for the grinding, shown in equation (32). Once P_{80} and E_0 were calculated, the Mergan work index, M-W_i, could be calculated from equation (10).

$$E_0 = \frac{\sum P}{3600000\frac{M}{10^6}} = \frac{\sum P}{3{,}6M} \tag{32}$$

where E_0 is energy consumption [kWh/t]
P is power [W]
M is weight of the mill feed [g]

6 RESULTS AND ANALYSIS

6.1 Bond tests

The results of the 15 Bond tests can be seen in Table 8. The table shows the W_i and P_{80} acquired from the tests. More detailed information on the tests can be found in the appendices.

Table 8. Results from the Bond tests

Test	Sieve Closing size (µm)	Refractory gold ore		Massive sulphide ore		Limestone	
		P80 (µm)	Wi (kWh/t)	P80 (µm)	Wi (kWh/t)	P80 (µm)	Wi (kWh/t)
1	**150**	97	19,39	105	13,99	106	9,21
2	**106**	71	19,74	75	14,62	76	10,19
3	**106**	69	19,32	76	14,58	76	10,14
4	**106**	67	18,81	72	14,83	75	10,29
5	**75**	33	20,02	39	15,74	42	11,14

At first the reproducibility of the tests was analyzed. The maximum error in the 106 µm Bond test Work indices for each material is 4.9%, 1.7%, and 1.5% respectively. The difference in results show that the tests can be done with good reproducibility, and if the error margin in full Bond tests is set to ±3.5 %, the average W_i for the refractory gold ore is 19.29 kWh/t and comparison of the maximum and minimum from the tests shows that the work indices are still within the error margin. The average W_i values for the massive sulphide ore and limestone are 14.68 kWh/t and 10.21 kWh/t, respectively.

It should be noted that refractory gold ore sample was definitely most resistant to grinding, and as such it affects the results and error in the tests somewhat. Also, since the ball mill grindability G_{bp} is the lowest for RGO, slight differences in G_{bp} seem to affect the Work indices more so than with the softer materials.

Based on the mineralogy data presented in chapter 5.1, the massive sulphide ore has the highest Mohs hardness value. This shows that hardness based on mineralogical data is not a sum of its parts when determining a material's resistance to grinding, as it doesn't take into account structure, mineral size etc.

Based on the results, the more resistant to grinding the ore is, the lower the P_{80} value seems to be in comparison to ores that are easier to grind. This can be explained by the fact that lower G_{bp} means that the number of mill revolutions to produce 250% circulating load increases. This increase then means that the material that would pass the sieve gets ground more than would be necessary. From equation (9) it can also be seen, that when P_{80} decreases, the W_i value also decreases, if other parameters remain unchanged.

One very interesting aspect of the tests that can be seen in Table 8 is the P_{80} values from the tests when 75µm sieve closing size was used. When compared to tests where other closing sieves were used, the P_{80} values seem a lot smaller in comparison. Bond (1961a) states that if P_{80} value can't be found from particle size analysis results, P_{80} value of 50 µm should be used when closing sieve size of 75 µm is used. For comparison, Bond also states that when 150 µm closing sieve is used, P_{80} value of 114 µm should be used, and when 106 µm sieve closing size is used, P_{80} value of 76 µm should be used. (Bond, 1961a)

The measured P_{80} value from particle size analysis is a lot lower in all 75 µm tests than the one Bond gives. This is most likely a result of the fluidity of the material decreasing as it is ground to finer sizes, which causes problems in dry sieving. If the P_{80} value of 50 µm was used instead of the one that was measured, the work index values would increase significantly. When 106 µm sieve closing size is used, the P_{80} value seems to be in line with the value that Bond gives, except in the case of RGO. For 150 µm closing sieve, the P_{80} values are again lower than the ones that Bond gives, with no apparent explanation. The P_{80} value of 114 µm that should be used with 150 µm closing sieve seems to be a little high though.

During one 106 µm test for each material, sieve analysis was done for the mill over-size after each grinding cycle. Results for the Sieve analysis are shown in Figure 29, where D_{80} of the material is shown after each grinding cycle.

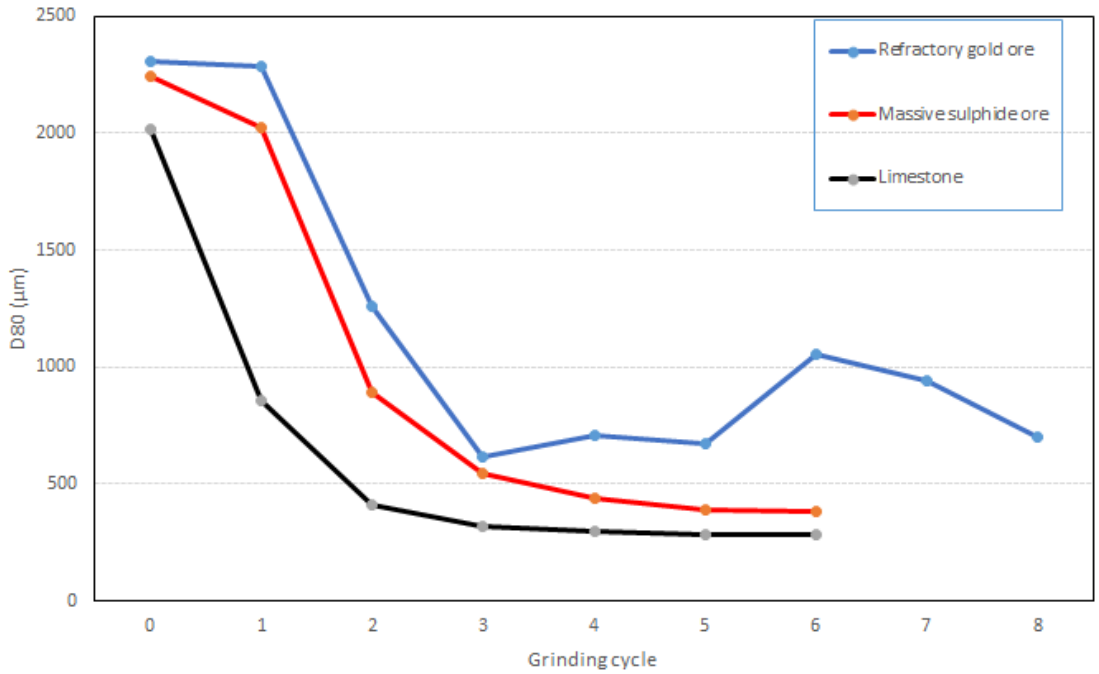

Figure 29. Measured D_{80} values for the Bond test sieve over-sizes.

From Figure 29 it can be seen that the easier the material is to grind, the faster the +106 µm material in the mill seems to reach a state of equilibrium. The refractory gold ore does show a noticeable spike in D_{80} after cycle 5, and doesn't seem to reach an equilibrium. During the test procedure nothing visibly different from normal happened.

The refractory gold ore, most resistant to grinding, seems to be more affected by the natural differences that occur during grinding cycles, which then affects G_{bp}. This causes fluctuations in the circulating load and number of revolutions required in the cycle, which then affects the results, as the G_{bp} value avoids reaching equilibrium. In the Bond tests, the RGO had significant troubles, at least when compared to the other two ores, in reaching the parameters set to consider the test finished, and every Bond test required more than 6 cycles.

This effect, along with the "overgrinding" that effects P_{80} should explain the relatively larger error in W_i values for the Bond tests for RGO. Other explanation for the spike in the D_{80} could be that once the material gets finer, a larger portion of the material passes the sieve. When fresh material is then added to the feed, it increases the D_{80} of the feed, and as the material is very resistant to grinding, the G_{bp} lowers again, causing a sort of oscillation effect in the D_{80}. Also it should be mentioned that the F_{80} value was calculated for the whole ore sample used in the testwork after blending, and even though the material could be divided into representative samples of less than 10 g, there might be tiny changes in the fineness of the fresh unsegregated feed, that then affect the grindability.

It was also noted, that the Work indices in almost all cases showed noticeable difference when the closing sieve size was changed. This shows that the material is not homogenous to grinding when ground to different size. The only exception is yet again the refractory gold ore, where the W_i when ground to pass 150 µm sieve seems to be the average of when ground to pass 106 µm sieve. This strongly indicates that the Bond Work index is not a material specific constant, but that it changes depending on the size the product is ground to. It seems natural that when the material is ground to a finer size, more energy is consumed in the process.

As said before, the test procedure for the 75 µm tests was different from the others, where sieving was done with the Sweco sieve. The results with this sieving method give some promise for the usability of this method, but the material losses during sieving cycles, along with the fact that dry sieving below 106 µm is far from the optimal method, make the results questionable. Especially when considering the difficulties dry sieving presents when material is this fine, an assumption can be made that the P_{80} value should be higher than the results of the sieving shows. If the P_{80} value actually is higher than what was determined based on particle size analysis, the work index values should then increase as well. If these assumptions are correct, the Bond tests where 75µm sieve closing size was used give questionable results.

Table 9 shows that the maximum of 0.5% material losses during sieving cycles was not achieved with the Sweco sieving method. This is especially noticeable during the first

cycles, and whenever the sieve was removed for washing. This can be explained by the fact that the Sweco sieve, even when properly set up, is not compact enough for the sieving until the fine material blocks all the seams of the sieve. So the results, although seemingly useful, contain more errors and aren't as reliable as the other Bond tests done during this thesis. This shows really well that the Bond test is quite limited when going to finer sieve sizes, when dry sieving is used.

Table 9. Percentage of material losses during 75 µm sieving.

	Refractory gold ore	Massive sulphide ore	Limestone
Cycle 1	4,3	7,4	1,7
Cycle 2	0,7	0,0	1,0
Cycle 3	0,9	0,5	0,6
Cycle 4	0,9	0,9	0,6
Cycle 5	2,4	1,4	0,8
Cycle 6	0,7	0,5	0,7
Cycle 7	0,6		

6.2 Mergan tests

The results of the nine Mergan tests are shown Table 10. The table shows the M-W_i calculated based on the data from the torque meter, along with P_{80} acquired from particle size analysis, and number of total mill revolutions. The aim of the Mergan tests was to grind the material so that $P_{80} < 150$ µm. Also, RGO was ground for same number of mill revolutions for each test to ensure reproducibility of the tests.

Table 10. The results of the Mergan tests

	Refractory gold ore			Massive sulphide ore			Limestone		
	M-Wi (kWh/t)	**P80 (µm)**	**Revolutions**	**M-Wi (kWh/t)**	**P80 (µm)**	**Revolutions**	**M-Wi (kWh/t)**	**P80 (µm)**	**Revolutions**
Test 1	14,63	115	1500	10,98	138	1500	6,88	141	600
Test 2	14,02	112	1500	10,38	97	1700	7,05	119	700
Test 3	13,99	113	1500	10,03	101	1600	7,28	123	700

Again, first thing that was analyzed from the results is the reproducibility of the tests. For RGO, three different tests were done with the same number of total mill revolutions. The difference in calculated M-W_i values between the lowest and highest value is 4.6%, which indicates good reproducibility. The error in the three tests can be explained by the minute difference in the testwork. The first test for each material was always done in cycles. For RGO, the first grinding cycle was 100 total revolutions, second 500 total revolutions, third 1000 total revolutions and finally 1500 total revolutions on the fourth cycle. After each grinding cycle, the mill was emptied and the material was sieved. These sieving cycles could have tiny losses in sample material or the pulp density might change a little bit due to weighing errors, which would affect the torque of the mill and thus the work index. Other explanation is the aforementioned possibility of small differences in the feed.

One rather interesting aspect of the results shown in Table 10 is that for massive sulphide ore, the highest M-W_i value was gained on the test where the material was ground to the coarsest size. From equation (10) it can be seen that when P_{80} lowers, the M-W_i also lowers, if other parameters in the equation remain the same. One explanation could be that even though all the sample material was blended, material used for test one could have been a little more resistant to grinding, thus increasing the P_{80} and W_i value. Another explanation could be the aforementioned difference in the first test, which was done in cycles to gain the grindability of the material, or some other small changes that affected the tests.

The prediction method used after particle size analysis for each grinding cycle can be seen in Figure 30, where 106 µm sieve passing% is plotted against total mill revolutions in the test.

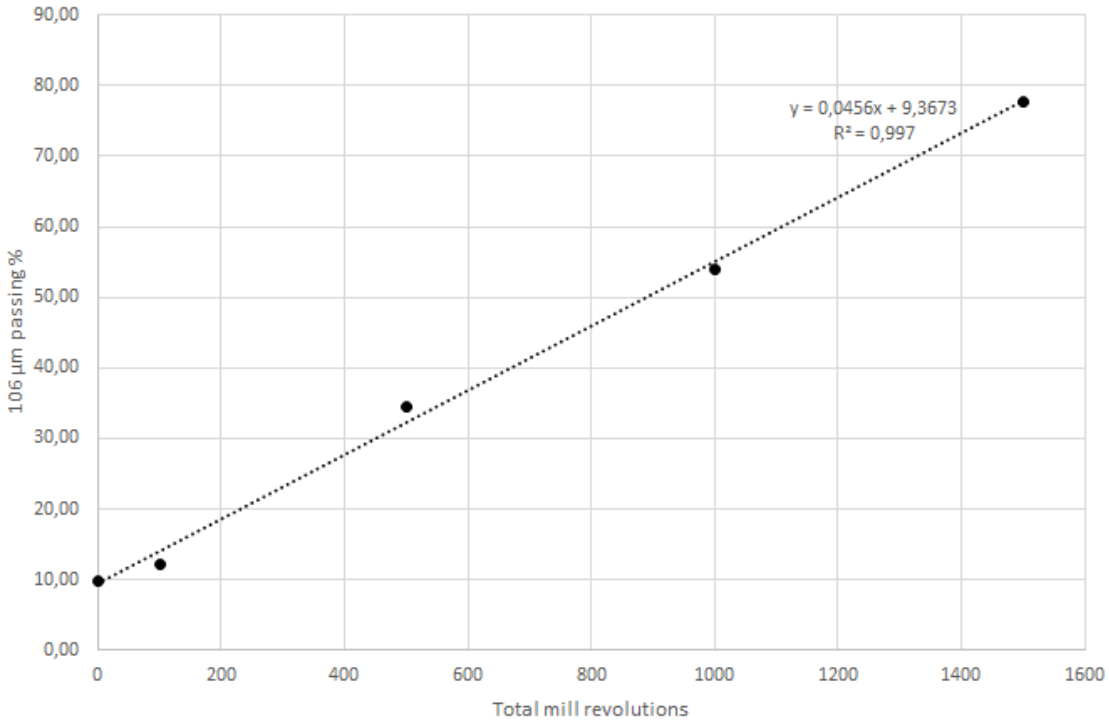

Figure 30. Refractory gold ore Mergan test 1 particle size analysis after each grinding cycle used to predict grindability in the Mergan mill.

Figure 30 shows that total number of mill revolutions is directly proportional to the 106 µm passing%. When a trendline is added between the points, it can be seen, that when ground to this fineness, the grindability of the material acts very much like a line, and this line can be used to predict the grindability of the material after each grinding cycle. Thus it can also be said, that the ball mill charge, and thus grindability seems to be at an optimum conditions in the Mergan mill when material is ground to this fineness, as no significant decrease or increase between the points can be seen. The same effect could also be observed with the other 2 sample materials used.

6.3 Comparison between Bond tests and Mergan tests

The Mergan test and Bond test are quite different. First of all, the mills are of different size, however, the size difference between the two is proportionate and quite small. The Bond test is locked cycle test, and the Mergan is a batch test. The mill rotation speed, as percentage of the critical mill speed, is different. Also, the Mergan mill, even though smaller in proportions, uses larger ball charge, both in terms of mass and volume. The amount of material ground in the mills is also vastly different. The Mergan test is done wet, and Bond test is done dry. In Bond test the P_{80} is calculated for the sieve under-size, meanwhile in the Mergan test the P_{80} value is calculated for the whole test material batch.

It should be noted that both the Bond mill and Mergan mill have been tested extensively by their creators to find the optimum operating conditions for the mill, so one could assume that the most notable difference between the two is the fact that that Bond test is done dry, and the Mergan test is done wet. It should be noted that since the Mergan test is done in wet conditions, sieving proved to be a lot more flexible with the Mergan method, and as such, the Mergan method could be a lot more usable when ground to finer sizes than what can be analyzed with dry sieving.

Table 11 shows the comparison of the three M-W_i values acquired against the average W_i acquired from the Bond tests when 106 µm sieve was used. The Bond test average is used because of the fact that the Bond test results have a small error margin, and based on only three Bond test results it would be safe to assume that the average of those three tests is the closest to the real Bond work index value. The material in this comparison is the refractory gold ore.

Table 11. Comparison of the W_i values and M-W_i values for the refractory gold ore.

	Wi (kWh/t)	Sieve opening (µm)	M-Wi (kWh/t)	P80 (µm)	Difference (%)
Test 1	19,29	106	14,63	115	31,85
Test 2	19,29	106	14,02	112	37,59
Test 3	19,29	106	13,99	113	37,88

There is some sort of correlation between the two work indices. The correlation coefficient value 1.3 from chapter 4.4 is not too far off, but still doesn't seem very satisfactory. Table 12 shows the results of the rest of the materials, and comparison is done to the Bond test where sieve opening is closest to the P_{80} value gained from the Mergan tests.

Table 12. Comparison of the W_i values and M-W_i values

		Wi (kWh/t)	Sieve opening (µm)	M-Wi (kWh/t)	P80 (µm)	Difference (%)
Refractory gold ore	**Test 1**	19,29	106	14,63	115	31,85
	Test 2	19,29	106	14,02	112	37,59
	Test 3	19,29	106	13,99	113	37,88
Massive sulphide ore	**Test 1**	13,99	150	10,98	138	27,41
	Test 2	14,68	106	10,38	97	41,43
	Test 3	14,68	106	10,03	101	46,36
Limestone	**Test 1**	9,21	150	6,88	141	33,87
	Test 2	10,21	106	7,05	119	44,82
	Test 3	10,21	106	7,28	123	40,25

From Table 12 it is even more visible that there is some sort of correlation between the two tests, but can't be explained by a single correlation coefficient. However, when the two Work indices are plotted against each other, as is done in Figure 31, a more satisfactory model can be found.

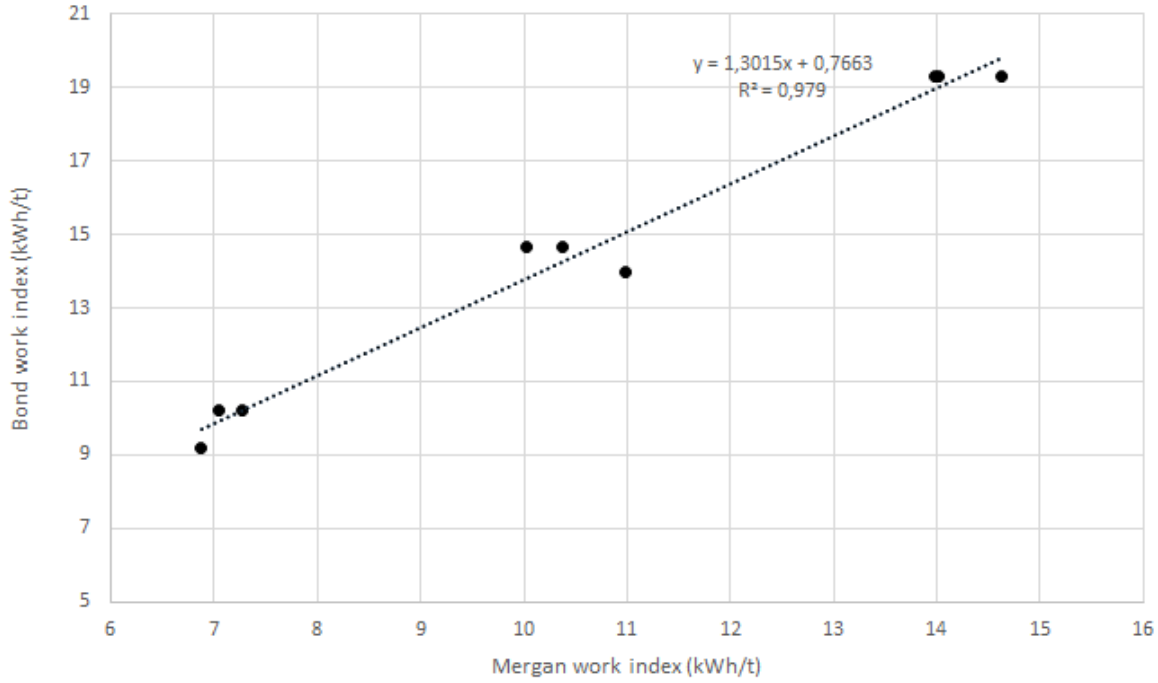

Figure 31. Comparison of the Bond work index values and Mergan work index values, with a linear model.

It can be seen from Figure 31 that there seems to be a linear correlation between the two work indices. A linear model was chosen as there wasn't much difference in the R^2 value even if the model was changed to, for example, power regression model. This is a result of the fact that there are only 9 test results for comparison, so further testwork should be conducted to enhance the model. Regression analysis was also done for the test results, but the analysis results didn't show anything further to note. However, if we take the model now to predict Bond work index from Mergan Work index, we get equation (33).

$$W_{i,MP} = 1{,}3015(M - W_i) + 0{,}7663 \tag{33}$$

where W_i,MP is Mergan predicted Bond work index [kWt/h]

M-W_i is Mergan work index [kWt/h]

Using Mergan work indices to calculate Mergan predicted work indices from equation (33), and comparing the Mergan predicted work indices to Bond work indices acquired from the experimental model, we get Table 13.

Table 13. Comparison of Mergan predicted work indices and Bond work indices.

		M-Wi (kWh/t)	Wi (kWh/t)	Wi,MP (kWh/t)	Error (%)
Refractory gold ore	**Test 1**	14,63	19,29	19,81	-2,61
	Test 2	14,02	19,29	19,01	1,46
	Test 3	13,99	19,29	18,97	1,66
Massive sulphide ore	**Test 1**	10,98	13,99	15,06	-7,08
	Test 2	10,38	14,68	14,28	2,83
	Test 3	10,03	14,68	13,82	6,22
Limestone	**Test 1**	6,88	9,21	9,72	-5,25
	Test 2	7,05	10,21	9,94	2,70
	Test 3	7,28	10,21	10,24	-0,30

Table 13 shows that for the 9 Mergan tests done during this thesis, the model presented in equation (33) can predict the Bond work index with a minimum error of 0.30%, and a maximum of 7.08%, with an average error of 3.35%. The presented experimental model shows good promise, if it can be believed, that the Mergan mill can indeed be used to predict the Bond work index for the material. The Work indices are further compared in Figure 32, where Mergan predicted work indices are plotted against the Bond work indices from testwork.

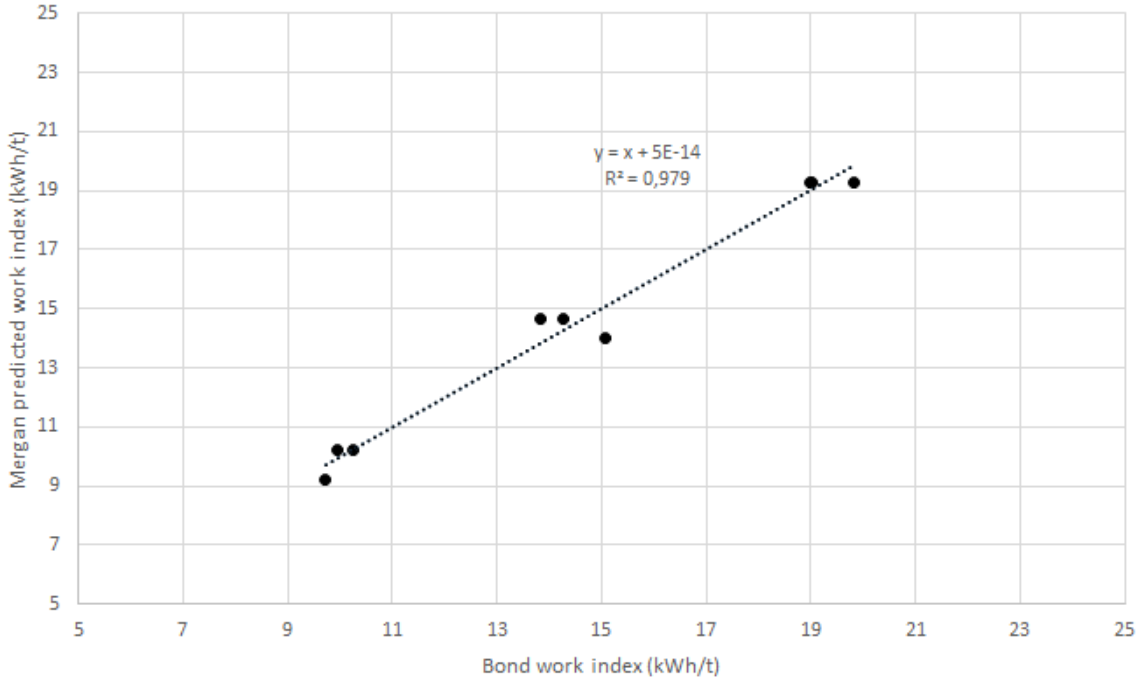

Figure 32. Comparison of Mergan predicted work indices and Bond work indices.

Going back and taking a look at Table 12 raises one question. Can this comparison be trusted? The P_{80} values from the Mergan tests aren't anywhere near the P_{80} values from the Bond tests. Comparison like this can be considered faulty, because the materials aren't ground to the same fineness, P_{80}, in both tests. However, Mergan test data can be normalized mathematically, if a couple of assumptions are made. If we assume that during the Mergan test, the grindability of the material per mill revolutions is a constant when going from F_{80} value to P_{80} of 75 µm, then the E_0 it would take to grind the material to P_{80} of 75 µm based on the test data can be calculated, and then the new M-W_i can be calculated using the new E_0 value and assuming that the P_{80} will be 75 µm. It should be noted that the Bond test P_{80} values for RGO were on average 69 µm, but the difference between 69 and 75 µm is small, and the normalization had to be done to the closest sieve size possible (75 µm).

This assumption was tested by calculating the mill revolutions it would require for the massive sulphide ore to be ground to P_{80} value of 75 µm. After that, one final Mergan test was conducted, and the results were that M-W_i was 10.46 kWh/t, and the P_{80} was 77 µm.

It was interesting to note that even though the E_0 value increased, the decrease in the P_{80} caused the Mergan work index to stay relatively the same when compared to the other tests. The minute error of 2 µm caused an error of 1.6% between the W_i values of the one calculated by normalization and the actual test data. Based on the test, it can be stated that the grindability for the massive sulphide ore is indeed a constant when ground to P_{80} of 75 µm. Due to time constraints, the tests couldn't be conducted to the refractory gold ore and the limestone to verify this, so the normalization of the data has to be based on the assumption that the grindability of the limestone and the refractory gold ore also is a constant when ground to P_{80} value of 75µm. While this assumption seems reasonable, since it could not be validated in the testwork, it must be taken with some uncertainty.

The normalized Mergan test data is shown in Table 14. The Mergan predicted Bond work index are also calculated in Table 14 and compared to the Bond work index averages when 106 µm sieve closing size was used.

Table 14. Comparison of the Mergan predicted work index values based on data normalization and Bond work index values from the testwork

		Normalized M-Wi (kWh/t)	P80 (µm)	Wi (kWh/t)	Wi,MP (kWh/t)	Error (%)
Refractory gold ore	**Test 1**	13,68	75	19,29	18,57	3,85
	Test 2	13,35	75	19,29	18,15	6,31
	Test 3	13,25	75	19,29	18,01	7,11
Massive sulphide ore	**Test 1**	9,80	75	14,68	13,52	8,62
	Test 2	10,25	75	14,68	14,11	4,06
	Test 3	10,26	75	14,68	14,12	3,95
	Test 4	10,46	77	14,68	14,38	2,09
Limestone	**Test 1**	7,01	75	10,21	9,89	3,21
	Test 2	6,89	75	10,21	9,74	4,83
	Test 3	6,98	75	10,21	9,86	3,60

From Table 14 it is visible that based on the normalized test data, the experimental model seems a little bit worse, with a maximum error of 8.62% and average error of 4.76%. The comparison this time however is to same product fineness, and as a result the comparison is be more reliable.

The normalized Mergan work index values are compared to the Bond work index values in Figure 33 to see if a better model can be based on the normalized Mergan work index values.

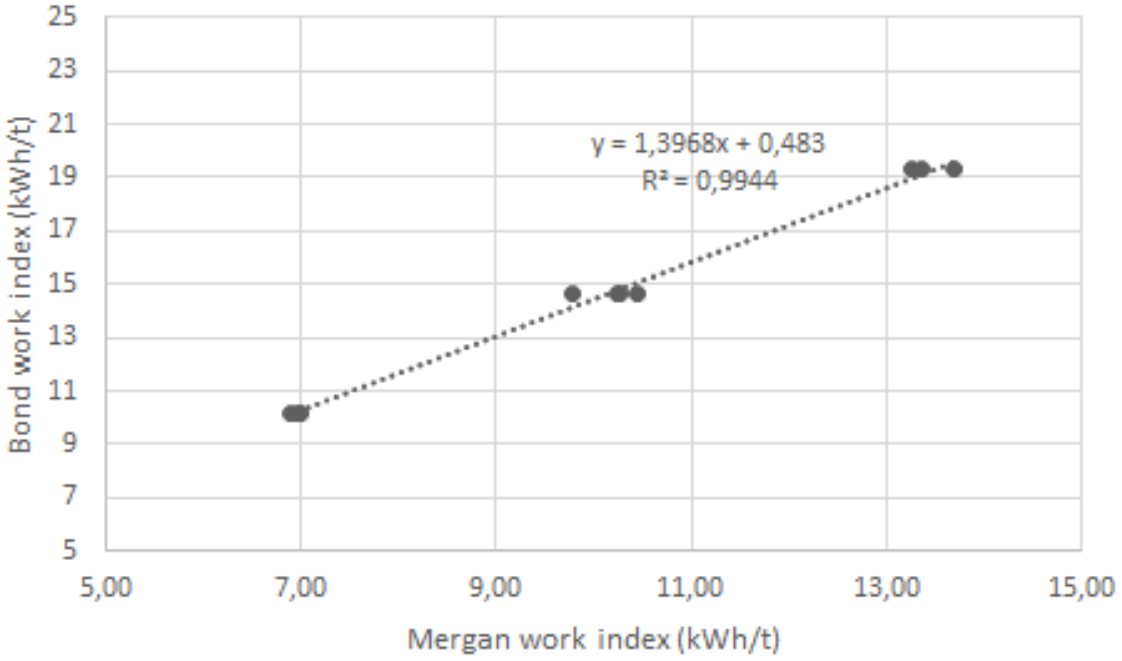

Figure 33. Comparison of the normalized Mergan work index values and the Bond work index values from the testwork.

We again get a new experimental equation (34) that seems to fit the data better. It is clear though that the equation is based only on 10 Mergan tests, and their comparison to the Bond test values, so it is in a sense forced to fit the test data.

$$W_{i,MP} = 1{,}3968(M - W_i) + 0{,}483 \tag{34}$$

Equation (34) is then again used in Table 15, where Mergan predicted Bond work index values are calculated and compared to the Bond work index values from the testwork. It

is visibly clear that the model from equation (34) seems to give better results, and is also based on a comparison that seems more reliable.

Table 15. Comparison of the normalized Mergan predicted work index values (eq. 34) and the Bond work index values from the testwork.

Normalized M-Wi (kWh/t)	Wi (kWh/t)	Wi,MP (kWh/t)	Error (%)
13,68	19,29	19,60	1,56
13,35	19,29	19,13	-0,81
13,25	19,29	18,99	-1,59
9,80	14,68	14,17	-3,63
10,25	14,68	14,80	0,81
10,26	14,68	14,82	0,92
10,46	14,68	15,09	2,73
7,01	10,21	10,28	0,65
6,89	10,21	10,11	-0,96
6,98	10,21	10,24	0,27

The model from equation (34) seems to fit the data very well. However, given that the small sample size that the data presents, and due to the fact that a model that seemed to fit the data well could be given when a questionable comparison was made to present equation (33), it is clear that in order to give a better model more test data is required. It should be also noted that because the data had to be mathematically normalized, small errors might be present in the normalized Mergan work index values, due to minor changes in E_0 values or differences of a few microns in the P_{80} value. In my opinion, to validate this method, up to tens or even hundreds of Mergan tests should be conducted and compared to Bond work index values, using different materials. Only then it can be seen if the model is satisfactory across a scale of different materials, and not only fit to the low amount of test data.

However, based on all of the test data in this thesis, it is safe to assume that the Mergan test can be used to predict Bond work index values. Niitti (1970) compared W_{74} values of Mergan mill and wet industrial grinding process, where he found that the industrial process had a W_{74} value of approximately 1.33 times larger than the Mergan mill (Niitti,

1970). The results from the testwork seem to correlate with this data as well. Kurki (2006) also compared Mergan and Bond tests for two ore samples to their grinding circuits, and found out that the Mergan work index values were approximately 13% and 30% lower than the Bond work index values (Kurki, 2006).

It is also clear that one should be very careful when comparing grinding tests in terms of the fineness ground to. Grinding tests should only be compared when ground to same fineness value in both tests. This taught the author a very valuable lesson about testwork comparison.

7 CONCLUSIONS

The aim of the thesis was to improve the Mergan method so that it could be used to test grindability and scaled to Bond work index. Literature review of the thesis gave good insight on how this could be done, and the results from the tests proved that developing this method seems indeed possible.

Results from the tests show that the Bond and Mergan tests could be done with good reproducibility. In doing these tests and when analyzing the results, I gained good knowledge about conducting research, and very good insight on both of these grindability tests. Bond test results seem to indicate that even though the Bond work index should be a material specific constant, grinding material to a different size is not always homogenous in terms of energy consumption. The Bond test also showed that the material most resistant to grinding had troubles reaching an equilibrium in terms of product created per mill revolutions. The Sweco sieving method that was used in 75 µm sieving, while giving reasonable results, had too much material losses and gave a comparably small P_{80} value, thus making the results questionable.

Based on mineralogical data, Mohs hardness values for each ore sample was also approximated. Data from the grindability tests showed that the Mohs hardness values didn't correlate with resistance to grinding very well.

The results from the Mergan tests indicate 106 µm sieve passing% has a very good linear correlation with the total number of mill revolutions, at least when ground to fineness where P_{80} is about 106 µm. The Mergan method also proved to be quite fast when information about the grindability of the ore is already known, and proved to be quite flexible since wet sieving could be used.

Comparison of the two grindability test showed that there is a correlation between the two work indices, and regression analysis resulted in the creation of an experimental linear model, where Mergan work index could be used to predict the Bond work index with good correlation. However, it was noticed that the Mergan tests weren't done to the same

fineness as the Bond tests, and the Mergan test data had to be mathematically normalized. Based on the normalization a new comparison was done, and another experimental model is presented. A conclusion is made that based on the test data, the Mergan method can be used to predict Bond work index values, but to improve and validate the method, more testwork is required.

8 FUTURE TESTWORK

For future testwork, more tests with Mergan mill should be conducted and compared to Bond test values to enhance the experimental model, using different ore samples and different sieve closing sizes. Special attention needs to be paid to the fact that P_{80} values, or the fineness the ore sample is ground to, should be as close as possible to each other in both tests.

Although the mathematical normalization of Mergan work index values can be done like it was done in this testwork, better way to do it is to slightly overgrind the material in the Mergan mill, and then do the normalization backwards. This way the normalization is not based on assumptions, but rather backed up with actual test data.

Also one should be very careful not to mix grinding energy consumption (E_0) and work index values with one another, even though both are expressed as kWh/t, they mean different things.

In terms of mineralogical information and geometallurgy, a good idea for future testing would be to test if mineralogical data can be used better to approximate grindability of an ore.

9 REFERENCES

Bbosa, L. S., Govender, I., Mainza, A. N. & Powell, M. S., 2011. Power draw estimation in experimental tumbling mills using PEPT. *Minerals Engineering,* Volume 24, pp. 319-324.

Bond, F. C., 1961a. Crushing and grinding calculations, part 1. *British Chemical Engineering,* 6(6), pp. 378-385.

Bond, F. C., 1961b. Crushing and grinding calculations, part 2. *British chemical engineering,* 6(8), pp. 543-548.

Burger, B. et al., 2006. *Batu Hijau Model for Throughput Forecast, Mining and Milling Optimisation and Expansion Studies.* [Online] Available at: http://www.metso.com/miningandconstruction/MaTobox7.nsf/DocsByID/15ADE568865ADF2EC2257DB700464EA1/$File/batu-hijau-throughput-forecast.pdf [Accessed 29 August 2017].

Cleary, P. W. & Morrison, R. D., 2016. Comminution mechanisms, particle shape evolution and collision energy partitioning in tumbling mills. *Minerals Engineering,* Volume 86, pp. 75-95.

Fuerstenau, M. C. & Han, K. N., 2003. *Principles of Mineral Processing.* Littleton, Colorado: Society for Mining, Metallurgy, and Exploration, Inc..

Gupta, A. & Yan, D. S., 2006. *Mineral Processing Design and Operation: An Introduction.* Amsterdam: Burlington Elsevier Science.

Hukki, R. T., 1964. *Mineraalien hienonnus ja rikastus.* s.l.:Hki: Teknillisten tieteiden akatemia.

Karra, R. C., Subodh, N. H. & Ashwin, J. B., 2016. Prediction of Bond's work index from field measurable rock properties. *International Journal of Mineral Processing,* Volume 157, pp. 134-144.

Kurki, P., 2006. *Jauhautuvuuden määritys panos-jauhatuskokeilla.* s.l.:Helsingin teknillinen korkeakoulu.

Lamberg, P., 2011. *Particles - the bridge between geology and metallurgy.* Luleå, Sweden, Conference in mineral engineering.

Lynch, A. J., 2015. *Comminution handbook.* Carlton, Victoria: Australian Institute of Mining and Metallurgy.

Magdalinović, N., 1989. A Procedure for Rapid Determination of the Bond Work Index. *International Journal of Mineral Processing,* 27(1-2), pp. 125-132.

Morrell, S., 2004. An alternative energy-size relationship to that proposed by Bond for the design and optimisation of grinding circuits. *International Journal of Mineral Processing,* 74(1-4), pp. 133-141.

Mwanga, A., Rosenkranz, J. & Lamberg, P., 2017. Development and experimental validation of the Geometallurgical Comminution Test (GCT). *Minerals Engineering,* Volume 108, pp. 109-114.

Mörsky, P., Klementti, M. & Knuutinen, T., 1995. *A Comparison of High Pressure Roller Mill and Conventional Grinding.* San Francisco, Society for Mining, Metallurgy, and Exploration, Inc..

Nematollahi, H., 1994. New size laboratory ball mill for Bond work index determination. *Mining Engineering,* 46(4), pp. 352-353.

Niitti, T., 1970. *Rapid evaluation of grindability by a simple batch test.* Praha, Proceedings of IX IMPC.

Norazirah, A., Fuad, S. & Hazizan, M., 2016. The Effect of Size and Shape on Breakage Characteristics of Mineral. *Procedia Chemistry,* Volume 19, pp. 702-708.

Rose, H. E. & Sullivan, R., 1958. *A Treatise on the internal mechanics of ball, tube and rod mills.* London: s.n.

Starkey, J. & Scinto, P., 2010. *SAG Mill Grinding Design Versus Geometallurgy - Getting It Right For Competent Ores.* [Online] Available at: http://www.sagdesign.com/Papers_for_Website/Brisbane%20Paper.pdf [Accessed 28 August 2017].

Steiner, H. J., 1996. Characterization of laboratory-scale tumbling mills. *International Journal of Mineral Processing,* Volume 44-45, pp. 373-382.

Tüzün, M. A., 2001. Wet bond mill test. *Minerals Engineering,* 14(3), pp. 369-373.

Walters, S. G., 2008. An overview of new integrated geometallurgical research. *Australian Institute of Mining and Metallurgy Publication Series,* pp. 79-82.

Wills, B. A. & Finch, J., 2015. *Wills Mineral Processing Technology.* 8th ed. Burlington: Butterworth-Heinemann.

Zhitie, Z., 1995. *Catastrophe Theory and Dissipative Structure in Mineral Comminution.* San Francisco, Society for Mining, Metallurgy, and Exploration, Inc..

10 APPENDICES

Appendix 1-5. RGO Bond tests

Appendix 6-10. MSO Bond tests

Appendix 11-15. Limestone Bond tests

Appendix 16. RGO Mergan test data

Appendix 17-18. MSO Mergan test data

Appendix 19. Limestone Mergan test data

Appendix 20. RGO and MSO XRD results

Appendix 21. Limestone XRD results

Appendix 22. Mineralogy and hardness calculations

Appendix 23. RGO optical microscope pictures

Appendix 24. MSO optical microscope pictures

Appendix 25. Limestone optical microscope pictures

Appendix 1. RGO Bond test, 106µm

Jauhettava materiaali:	RGO
Koe:	19.4.2017

Jauhatuspanos, g	1283,3
Hienoainesta, %	9,8
Kiertokuorma, g	366,7
Katkaisuseula, µm	106
Aloituskierrokset	100

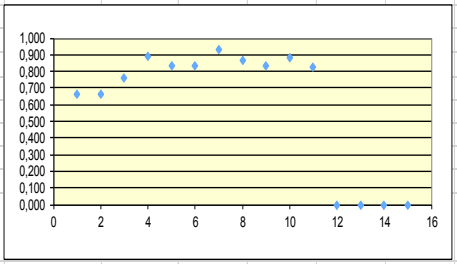

Kierros	Karkeaa g	Hienoa g	Hävikki g	Täydennys g	Jossa hienoa,g	Tuotettu hienoa,g	Hienoa/ myllyn kierros,g	Tuotettava hienoa,g	Tarvittavat seuraavat kierrokset	Kierto-kuorma,%	Hävikki, %:a syötteestä	Suunta
1	1091,9	188,7	2,7	191,4	18,7	66,2	0,662	348,0	526	570	0,2	
2	917,1	362	4,2	366,2	35,7	347,5	0,661	330,9	501	250	0,3	
3	869	410,4	3,9	414,3	40,4	378,6	0,756	326,2	431	210	0,3	
4	857,2	422,9	3,2	426,1	41,6	385,7	0,894	325,1	364	201	0,2	
5	937,5	342,2	3,6	345,8	33,7	304,2	0,837	332,9	398	271	0,3	
6	919,4	356	7,9	363,9	35,5	330,2	0,830	331,2	399	253	0,6	
7	877,9	402,8	2,6	405,4	39,5	369,9	0,927	327,1	353	217	0,2	
8	937,9	342,8	2,6	345,4	33,7	305,9	0,867	333,0	384	272	0,2	
9	928,8	344,4	10,1	354,5	34,6	320,8	0,835	332,1	398	262	0,8	
10	897,4	383,8	2,1	385,9	37,6	351,3	0,883	329,0	372	233	0,2	
11	938,8	341,4	3,1	344,5	33,6	306,9	0,824	333,0	404	273	0,2	
12												
13												
14												
15												

Gbp=	**0,848**	g/ kierros		**Syöte d80 =** **2304 µm**
Keskihaj.	**0,026**		*** VALMIS ***	**Tuote d80 =** **71 µm**
Keskihaj.	**3,0**	% keskiarvosta		**Wi=19,74 kWh/t**
Gbp min	0,8240			
Gbp max	0,8835			
max/min	**7,2208**			

Syöte: Raekoko,µm	Seulalle jäi, g		Kumulat. summa,g	Läpäisy,% Syöte	Tuote: Raekoko,µm	Seulalle jäi g	Kumulat. massa,g	Raeluokan massa,g	Läpäisy, Tuote	Raeluokan osuus,%
3350	0			100	106	0	0,0	0,0	100,0	0,0
2360	109,2	17,90	17,90	82,10	90	1,1	1,1	1,1	94,7	5,3
1700	151,7	24,87	42,78	57,22	75	2,5	3,6	2,5	82,7	12,0
1180	94,8	15,54	58,32	41,68	53	3,5	7,1	3,5	65,9	16,8
850	50	8,20	66,52	33,48	45	1,2	8,3	1,2	60,1	5,8
600	42,1	6,90	73,42	26,58	-45	12,5	20,8	12,5	0,0	60,1
425	31,2	5,12	78,54	21,46			20,8	0,0		0,0
300	26,7	4,38	82,92	17,08			**Yhteensä**	**20,8**		**100,0**
212	19	3,12	86,03	13,97						
150	16,6	2,72	88,75	11,25						
106	9,1	1,49	90,24	9,76						
75	11,1	1,82	92,06	7,94						
Pan	48,4	7,94	100,00							
	609,9	100,00								

Index (S)	x	y	X80, µm
1	75	82,7	**71**
2	53	65,9	

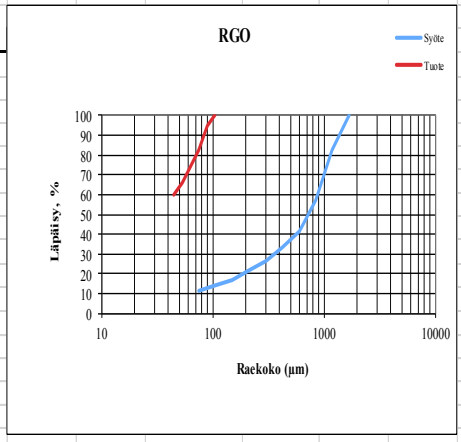

Huom! alkupunnituksesta kamaa +0,5g!!!!!

Index (S)	x	y	X80, µm
1	2360	82,1	**2304**
2	1700	57,2	

Wi	**19,740**

Appendix 2. RGO Bond test, 106µm

Jauhettava materiaali:	RGO
Koe:	3.5.2017

Jauhatuspanos, g	1283,3
Hienoainesta, %	9,8
Kiertokuorma, g	366,7
Katkaisuseula, µm	106
Aloituskierrokset	100

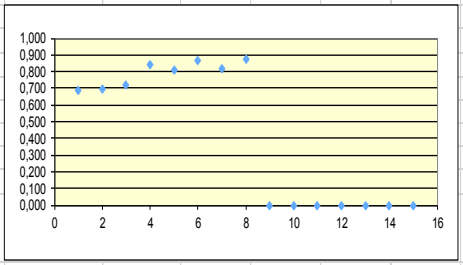

Kierros	Karkeaa g	Hienoa g	Hävikki g	Täydennys g	Jossa hienoa,g	Tuotettu hienoa,g	Hienoa/ myllyn kierros,g	Tuotettava hienoa,g	Tarvittavat seuraavat kierrokset	Kierto-kuorma,%	Hävikki, %:a syötteestä	Suunta
1	1089,8	190,6	2,9	193,5	18,9	68,3	0,683	347,8	509	563	0,2	
2	910	371	2,3	373,3	36,4	354,4	0,696	330,2	474	244	0,2	
3	904,9	375,9	2,5	378,4	36,9	342,0	0,721	329,7	457	239	0,2	
4	860,9	420,5	1,9	422,4	41,2	385,5	0,843	325,4	386	204	0,1	
5	931,1	349,5	2,7	352,2	34,4	311,0	0,805	332,3	413	264	0,2	
6	890,8	388,9	3,6	392,5	38,3	358,1	0,868	328,4	378	227	0,3	
7	936	343	4,3	347,3	33,9	309,0	0,817	332,8	407	270	0,3	
8	894,7	384,9	3,7	388,6	37,9	354,7	0,871	328,7	378	230	0,3	
9												
10												
11												
12												
13												
14												
15												

Gbp=	**0,852**	g/ kierros	
Keskihaj.	**0,025**		*** VALMIS ***
Keskihaj.	**2,9**	% keskiarvosta	
Gbp min	0,8167		
Gbp max	0,8706		
max/min	6,5939		

Syöte d80 =	**2304 µm**
Tuote d80 =	**69 µm**
Wi=19,32 kWh/t	

Syöte: Raekoko,µm	Seulalle jäi, g		Kumulat. summa,g	Läpäisy,% Syöte	Tuote: Raekoko,µm	Seulalle jäi g	Kumulat. massa,g	Raeluokan massa,g	Läpäisy, Tuote	Raeluokan osuus,%
3350				100	106	0	0,0	0,0	100,0	0,0
2360	109,2	17,90	17,90	82,10	90	0,7	0,7	0,7	96,8	3,2
1700	151,7	24,87	42,78	57,22	75	2,8	3,5	2,8	84,2	12,6
1180	94,8	15,54	58,32	41,68	53	3,7	7,2	3,7	67,6	16,7
850	50	8,20	66,52	33,48	45	1,5	8,7	1,5	60,8	6,8
600	42,1	6,90	73,42	26,58	-45	13,5	22,2	13,5	0,0	60,8
425	31,2	5,12	78,54	21,46			22,2	0,0		0,0
300	26,7	4,38	82,92	17,08			**Yhteensä**	**22,2**		**100,0**
212	19	3,12	86,03	13,97						
150	16,6	2,72	88,75	11,25						
106	9,1	1,49	90,24	9,76						
75	11,1	1,82	92,06	7,94						
Pan	48,4	7,94	100,00							
	609,9	100,00								

Index (S)	x	y	X80, µm
1	75	84,2	**69**
2	53	67,6	

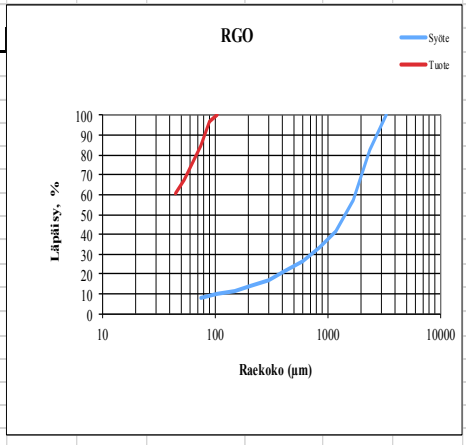

Huom! alkupunnituksesta kamaa +0,5g!!!!!

Index (S)	x	y	X80, µm
1	2360	82,1	**2304**
2	1700	57,2	

Wi	**19,319**

Appendix 3. RGO Bond test, 106µm

Jauhettava materiaali:	RGO
Koe:	26.7.2017

Jauhatuspanos, g	1283,3
Hienoainesta, %	9,8
Kiertokuorma, g	366,7
Katkaisuseula, µm	106
Aloituskierrokset	100

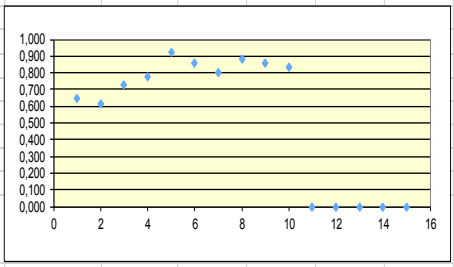

Kierros	Karkeaa g	Hienoa g	Hävikki g	Täydennys g	Jossa hienoa,g	Tuotettu hienoa,g	Hienoa/ myllyn kierros,g	Tuotettava hienoa,g	Tarvittavat seuraavat kierrokset	Kierto-kuorma,%	Hävikki, %:a syötteestä	Suunta
1	1093,1	188,2	2,0	190,2	18,6	65,0	0,650	348,1	535	575	0,2	
2	936,2	344,3	2,8	347,1	33,9	328,5	0,614	332,8	542	270	0,2	
3	855,5	424,3	3,5	427,8	41,7	393,9	0,726	324,9	447	200	0,3	
4	894,5	385,6	3,2	388,8	37,9	347,1	0,776	328,7	424	230	0,2	
5	855,8	424,1	3,4	427,5	41,7	389,6	0,919	325,0	353	200	0,3	
6	939,5	341,2	2,6	343,8	33,5	302,1	0,855	333,1	390	273	0,2	
7	936,5	344,6	2,2	346,8	33,8	313,3	0,804	332,8	414	270	0,2	
8	885	395,3	3,0	398,3	38,9	364,5	0,880	327,8	372	222	0,2	
9	924,2	353,1	6	359,1	35,0	320,2	0,860	331,6	386	257	0,5	
10	928	351,5	3,8	355,3	34,7	320,3	0,830	332,0	400	261	0,3	
11												
12												
13												
14												
15												

Gbp=	0,857	g/ kierros		Syöte d80 = 2304 µm
Keskihaj.	0,020		* VALMIS *	Tuote d80 = 67 µm
Keskihaj.	2,4	% keskiarvosta		Wi=18,81 kWh/t
Gbp min	0,8304			
Gbp max	0,8801			
max/min	5,9896			

Syöte: Raekoko,µm	Seulalle jäi, g		Kumulat. summa,g	Läpäisy,% Syöte	Tuote: Raekoko,µm	Seulalle jäi g	Kumulat. massa,g	Raeluokan massa,g	Läpäisy, Tuote	Raeluokan osuus,%
3350	0			100	106	0	0,0	0,0	100,0	0,0
2360	109,2	17,90	17,90	82,10	90	0,6	0,6	0,6	97,3	2,7
1700	151,7	24,87	42,78	57,22	75	2,4	3,0	2,4	86,4	10,9
1180	94,8	15,54	58,32	41,68	53	3,9	6,9	3,9	68,8	17,6
850	50	8,20	66,52	33,48	45	1,4	8,3	1,4	62,4	6,3
600	42,1	6,90	73,42	26,58	-45	13,8	22,1	13,8	0,0	62,4
425	31,2	5,12	78,54	21,46			22,1	0,0		0,0
300	26,7	4,38	82,92	17,08			Yhteensä	22,1		100,0
212	19	3,12	86,03	13,97						
150	16,6	2,72	88,75	11,25						
106	9,1	1,49	90,24	9,76						
75	11,1	1,82	92,06	7,94						
Pan	48,4	7,94	100,00							
	609,9	100,00								

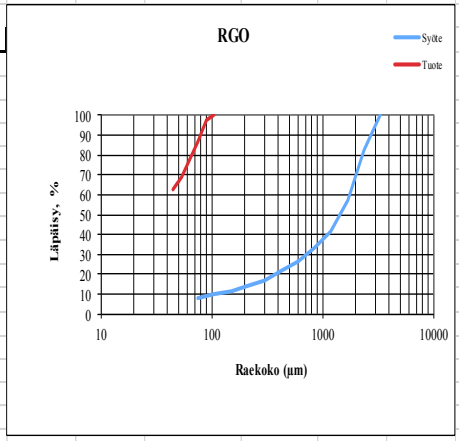

Index (S)	x	y	X80, µm
1	75	86,42533937	67
2	53	68,77828054	

Huom! alkupunnituksesta kamaa +0,5g!!!!!

Index (S)	x	y	X80, µm
1	2360	82,1	2304
2	1700	57,2	

Wi	18,815

Appendix 4. RGO Bond test, 150µm

Jauhettava materiaali:	RGO
Koe:	28.4.2017

Jauhatuspanos, g	1283,3
Hienoainesta, %	11,2
Kiertokuorma, g	366,7
Katkaisuseula, µm	150
Aloituskierrokset	100

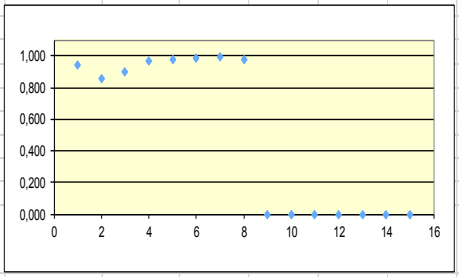

Kierros	Karkeaa g	Hienoa g	Hävikki g	Täydennys g	Jossa hienoa,g	Tuotettu hienoa,g	Hienoa/ myllyn kierros,g	Tuotettava hienoa,g	Tarvittavat seuraavat kierrokset	Kierto-kuorma,%	Hävikki, %:a syötteestä	Suunta
1	1045,2	235,3	2,8	238,1	26,8	93,8	0,938	339,9	363	439	0,2	
2	947,5	333,7	2,1	335,8	37,8	309,0	0,852	328,9	386	282	0,2	
3	897,8	382,2	3,3	385,5	43,4	347,7	0,901	323,3	359	233	0,3	
4	893,5	388,3	1,5	389,8	43,8	346,4	0,966	322,8	334	229	0,1	
5	912,8	369,1	1,4	370,5	41,7	326,7	0,977	325,0	333	246	0,1	
6	913,9	366,6	2,8	369,4	41,5	327,7	0,986	325,1	330	247	0,2	
7	914,9	366	2,4	368,4	41,4	326,9	0,991	325,2	328	248	0,2	
8	920,1	360	3,2	363,2	40,9	321,8	0,980	325,8	332	253	0,2	
9												
10												
11												
12												
13												
14												
15												

Gbp=	0,986	g/kierros		Syöte d80 = 2304 µm
Keskihaj.	0,004		* VALMIS *	Tuote d80 = 97 µm
Keskihaj.	0,4	% keskiarvosta		Wi=19,39 kWh/t
Gbp min	0,9803			
Gbp max	0,9908			
max/min	1,0744			

Syöte: Raekoko,µm	Seulalle jäi, g		Kumulat. summa,g	Läpäisy,% Syöte	Tuote: Raekoko,µm	Seulalle jäi g	Kumulat. massa,g	Raeluokan massa,g	Läpäisy, Tuote	Raeluokan osuus,%
3350				100	125	1,7	1,7	1,7	92,1	7,9
2360	109,2	17,90	17,90	82,10	106	1,4	3,1	1,4	85,5	6,5
1700	151,7	24,87	42,78	57,22	90	2	5,1	2,0	76,2	9,3
1180	94,8	15,54	58,32	41,68	75	1,9	7,0	1,9	67,3	8,9
850	50	8,20	66,52	33,48	53	3,1	10,1	3,1	52,8	14,5
600	42,1	6,90	73,42	26,58	45	0,6	10,7	0,6	50,0	2,8
425	31,2	5,12	78,54	21,46	-45	10,7	21,4	10,7		50,0
300	26,7	4,38	82,92	17,08			Yhteensä	21,4		100,0
212	19	3,12	86,03	13,97						
150	16,6	2,72	88,75	11,25						
106	9,1	1,49	90,24	9,76						
75	11,1	1,82	92,06	7,94						
Pan	48,4	7,94	100,00							
	609,9	100,00								

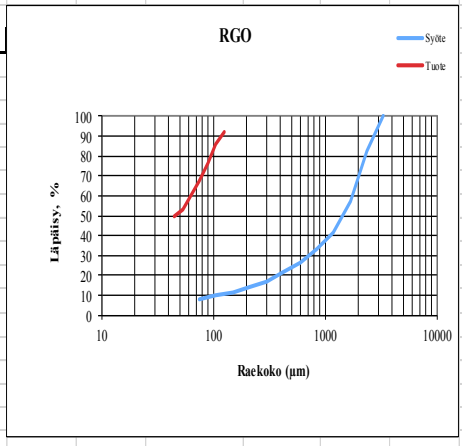

Index (S)	x	y	X80, µm
1	106	85,5	97
2	90	76,2	

Huom! alkupunnituksesta kamaa +0,5g!!!!!

Index (S)	x	y	X80, µm
1	2360	82,1	2304
2	1700	57,2	

Wi	19,389

Appendix 5. RGO Bond test, 75 µm

Jauhettava materiaali:	RGO
Koe:	20.7.2017

Jauhatuspanos, g	1283,3
Hienoainesta, %	7,9
Kiertokuorma, g	366,7
Katkaisuseula, µm	75
Aloituskierrokset	100

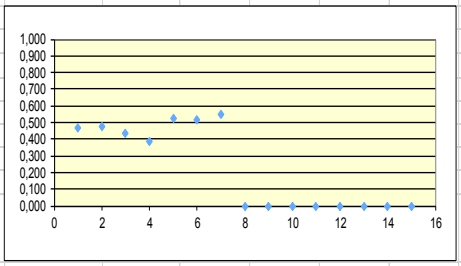

Kierros	Karkeaa g	Hienoa g	Hävikki g	Täydennys g	Jossa hienoa,g	Tuotettu hienoa,g	Hienoa/ myllyn kierros,g	Tuotettava hienoa,g	Tarvittavat seuraavat kierrokset	Kierto-kuorma,%	Hävikki, %:a syötteestä	Suunta
1	1134,5	93,3	55,5	148,8	11,8	47,0	0,470	354,8	756	762	4,3	
2	914,7	359,6	9,0	368,6	29,3	356,8	0,472	337,4	715	248	0,7	
3	945	327,1	11,2	338,3	26,8	309,0	0,432	339,8	786	279	0,9	
4	955,9	315,7	11,7	327,4	26,0	300,6	0,383	340,7	891	292	0,9	
5	790,6	462,5	30,2	492,7	39,1	466,7	0,524	327,6	625	160	2,4	
6	920,8	353,3	9,2	362,5	28,8	323,4	0,517	337,9	653	254	0,7	
7	898,1	378,1	7,1	385,2	30,6	356,4	0,546	336,1	616	233	0,6	
8												
9												
10												
11												
12												
13												
14												
15												

Gbp=	0,529	g/ kierros		Syöte d80 = 2304 µm
Keskihaj.	0,012		* VALMIS *	Tuote d80 = 33 µm
Keskihaj.	2,3	% keskiarvosta		Wi=20,02 kWh/t

Gbp min	0,5174
Gbp max	0,5458
max/min	5,4878

Syöte: Raekoko,µm	Seulalle jäi, g		Kumulat. summa,g	Läpäisy,% Syöte	Tuote: Raekoko,µm	Seulalle jäi g	Kumulat. massa,g	Raeluokan massa,g	Läpäisy, Tuote	Raeluokan osuus,%
3350	0			100			0,0	0,0	100,0	0,0
2360	109,2	17,90	17,90	82,10			0,0	0,0	100,0	0,0
1700	151,7	24,87	42,78	57,22	75	0	0,0	0,0	100,0	0,0
1180	94,8	15,54	58,32	41,68	45	0,7	0,7	0,7	96,1	3,9
850	50	8,20	66,52	33,48	38	0,9	1,6	0,9	91,0	5,1
600	42,1	6,90	73,42	26,58	20	7,1	8,7	7,1	51,1	39,9
425	31,2	5,12	78,54	21,46	-20	9,1	17,8	9,1		51,1
300	26,7	4,38	82,92	17,08			Yhteensä	17,8		100,0
212	19	3,12	86,03	13,97						
150	16,6	2,72	88,75	11,25						
106	9,1	1,49	90,24	9,76						
75	11,1	1,82	92,06	7,94						
Pan	48,4	7,94	100,00							
	609,9	100,00								

Index (S)	x	y	X80, µm
1	38	91,01123596	33
2	20	51,12359551	

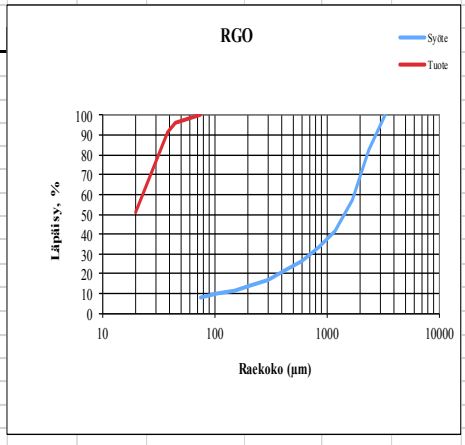

Huom! alkupunnituksesta kamaa +0,5g!!!!!

Index (S)	x	y	X80, µm
1	2360	82,1	2304
2	1700	57,2	

Wi	20,015

Appendix 6. MSO Bond test, 106 µm

Jauhettava materiaali:	MSO
Koe:	19.5.2017

Jauhatuspanos, g	1704,2
Hienoainesta, %	10,7
Kiertokuorma, g	486,9
Katkaisuseula, µm	106
Aloituskierrokset	100

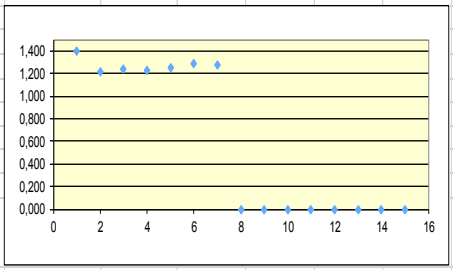

Kierros	Karkeaa g	Hienoa g	Hävikki g	Täydennys g	Jossa hienoa,g	Tuotettu hienoa,g	Hienoa/ myllyn kierros,g	Tuotettava hienoa,g	Tarvittavat seuraavat kierrokset	Kierto-kuorma,%	Hävikki, %:a syötteestä	Suunta
1	1382	318,6	3,6	322,2	34,5	139,6	1,396	452,4	324	429	0,2	
2	1276,1	425,7	2,4	428,1	45,9	393,6	1,214	441,0	363	298	0,1	
3	1208,9	490,5	4,8	495,3	53,1	449,4	1,237	433,8	351	244	0,3	
4	1221	480,5	2,7	483,2	51,8	430,1	1,227	435,1	355	253	0,2	
5	1208,4	492	3,8	495,8	53,1	444,0	1,252	433,8	347	244	0,2	
6	1205,2	496,1	2,9	499	53,5	445,9	1,287	433,4	337	242	0,2	
7	1220,7	479	4,5	483,5	51,8	430,0	1,276	435,1	341	252	0,3	
8												
9												
10												
11												
12												
13												
14												
15												

Gbp=	1,272 g/ kierros		Syöte d80 = 2244 µm
Keskihaj.	0,015	* VALMIS *	Tuote d80 = 75 µm
Keskihaj.	1,2 % keskiarvosta		Wi=14,62 kWh/t
Gbp min	1,2517		
Gbp max	1,2866		
max/min	2,7861		

Syöte: Raekoko,µm	Seulalle jää, g		Kumulat. summa,g	Läpäisy,% Syöte	Tuote: Raekoko,µm	Seulalle jää g	Kumulat. massa,g	Raeluokan massa,g	Läpäisy, Tuote	Raeluokan osuus,%
3350	0			100	106	0	0,0	0,0	100,0	0,0
2360	143,80	15,74	15,74	84,26	90	0,9	0,9	0,9	94,2	5,8
1700	220,80	24,17	39,91	60,09	75	2,2	3,1	2,2	80,0	14,2
1180	166,30	18,20	58,12	41,88	53	2,9	6,0	2,9	61,3	18,7
850	86,40	9,46	67,58	32,42	45	1,3	7,3	1,3	52,9	8,4
600	61,50	6,73	74,31	25,69	-45	8,2	15,5	8,2	0,0	52,9
425	42,10	4,61	78,92	21,08			15,5	0,0		0,0
300	33,90	3,71	82,63	17,37			Yhteensä	15,5		100,0
212	25,20	2,76	85,39	14,61						
150	24,00	2,63	88,01	11,99						
106	11,60	1,27	89,28	10,72						
75	20,20	2,21	91,49	8,51						
Pan	77,70	8,51	100,00							
	913,5	100,00								

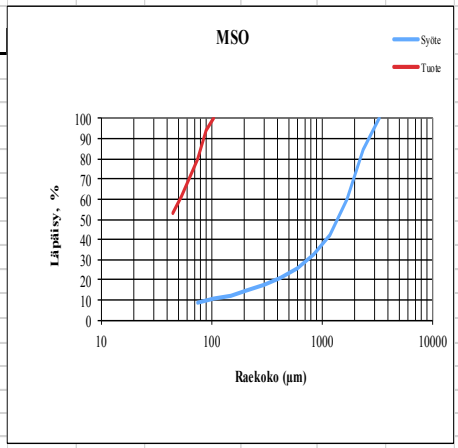

Index (S)	x	y	X80, µm
1	75	80	75
2			

Huom! alkupunnituksesta kamaa +0,5g!!!!!

Index (S)	x	y	X80, µm
1	2360	84,3	2244
2	1700	60,1	

Wi	14,619

Appendix 7. MSO Bond test, 106 µm

Jauhettava materiaali:	MSO
Koe:	24.5.2017

Jauhatuspanos, g	1704,2
Hienoainesta, %	10,7
Kiertokuorma, g	486,9
Katkaisuseula, µm	106
Aloituskierrokset	100

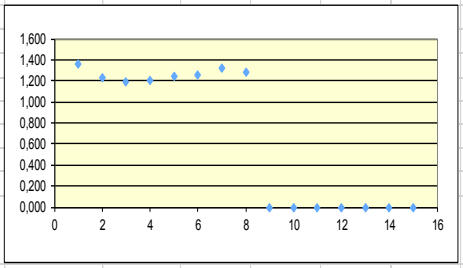

Kierros	Karkeaa g	Hienoa g	Hävikki g	Täydennys g	Jossa hienoa,g	Tuotettu hienoa,g	Hienoa/ myllyn kierros,g	Tuotettava hienoa,g	Tarvittavat seuraavat kierrokset	Kierto-kuorma,%	Hävikki, %:a syötteestä	Suunta
1	1385,6	314,1	4,5	318,6	34,1	136,0	1,360	452,8	333	435	0,3	
2	1261,7	437,7	4,8	442,5	47,4	408,4	1,226	439,5	358	285	0,3	
3	1232,2	468,3	3,7	472	50,6	424,6	1,185	436,3	368	261	0,2	
4	1211,2	490	3,0	493	52,8	442,4	1,201	434,1	361	246	0,2	
5	1204,1	496,9	3,2	500,1	53,6	447,3	1,238	433,3	350	241	0,2	
6	1209,4	491,6	3,2	494,8	53,0	441,2	1,260	433,9	344	244	0,2	
7	1197,9	502,8	3,5	506,3	54,3	453,3	1,316	432,7	329	237	0,2	
8	1228,6	471,8	3,8	475,6	51,0	421,3	1,282	435,9	340	258	0,2	
9												
10												
11												
12												
13												
14												
15												

Gbp=	1,286	g/ kierros		Syöte d80 = 2244 µm
Keskihaj.	0,023		* VALMIS *	Tuote d80 = 76 µm
Keskihaj.	1,8	% keskiarvosta		Wi=14,58 kWh/t
Gbp min	1,2602			
Gbp max	1,3165			
max/min	4,4679			

Syöte: Raekoko,µm	Seulalle jäi, g		Kumulat. summa,g	Läpäisy,% Syöte
3350	0			100
2360	143,8	15,74	15,74	84,26
1700	220,8	24,17	39,91	60,09
1180	166,3	18,20	58,12	41,88
850	86,4	9,46	67,58	32,42
600	61,5	6,73	74,31	25,69
425	42,1	4,61	78,92	21,08
300	33,9	3,71	82,63	17,37
212	25,2	2,76	85,39	14,61
150	24	2,63	88,01	11,99
106	11,6	1,27	89,28	10,72
75	20,2	2,21	91,49	8,51
Pan	77,7	8,51	100,00	
	913,5	100,00		

Tuote: Raekoko,µm	Seulalle jäi g	Kumulat. massa,g	Raeluokan massa,g	Läpäisy, Tuote	Raeluokan osuus,%
106		0,0	0,0	100,0	0,0
90	1	1,0	1,0	93,3	6,7
75	2,1	3,1	2,1	79,2	14,1
53	2,7	5,8	2,7	61,1	18,1
45	1,2	7,0	1,2	53,0	8,1
-45	7,9	14,9	7,9	0,0	53,0
		14,9	0,0		0,0
		Yhteensä	14,9		100,0

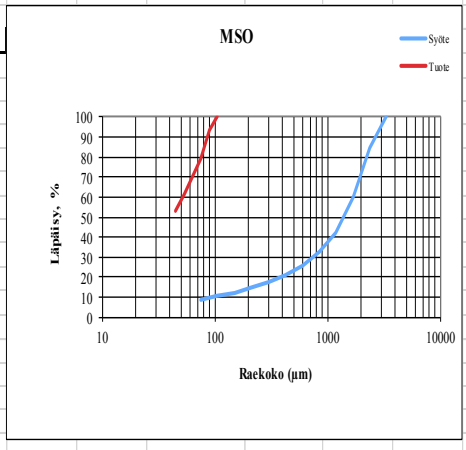

Index (S)	x	y	X80, µm
1	90	93,3	76
2	75	79,2	

Huom! alkupunnituksesta kamaa +0,5g!!!!!

Index (S)	x	y	X80, µm
1	2360	84,26	2244
2	1700	60,09	

Wi	14,583

Appendix 8. MSO Bond test, 106 µm

Jauhettava materiaali:	MSO
Koe:	2.8.2017

Jauhatuspanos, g	1704,2
Hienoainesta, %	10,7
Kiertokuorma, g	486,9
Katkaisuseula, µm	106
Aloituskierrokset	100

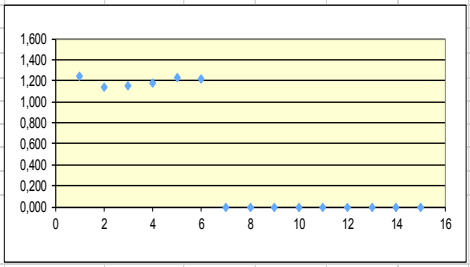

Kierros	Karkeaa g	Hienoa g	Hävikki g	Täydennys g	Jossa hienoa,g	Tuotettu hienoa,g	Hienoa/ myllyn kierros,g	Tuotettava hienoa,g	Tarvittavat seuraavat kierrokset	Kierto-kuorma,%	Hävikki, %:a syötteestä	Suunta
1	1397,4	303,6	3,2	306,8	32,9	124,2	1,242	454,0	366	455	0,2	
2	1254,1	446,6	3,5	450,1	48,2	417,2	1,141	438,7	384	279	0,2	
3	1214,2	488,6	1,4	490	52,5	441,8	1,149	434,4	378	248	0,1	
4	1204,3	498	1,9	499,9	53,6	447,4	1,183	433,3	366	241	0,1	
5	1198,4	501,8	4,0	505,8	54,2	452,2	1,235	432,7	350	237	0,2	
6	1223,7	478,1	2,4	480,5	51,5	426,3	1,217	435,4	358	255	0,1	
7												
8												
9												
10												
11												
12												
13												
14												
15												

Gbp=	1,212	g/kierros	* VALMIS *
Keskihaj.	0,021		
Keskihaj.	1,8	% keskiarvosta	
Gbp min	1,1833		
Gbp max	1,2349		
max/min	4,3582		

Syöte: Raekoko,µm	Seulalle jäi, g		Kumulat. summa,g	Läpäisy,% Syöte	Tuote: Raekoko,µm	Seulalle jäi g	Kumulat. massa,g	Raeluokan massa,g	Läpäisy, Tuote	Raeluokan osuus,%
3350	0			100	106	0	0,0	0,0	100,0	0,0
2360	143,8	15,74	15,74	84,26	90	0,7	0,7	0,7	95,6	4,4
1700	220,8	24,17	39,91	60,09	75	2,1	2,8	2,1	82,3	13,3
1180	166,3	18,20	58,12	41,88	53	2,6	5,4	2,6	65,8	16,5
850	86,4	9,46	67,58	32,42	45	1,1	6,5	1,1	58,9	7,0
600	61,5	6,73	74,31	25,69	-45	9,3	15,8	9,3	0,0	58,9
425	42,1	4,61	78,92	21,08			15,8	0,0		0,0
300	33,9	3,71	82,63	17,37			Yhteensä	15,8		100,0
212	25,2	2,76	85,39	14,61						
150	24	2,63	88,01	11,99						
106	11,6	1,27	89,28	10,72						
75	20,2	2,21	91,49	8,51						
Pan	77,7	8,51	100,00							
	913,5	100,00								

Index (S)	x	y	X80, µm
1	75	82,27848101	72
2	53	65,82278481	

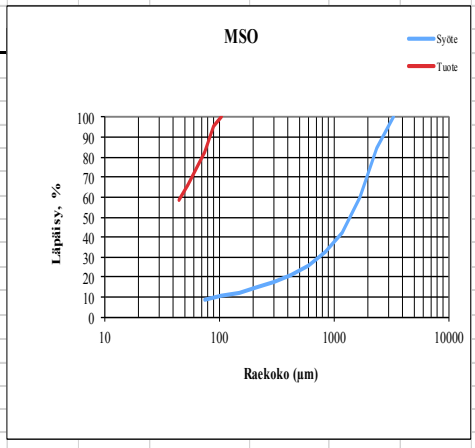

Huom! alkupunnituksesta kamaa +0,5g!!!!!

Index (S)	x	y	X80, µm
1	2360	84,3	2244
2	1700	60,1	

Wi	14,830

Appendix 9. MSO Bond test, 150 µm

Jauhettava materiaali:	MSO
Koe:	22.5.2017

Jauhatuspanos, g	1704,2
Hienoainesta, %	12,0
Kiertokuorma, g	486,9
Katkaisuseula, µm	150
Aloituskierrokset	100

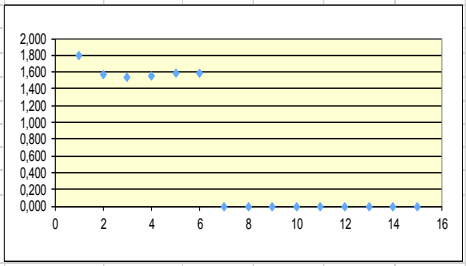

Kierros	Karkeaa g	Hienoa g	Hävikki g	Täydennys g	Jossa hienoa,g	Tuotettu hienoa,g	Hienoa/ myllyn kierros,g	Tuotettava hienoa,g	Tarvittavat seuraavat kierrokset	Kierto-kuorma,%	Hävikki, %:a syötteestä	Suunta
1	1320	381,4	2,8	384,2	46,1	179,9	1,799	440,9	245	344	0,2	
2	1273,2	427,9	3,1	431	51,7	384,9	1,571	435,3	277	295	0,2	
3	1228,7	471,4	4,1	475,5	57,0	423,8	1,530	429,9	281	258	0,2	
4	1212,6	488	3,6	491,6	58,9	434,6	1,546	428,0	277	247	0,2	
5	1206,5	494,2	3,5	497,7	59,7	438,8	1,585	427,3	269	242	0,2	
6	1219,1	481,9	3,2	485,1	58,1	425,4	1,579	428,8	272	251	0,2	
7												
8												
9												
10												
11												
12												
13												
14												
15												

Gbp=	1,570	g/ kierros		Syöte d80 = 2244 µm
Keskihaj.	0,017		* VALMIS *	Tuote d80 = 105 µm
Keskihaj.	1,1	% keskiarvosta		Wi= 13,99 kWh/t
Gbp min	1,5465			
Gbp max	1,5855			
max/min	2,5201			

Syöte: Raekoko,µm	Seulalle jäi, g		Kumulat. summa,g	Läpäisy,% Syöte	Tuote: Raekoko,µm	Seulalle jäi g	Kumulat. massa,g	Raeluokan massa,g	Läpäisy, Tuote	Raeluokan osuus,%
3350	0			100	150	0	0,0	0,0	100,0	0,0
2360	143,80	15,74	15,74	84,26	106	2,8	2,8	2,8	80,7	19,3
1700	220,80	24,17	39,91	60,09	90	1,3	4,1	1,3	71,7	9,0
1180	166,30	18,20	58,12	41,88	75	1,4	5,5	1,4	62,1	9,7
850	86,40	9,46	67,58	32,42	53	1,9	7,4	1,9	49,0	13,1
600	61,50	6,73	74,31	25,69	45	0,8	8,2	0,8	43,4	5,5
425	42,10	4,61	78,92	21,08	-45	6,3	14,5	6,3		43,4
300	33,90	3,71	82,63	17,37			Yhteensä	14,5		100,0
212	25,20	2,76	85,39	14,61						
150	24,00	2,63	88,01	11,99						
106	11,60	1,27	89,28	10,72						
75	20,20	2,21	91,49	8,51						
Pan	77,70	8,51	100,00							
	913,5	100,00								

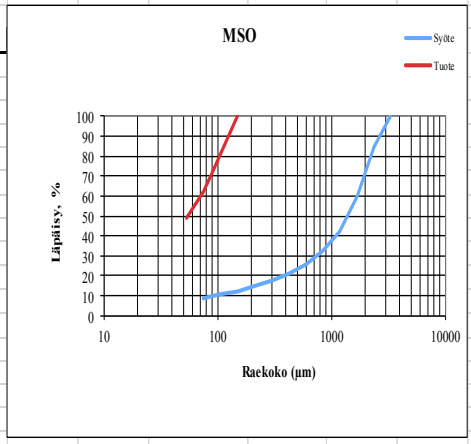

Index (S)	x	y	X80, µm
1	106	80,7	105
2	90	71,7	

Huom! alkupunnituksesta kamaa +0,5g!!!!!

Index (S)	x	y	X80, µm
1	2360	84,3	2244
2	1700	60,1	

Wi	13,986

Appendix 10. MSO Bond test, 75 µm

Jauhettava materiaali:	MSO
Koe:	24.5.2017

Jauhatuspanos, g	1704,2
Hienoainesta, %	8,5
Kiertokuorma, g	486,9
Katkaisuseula, µm	75
Aloituskierrokset	100

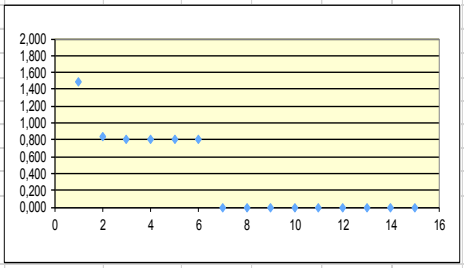

Kierros	Karkeaa g	Hienoa g	Hävikki g	Täydennys g	Jossa hienoa,g	Tuotettu hienoa,g	Hienoa/ myllyn kierros,g	Tuotettava hienoa,g	Tarvittavat seuraavat kierrokset	Kierto-kuorma,%	Hävikki, %:a syötteestä	Suunta
1	1410,6	167,4	126,2	293,6	25,0	148,6	1,486	461,9	311	480	7,4	
2	1419,7	283,7	0,8	284,5	24,2	259,5	0,835	462,7	554	499	0,0	
3	1237,6	457,3	9,3	466,6	39,7	442,4	0,798	447,2	560	265	0,5	
4	1214,9	474,7	14,6	489,3	41,6	449,6	0,803	445,3	555	248	0,9	
5	1220,2	460,5	23,5	484	41,2	442,4	0,797	445,7	559	252	1,4	
6	1211,6	484,1	8,5	492,6	41,9	451,4	0,808	445,0	551	246	0,5	
7												
8												
9												
10												
11												
12												
13												
14												
15												

Gbp=	0,803	g/ kierros		Syöte d80 = 2244 µm
Keskihaj.	0,004		* VALMIS *	Tuote d80 = 39 µm
Keskihaj.	0,5	% keskiarvosta		Wi= 15,74 kWh/t
Gbp min	0,7975			
Gbp max	0,8076			
max/min	1,2755			

Syöte: Raekoko,µm	Seulalle jäi, g	Seulalle jäi, %	Kumulat. summa,g	Läpäisy,% Syöte	Tuote: Raekoko,µm	Seulalle jäi g	Kumulat. massa,g	Raeluokan massa,g	Läpäisy, Tuote	Raeluokan osuus,%
3350	0,0	0,0	0	100			0,0	0,0	100,0	0,0
2360	143,8	15,7	15,74	84,3			0,0	0,0	100,0	0,0
1700	220,8	24,2	39,91	60,1	75	0	0,0	0,0	100,0	0,0
1180	166,3	18,2	58,12	41,9	45	1,7	1,7	1,7	88,0	12,0
850	86,4	9,5	67,58	32,4	38	1,4	3,1	1,4	78,2	9,9
600	61,5	6,7	74,31	25,7	-38	11,1	14,2	11,1	0,0	78,2
425	42,1	4,6	78,92	21,1			14,2	0,0		0,0
300	33,9	3,7	82,63	17,4			Yhteensä	14,2		100,0
212	25,2	2,8	85,39	14,6						
150	24	2,6	88,01	12,0						
106	11,6	1,3	89,28	10,7						
75	20,2	2,2	91,49	8,5						
Pan	77,7	8,5	100,00							
	913,5	100,0								

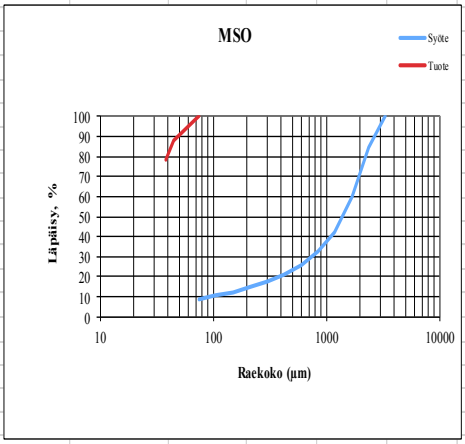

Index (S)	x	y	X80, µm
1	45	88	39
2	38	78,2	

Huom! alkupunnituksesta kamaa +0,5g!!!!!

Index (S)	x	y	X80, µm
1	2360	84,3	2244
2	1700	60,1	

Wi	15,736

Appendix 11. Limestone Bond test, 106 µm

Jauhettava materiaali:	Limestone
Koe:	10.7.2017

Jauhatuspanos, g	1244,1
Hienoainesta, %	12,5
Kiertokuorma, g	355,5
Katkaisuseula, µm	106
Aloituskierrokset	100

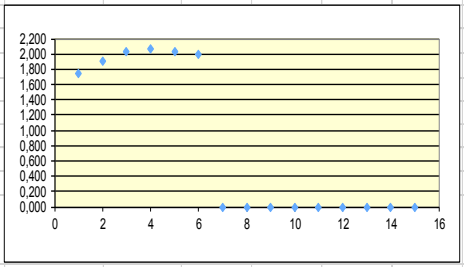

Kierros	Karkeaa g	Hienoa g	Hävikki g	Täydennys g	Jossa hienoa,g	Tuotettu hienoa,g	Hienoa/ myllyn kierros,g	Tuotettava hienoa,g	Tarvittavat seuraavat kierrokset	Kierto-kuorma,%	Hävikki, %:a syötteestä	Suunta
1	914,1	327,8	2,2	330	41,1	174,9	1,749	314,3	180	277	0,2	
2	860,1	380,4	3,6	384	47,9	342,9	1,908	307,6	161	224	0,3	
3	868,5	373,1	2,5	375,6	46,8	327,7	2,033	308,6	152	231	0,2	
4	883	358,5	2,6	361,1	45,0	314,3	2,070	310,4	150	245	0,2	
5	894,8	346,6	2,7	349,3	43,5	304,3	2,029	311,9	154	256	0,2	
6	894	348,2	1,9	350,1	43,6	306,6	1,994	311,8	156	255	0,2	
7												
8												
9												
10												
11												
12												
13												
14												
15												

Gbp=	2,031	g/ kierros		Syöte d80 =	2018 µm
Keskihaj.	0,031		* VALMIS *	Tuote d80 =	76 µm
Keskihaj.	1,5	% keskiarvosta		Wi=	10,19 kWh/t
Gbp min	1,9943				
Gbp max	2,0703				
max/min	3,8063				

Syöte: Raekoko,µm	Seulalle jäi, g		Kumulat. summa,g	Läpäisy,% Syöte	Tuote: Raekoko,µm	Seulalle jäi g	Kumulat. massa,g	Raeluokan massa,g	Läpäisy, Tuote	Raeluokan osuus,%
3350	0			100	106	0	0,0	0,0	100,0	0,0
2360	51,1	9,65	9,65	90,35	90	1,3	1,3	1,3	93,8	6,2
1700	105,8	19,98	29,63	70,37	75	3,2	4,5	3,2	78,7	15,2
1180	92,6	17,49	47,12	52,88	53	4,3	8,8	4,3	58,3	20,4
850	58,2	10,99	58,11	41,89	45	1,7	10,5	1,7	50,2	8,1
600	44,1	8,33	66,44	33,56	-45	10,6	21,1	10,6	0,0	50,2
425	32,2	6,08	72,52	27,48			21,1	0,0		0,0
300	27,7	5,23	77,75	22,25			Yhteensä	21,1		100,0
212	20,6	3,89	81,64	18,36						
150	19,9	3,76	85,40	14,60						
106	11,3	2,13	87,54	12,46						
75	15,6	2,95	90,48	9,52						
Pan	50,4	9,52	100,00							
	529,5	100,00								

Index (S)	x	y	X80, µm
1	90	93,8	76
2	75	78,7	

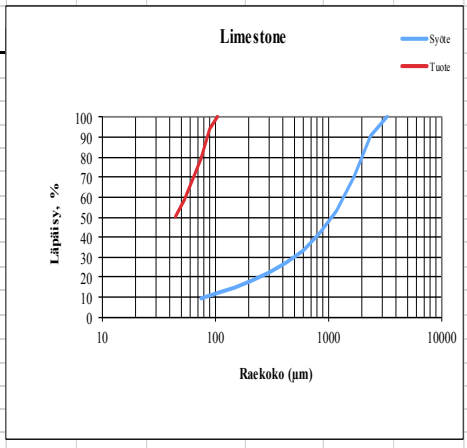

Huom! alkupunnituksesta kamaa +0,5g!!!!!

Index (S)	x	y	X80, µm
1	2360	90,3	2018
2	1700	70,4	

Wi	10,187

Appendix 12. Limestone Bond test, 106 µm

Jauhettava materiaali:	Limestone
Koe:	13.7.2017

Jauhatuspanos, g	1244,1
Hienoainesta, %	12,5
Kiertokuorma, g	355,5
Katkaisuseula, µm	106
Aloituskierrokset	100

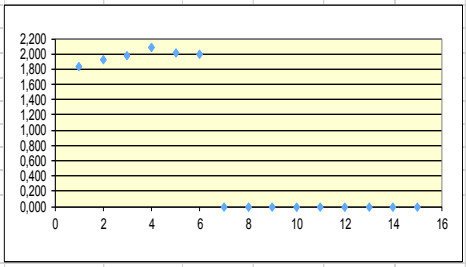

Kierros	Karkeaa g	Hienoa g	Hävikki g	Täydennys g	Jossa hienoa,g	Tuotettu hienoa,g	Hienoa/ myllyn kierros,g	Tuotettava hienoa,g	Tarvittavat seuraavat kierrokset	Kierto-kuorma,%	Hävikki, %:a syötteestä	Suunta
1	905,1	336,3	2,7	339	42,3	183,9	1,839	313,2	170	267	0,2	
2	874,5	368,1	1,5	369,6	46,1	327,3	1,922	309,4	161	237	0,1	
3	880,7	360,5	2,9	363,4	45,3	317,3	1,972	310,2	157	242	0,2	
4	871,6	370,3	2,2	372,5	46,4	327,2	2,080	309,0	149	234	0,2	
5	897,8	344,1	2,2	346,3	43,2	299,9	2,018	312,3	155	259	0,2	
6	893,3	348,2	2,6	350,8	43,7	307,6	1,988	311,7	157	255	0,2	
7												
8												
9												
10												
11												
12												
13												
14												
15												

Gbp=	2,029	g/ kierros		Syöte d80 = 2018 µm
Keskihaj.	0,038		* VALMIS *	Tuote d80 = 76 µm
Keskihaj.	1,9	% keskiarvosta		Wi=10,14 kWh/t

Gbp min	1,9883
Gbp max	2,0800
max/min	4,6138

Syöte: Raekoko,µm	Seulalle jäi, g		Kumulat. summa,g	Läpäisy,% Syöte	Tuote: Raekoko,µm	Seulalle jäi g	Kumulat. massa,g	Raeluokan massa,g	Läpäisy, Tuote	Raeluokan osuus,%
3350	0			100	106	0	0,0	0,0	100,0	0,0
2360	51,1	9,65	9,65	90,35	90	1,1	1,1	1,1	94,7	5,3
1700	105,8	19,98	29,63	70,37	75	3,2	4,3	3,2	79,3	15,4
1180	92,6	17,49	47,12	52,88	53	4,2	8,5	4,2	59,1	20,2
850	58,2	10,99	58,11	41,89	45	1,8	10,3	1,8	50,5	8,7
600	44,1	8,33	66,44	33,56	-45	10,5	20,8	10,5	0,0	50,5
425	32,2	6,08	72,52	27,48			20,8	0,0		0,0
300	27,7	5,23	77,75	22,25			Yhteensä	20,8		100,0
212	20,6	3,89	81,64	18,36						
150	19,9	3,76	85,40	14,60						
106	11,3	2,13	87,54	12,46						
75	15,6	2,95	90,48	9,52						
Pan	50,4	9,52	100,00							
	529,5	100,00								

Index (S)	x	y	X80, µm
1	90	94,71153846	76
2	75	79,32692308	

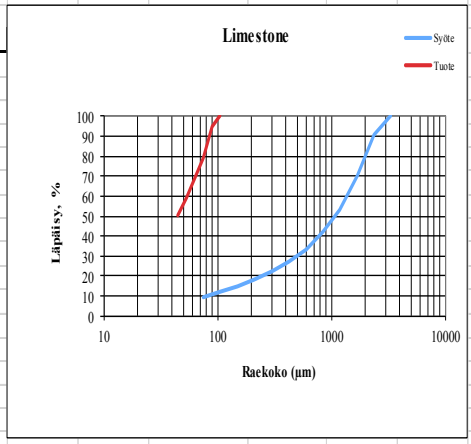

Huom! alkupunnituksesta kamaa +0,5g!!!!!

Index (S)	x	y	X80, µm
1	2360	90,3	2018
2	1700	70,4	

Wi	10,144

Appendix 13. Limestone Bond test, 106 µm

Jauhettava materiaali:	Limestone
Koe:	9.8.2017

Jauhatuspanos, g	1244,1
Hienoainesta, %	12,5
Kiertokuorma, g	355,5
Katkaisuseula, µm	106
Aloituskierrokset	100

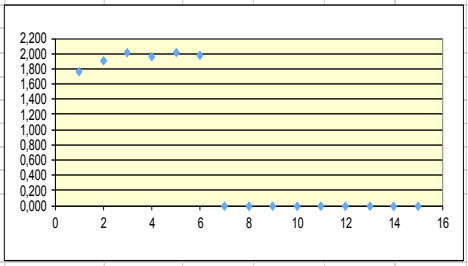

Kierros	Karkeaa g	Hienoa g	Hävikki g	Täydennys g	Jossa hienoa,g	Tuotettu hienoa,g	Hienoa/ myllyn kierros,g	Tuotettava hienoa,g	Tarvittavat seuraavat kierrokset	Kierto-kuorma,%	Hävikki, %:a syötteestä	Suunta
1	913	328,5	2,6	331,1	41,3	176,0	1,760	314,2	178	276	0,2	
2	864,3	376,9	2,9	379,8	47,3	338,5	1,897	308,1	162	228	0,2	
3	870,3	371,4	2,4	373,8	46,6	326,5	2,010	308,9	154	233	0,2	
4	895,9	345,8	2,4	348,2	43,4	301,6	1,962	312,1	159	257	0,2	
5	879,4	362,4	2,3	364,7	45,5	321,3	2,020	310,0	153	241	0,2	
6	894,9	346,4	2,8	349,2	43,5	303,7	1,980	311,9	158	256	0,2	
7												
8												
9												
10												
11												
12												
13												
14												
15												

Gbp=	**1,988**	g/ kierros	**Syöte d80 =** **2018 µm**
Keskihaj.	**0,024**		*** VALMIS *** **Tuote d80 =** **75 µm**
Keskihaj.	**1,2**	% keskiarvosta	**Wi=10,29 kWh/t**
Gbp min	1,9624		
Gbp max	2,0205		
max/min	**2,9619**		

Syöte: Raekoko,µm	Seulalle jäi, g		Kumulat. summa,g	Läpäisy,% Syöte	Tuote: Raekoko,µm	Seulalle jäi g	Kumulat. massa,g	Raeluokan massa,g	Läpäisy, Tuote	Raeluokan osuus,%
3350	0			100	106	0	0,0	0,0	100,0	0,0
2360	51,1	9,65	9,65	90,35	90	1,1	1,1	1,1	94,8	5,2
1700	105,8	19,98	29,63	70,37	75	3,2	4,3	3,2	79,6	15,2
1180	92,6	17,49	47,12	52,88	53	4,3	8,6	4,3	59,2	20,4
850	58,2	10,99	58,11	41,89	45	1,5	10,1	1,5	52,1	7,1
600	44,1	8,33	66,44	33,56	-45	11	21,1	11,0	0,0	52,1
425	32,2	6,08	72,52	27,48			21,1	0,0		0,0
300	27,7	5,23	77,75	22,25			**Yhteensä**	**21,1**		**100,0**
212	20,6	3,89	81,64	18,36						
150	19,9	3,76	85,40	14,60						
106	11,3	2,13	87,54	12,46						
75	15,6	2,95	90,48	9,52						
Pan	50,4	9,52	100,00							
	529,5	100,00								

Index (S)	x	y	X80, µm
1	90	94,78672986	**75**
2	75	79,62085308	

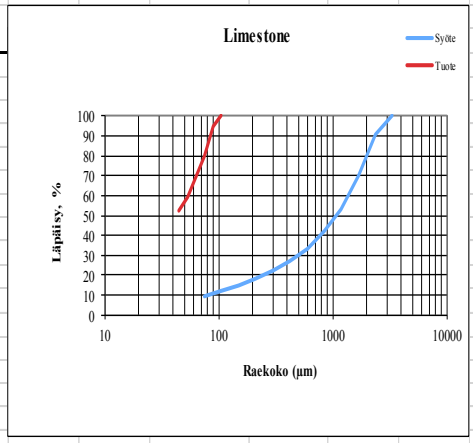

Huom! alkupunnituksesta kamaa +0,5g!!!!!

Index (S)	x	y	X80, µm
1	2360	90,3	**2018**
2	1700	70,4	

Wi	**10,293**

Appendix 14. Limestone Bond test, 150 µm

Jauhettava materiaali:	Limestone
Koe:	12.7.2017

Jauhatuspanos, g	1244,1
Hienoainesta, %	14,6
Kiertokuorma, g	355,5
Katkaisuseula, µm	150
Aloituskierrokset	100

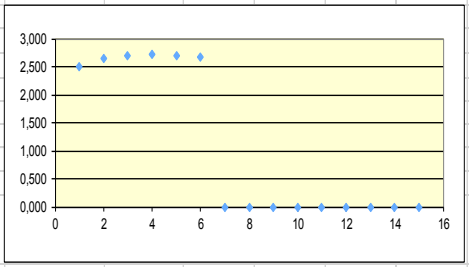

Kierros	Karkeaa g	Hienoa g	Hävikki g	Täydennys g	Jossa hienoa,g	Tuotettu hienoa,g	Hienoa/ myllyn kierros,g	Tuotettava hienoa,g	Tarvittavat seuraavat kierrokset	Kierto-kuorma,%	Hävikki, %:a syötteestä	Suunta
1	813,6	429,4	1,1	430,5	62,8	248,9	2,489	292,6	118	189	0,1	
2	869,2	372,2	2,7	374,9	54,7	312,1	2,654	300,7	113	232	0,2	
3	884,5	357,4	2,2	359,6	52,5	304,9	2,691	303,0	113	246	0,2	
4	886,6	355,9	1,6	357,5	52,2	305,0	2,709	303,3	112	248	0,1	
5	889,2	351,8	3,1	354,9	51,8	302,7	2,704	303,6	112	251	0,2	
6	891,6	350,1	2,4	352,5	51,5	300,7	2,678	304,0	114	253	0,2	
7												
8												
9												
10												
11												
12												
13												
14												
15												

Gbp=	2,697	g/ kierros	
Keskihaj.	0,014		* VALMIS *
Keskihaj.	0,5	% keskiarvosta	
Gbp min	2,6775		
Gbp max	2,7089		
max/min	1,1693		

Syöte: Raekoko,µm	Seulalle jäi, g		Kumulat. summa,g	Läpäisy,% Syöte	Tuote: Raekoko,µm	Seulalle jäi g	Kumulat. massa,g	Raeluokan massa,g	Läpäisy, Tuote	Raeluokan osuus,%
3350	0			100	150	0	0,0	0,0	100,0	0,0
2360	51,1	9,65	9,65	90,35	106	4,3	4,3	4,3	79,8	20,2
1700	105,8	19,98	29,63	70,37	90	1,9	6,2	1,9	70,9	8,9
1180	92,6	17,49	47,12	52,88	75	2,4	8,6	2,4	59,6	11,3
850	58,2	10,99	58,11	41,89	53	3,2	11,8	3,2	44,6	15,0
600	44,1	8,33	66,44	33,56	45	1,3	13,1	1,3	38,5	6,1
425	32,2	6,08	72,52	27,48	-45	8,2	21,3	8,2		38,5
300	27,7	5,23	77,75	22,25			Yhteensä	21,3		100,0
212	20,6	3,89	81,64	18,36						
150	19,9	3,76	85,40	14,60						
106	11,3	2,13	87,54	12,46						
75	15,6	2,95	90,48	9,52						
Pan	50,4	9,52	100,00							
	529,5	100,00								

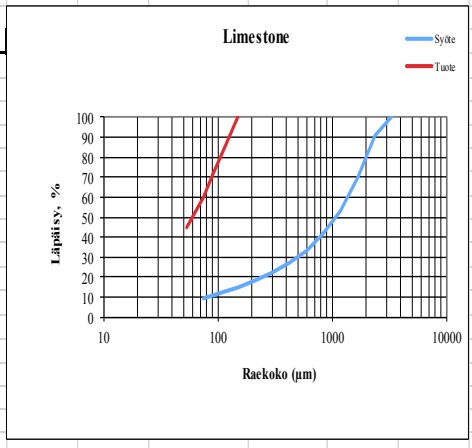

Index (S)	x	y	X80, µm
1	150	100	106
2	106	79,81220657	

Huom! alkupunnituksesta kamaa +0,5g!!!!!

Index (S)	x	y	X80, µm
1	2360	90,3	2018
2	1700	70,4	

Wi	9,206

Appendix 15. Limestone Bond test, 75 µm

Jauhettava materiaali:	Limestone
Koe:	19.7.2017

Jauhatuspanos, g	1244,1
Hienoainesta, %	9,5
Kiertokuorma, g	355,5
Katkaisuseula, µm	75
Aloituskierrokset	100

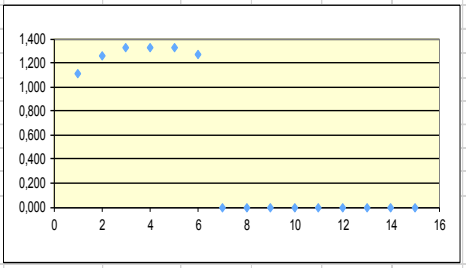

Kierros	Karkeaa g	Hienoa g	Hävikki g	Täydennys g	Jossa hienoa,g	Tuotettu hienoa,g	Hienoa/ myllyn kierros,g	Tuotettava hienoa,g	Tarvittavat seuraavat kierrokset	Kierto-kuorma,%	Hävikki, %:a syötteestä	Suunta
1	1015	207,7	21,4	229,1	21,8	110,7	1,107	333,7	301	443	1,7	
2	841,8	390,3	12,0	402,3	38,3	380,5	1,262	317,2	251	209	1,0	
3	872,2	364	7,9	371,9	35,4	333,6	1,328	320,1	241	235	0,6	
4	889,7	346,9	7,5	354,4	33,7	319,0	1,323	321,7	243	251	0,6	
5	889,3	344,4	10,4	354,8	33,8	321,1	1,321	321,7	244	251	0,8	
6	900,2	335,3	8,6	343,9	32,7	310,1	1,273	322,7	253	262	0,7	
7												
8												
9												
10												
11												
12												
13												
14												
15												

Gbp=	1,306	g/ kierros		Syöte d80 = 2018 µm
Keskihaj.	0,023		* VALMIS *	Tuote d80 = 42 µm
Keskihaj.	1,8	% keskiarvosta		Wi=11,14 kWh/t
Gbp min	1,2731			
Gbp max	1,3233			
max/min	3,9389			

Syöte: Raekoko,µm	Seulalle jäi, g		Kumulat. summa,g	Läpäisy,% Syöte	Tuote: Raekoko,µm	Seulalle jäi g	Kumulat. massa,g	Raeluokan massa,g	Läpäisy, Tuote	Raeluokan osuus,%
3350	0			100			0,0	0,0	100,0	0,0
2360	51,1	9,65	9,65	90,35	75	0	0,0	0,0	100,0	0,0
1700	105,8	19,98	29,63	70,37	45	3,2	3,2	3,2	84,3	15,7
1180	92,6	17,49	47,12	52,88	38	2,4	5,6	2,4	72,5	11,8
850	58,2	10,99	58,11	41,89	-38	14,8	20,4	14,8	0,0	72,5
600	44,1	8,33	66,44	33,56			20,4	0,0	0,0	0,0
425	32,2	6,08	72,52	27,48			20,4	0,0		0,0
300	27,7	5,23	77,75	22,25			Yhteensä	20,4		100,0
212	20,6	3,89	81,64	18,36						
150	19,9	3,76	85,40	14,60						
106	11,3	2,13	87,54	12,46						
75	15,6	2,95	90,48	9,52						
Pan	50,4	9,52	100,00							
	529,5	100,00								

Index (S)	x	y	X80, µm
1	45	84,31372549	42
2	38	72,54901961	

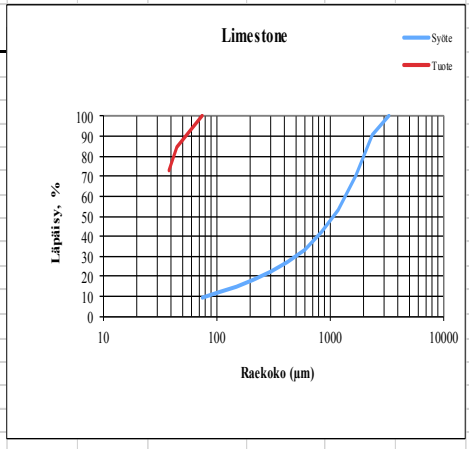

Huom! alkupunnituksesta kamaa +0,5g!!!!!

Index (S)	x	y	X80, µm
1	2360	90,3	2018
2	1700	70,4	

Wi	11,136

Appendix 16. RGO Mergan test data

> Log Filename: Fgo Mergan1 1500rev								Passing	P80 =	**115**	µm
								%	F80 =	**2305**	
Lämpö 1	16,33856	C	Momentin k.a		10,53971	Nm					
lämpö 2	16,19989	C	Keskihaj.		2,41095	Nm	Sieve		Sieve		
I	1,350754	A	Energiankulutus		0,0291	kWh	µm	Feed	µm	Product	
P(I)	0,155604	kW	Keskim.teho		0,066223	kW	2360	82	3550	100	
T	10,53971	Nm	Jauhettavaa		2,749		1700	57	2360	99	
			materiaalia			kg	1180	42	1700	99	
							850	33	850	99	
			E0	10,58564	kWh/t		600	27	600	98	
			Wi(op)=	14,62618	kWh/t		425	21	300	97	
							300	17	150	88	
			SGE	10,58564			212	14	106	78	
							150	11	75	66	
							106	10	45	51	
			P80(norm)	75	µm		75	8			
			E0(norm)	12,94977	kWh/t		**D_{80}**	**2305**		**115**	
			Wi(norm)	13,68288	kWh/t						

> Log Filename: FGO Mergan2 1500rev								Passing	P80 =	**112**	µm
								%	F80 =	**2305**	
Lämpö 1	24,53411	C	Momentin k.a		10,82591	Nm					
lämpö 2	24,01536	C	Keskihaj.		2,285875	Nm	Sieve		Sieve		
I	1,412621	A	Energiankulutus		0,028399	kWh	µm	Feed	µm	Product	
P(I)	0,154371	kW	Keskim.teho		0,068021	kW	2360	82	3550	100	
T	10,82591	Nm	Jauhettavaa		2,749		1700	57	2360	99	
			materiaalia			kg	1180	42	1700	99	
							850	33	850	98	
			E0	10,33061	kWh/t		600	27	600	98	
			Wi(op)=	14,02412	kWh/t		425	21	300	97	
							300	17	150	88	
			SGE	10,33061			212	14	106	79	
							150	11	75	67	
							106	10	45	53	
			P80(norm	75	µm		75	8			
			E0(norm)	12,63778	kWh/t		**D_{80}**	**2305**		**112**	
			Wi(norm)	13,35323	kWh/t						

> Log Filename: FGO Mergan3 1500rev								Passing	P80 =	**113**	µm
								%	F80 =	**2305**	
Lämpö 1	23,98916	C	Momentin k.a		10,73352	Nm					
lämpö 2	23,52212	C	Keskihaj.		2,314269	Nm	Sieve		Sieve		
I	1,415805	A	Energiankulutus		0,028175	kWh	µm	Feed	µm	Product	
P(I)	0,154269	kW	Keskim.teho		0,067441	kW	2360	82	3550	100	
T	10,73352	Nm	Jauhettavaa		2,749		1700	57	2360	100	
			materiaalia			kg	1180	42	1700	99	
							850	33	850	99	
			E0	10,24927	kWh/t		600	27	600	99	
			Wi(op)=	13,99329	kWh/t		425	21	300	98	
							300	17	150	89	
			SGE	10,24927			212	14	106	78	
							150	11	75	68	
							106	10	45	53	
			P80(norm	75	µm		75	8			
			E0(norm)	12,53827	kWh/t		**D_{80}**	**2305**		**113**	
			Wi(norm)	13,24809	kWh/t						

Appendix 17. MSO Mergan test data

> Log Filename: CLC mergan1 1500rev								Passing	P80 =	**138**	µm	Passing	P80 =	**138**	µm
								%	F80 =	**298**		%	F80 =	**2244**	
Lämpö 1	22,7024	C	Momentin k.a		9,882087	Nm									
lämpö 2	22,15033	C	Keskihaj.		2,324241	Nm	Sieve		Sieve						
I	1,402717	A	Energiankulutus		0,008762	kWh	µm	Feed	µm	Product					
P(I)	0,148642	kW	Keskim.teho		0,062091	kW	3350	100	3350	100					
T	9,882087	Nm	Jauhettavaa		3,652		2360	98	2360	98					
			materiaalia			kg	1700	94	1700	96					
							850	90	850	95					
			E0	2,399159	kWh/t		600	88	600	95					
			Wi(op)=	8,791173	kWh/t		300	80	300	93					
							150	62	150	83					
			SGE	2,399159			106	52	106	72					
							75	44	75	60					
				2,127983			45	32	45	44					
				2,51056											
				2,399159			D_{80}	**298**		**138**					
				7,037701											
			Wi(op)=	10,97794	kWh/t										
				P80(norm	75	µm									
				E0(norm)	9,242847	kWh/t									
				Wi(norm)	9,795434	kWh/t									

> Log Filename: CLC Mergan2 1700rev								Passing	P80 =	**97**	µm
								%	F80 =	**2244**	
Lämpö 1	23,36904	C	Momentin k.a		10,24894	Nm					
lämpö 2	22,92457	C	Keskihaj.		2,325613	Nm	Sieve		Sieve		
I	1,414601	A	Energiankulutus		0,030481	kWh	µm	Feed	µm	Product	
P(I)	0,152735	kW	Keskim.teho		0,064396	kW	2360	84	3350	100	
T	10,24894	Nm	Jauhettavaa		3,652		1700	60	2360	99	
			materiaalia			kg	1180	42	1700	98	
							850	32	850	98	
			E0	8,34632	kWh/t		600	26	600	98	
			Wi(op)=	10,37799	kWh/t		425	21	300	97	
							300	17	150	92	
			SGE	8,34632			212	15	106	84	
							150	12	75	69	
							106	11	45	52	
			P80(norm	75	µm		75	9			
			E0(norm)	9,671912	kWh/t		D_{80}	**2244**		**97**	
			Wi(norm)	10,25015	kWh/t						

Appendix 18. MSO Mergan test data

> Log Filename: CLC Mergan3 1600rev								Passing	P80 =	**101**	µm
								%	F80 =	**2244**	
Lämpö 1	22,18138	C	Momentin k.a		10,25288	Nm					
lämpö 2	21,74136	C	Keskihaj.		2,251767	Nm	Sieve		Sieve		
I	1,414062	A	Energiankulutus		0,028721	kWh	µm	Feed	µm	Product	
P(I)	0,152318	kW	Keskim.teho		0,064421	kW	2360	84	3350	100	
T	10,25288	Nm	Jauhettavaa		3,652		1700	60	2360	99	
			materiaalia			kg	1180	42	1700	98	
							850	32	850	97	
			E0	7,864434	kWh/t		600	26	600	97	
			Wi(op)=	10,03214	kWh/t		425	21	300	96	
							300	17	150	90	
			SGE	7,864434			212	15	106	81	
							150	12	75	71	
							106	11	45	54	
			P80(norm	75	µm		75	9			
			E0(norm)	9,683084	kWh/t		**D_{80}**	**2244**		**101**	
			Wi(norm)	10,26199	kWh/t						

> Log Filename: CLC Mergan4 1970rev								Passing	P80 =	**77**	µm
								%	F80 =	**2244**	
Lämpö 1	20,65895	C	Momentin k.a		10,29943	Nm					
lämpö 2	20,28099	C	Keskihaj.		2,177325	Nm	Sieve		Sieve		
I	1,41441	A	Energiankulutus		0,035466	kWh	µm	Feed	µm	Product	
P(I)	0,154653	kW	Keskim.teho		0,064713	kW	2360	84	3350	100	
T	10,29943	Nm	Jauhettavaa		3,652		1700	60	2360		
			materiaalia			kg	1180	42	1700	99	
							850	32	850	99	
			E0	9,71151	kWh/t		600	26	600	99	
			Wi(op)=	10,45944	kWh/t		425	21	300	99	
							300	17	150	96	
			SGE	9,71151			212	15	106	90	
							150	12	75	79	
							106	11	45	59	
							75	9			
							D_{80}	**2244**		**77**	

Appendix 19. Limestone Mergan test data

> Log Filename: Kalkki mergan1 600rev								Passing	P80 =	**141**	µm	Passing	P80 =	**141**	µm
								%	F80 =	**297**		%	F80 =	**2012**	
Lämpö 1	23,32977	C	Momentin k.a		10,30097	Nm									
lämpö 2	22,71445	C	Keskihaj.		2,685224	Nm	Sieve		Sieve						
I	1,391558	A	Energiankulutus		0,005537	kWh	µm	Feed	µm	Product					
P(I)	0,15039	kW	Keskim.teho		0,064723	kW	3350	100	3350	100					
T	10,30097	Nm	Jauhettavaa		2,666		2360	100	2360	100					
			materiaalia			kg	1700	99	1700	100					
							850	96	850	99					
			E0	2,077047	kWh/t		600	94	600	99					
			Wi(op)=	7,921779	kWh/t		300	80	300	98					
							150	56	150	83					
			SGE	2,077047			106	44	106	69					
							75	36	75	56					
							45	26	45	41					
			P80(norm	75											
			E0(norm)	6,533322			D_{80}	**297**		**141**					
			Wi(norm	7,011796											

> Log Filename: Kalkki Mergan2 700rev								Passing	P80 =	**119**	µm
								%	F80 =	**2012**	
Lämpö 1	21,92407	C	Momentin k.a		10,5601	Nm					
lämpö 2	21,44748	C	Keskihaj.		2,4658	Nm	Sieve		Sieve		
I	1,410566	A	Energiankulutus		0,013031	kWh	µm	Feed	µm	Product	
P(I)	0,154922	kW	Keskim.teho		0,066351	kW	2360	90	3350	100	
T	10,5601	Nm	Jauhettavaa		2,666		1700	70	2360	100	
			materiaalia			kg	1180	53	1700	100	
							850	42	850	100	
			E0	4,887701	kWh/t		600	34	600	100	
			Wi(op)=	7,046196	kWh/t		425	27	300	99	
							300	22	150	88	
			SGE	4,887701			212	18	106	76	
							150	15	75	63	
							106	12	45	45	
			P80(norm	75			75	10			
			E0(norm)	6,423836			D_{80}	**2012**		**119**	
			Wi(norm	6,894291							

> Log Filename: Kalkki Mergan3 700rev								Passing	P80 =	**123**	µm
								%	F80 =	**2012**	
Lämpö 1	22,47323	C	Momentin k.a		10,68184	Nm					
lämpö 2	21,92798	C	Keskihaj.		2,652035	Nm	Sieve		Sieve		
I	1,408319	A	Energiankulutus		0,013199	kWh	µm	Feed	µm	Product	
P(I)	0,154986	kW	Keskim.teho		0,067116	kW	2360	90	3350	100	
T	10,68184	Nm	Jauhettavaa		2,666		1700	70	2360	100	
			materiaalia			kg	1180	53	1700	100	
							850	42	850	100	
			E0	4,95104	kWh/t		600	34	600	100	
			Wi(op)=	7,281446	kWh/t		425	27	300	99	
							300	22	150	87	
			SGE	4,95104			212	18	106	75	
							150	15	75	62	
							106	12	45	44	
			P80(norm	75	µm		75	10			
			E0(norm)	6,507081	kWh/t		D_{80}	**2012**		**123**	
			Wi(norm	6,983633	kWh/t						

Appendix 20. RGO and MSO XRD results

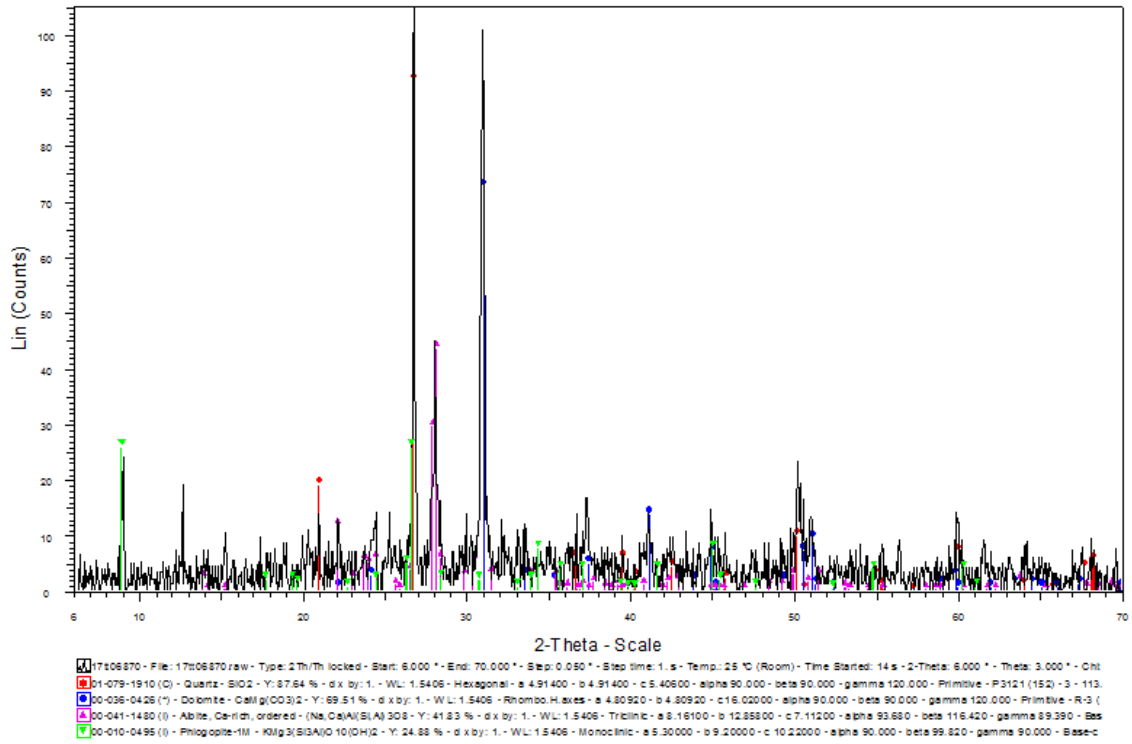

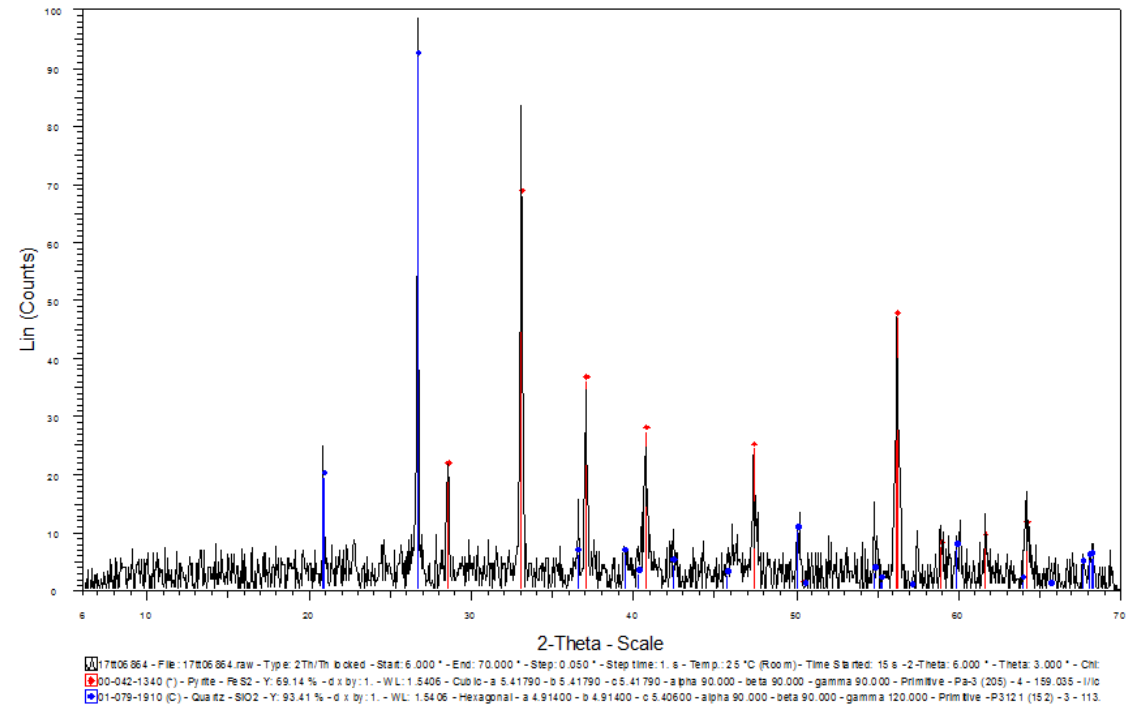

Appendix 21. Limestone XRD results

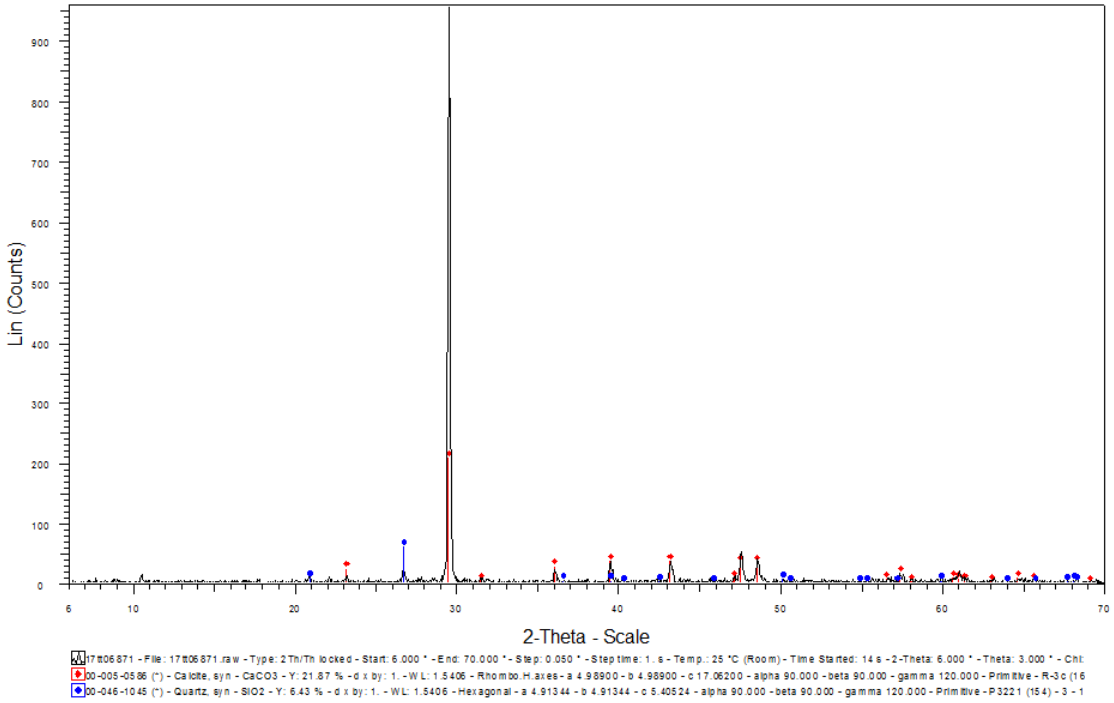

Appendix 22. Mineralogy and hardness calculations

ID	Cal %	Qtz %	Py %	Ccp %	Ab %	Phl %	Total	SG
Limestone	83,609	11,901	0,108	0,040	1,406	2,542	99,607	**2,705**

ID	Chal %	Bro %	Cc %	Ttrh %	Apy %	Gn %	Stnn %	Sp %	Ccp %	Py %	Qtz %	Cal %	Total	SG
Massive sulfide ore	0,024	1,957	5,572	0,099	0,628	0,521	0,125	0,151	1,146	60,098	28,602	1,258	100,180	**3,972**

ID	Py %	Apy %	Ttrh %	Sp %	Dol %	Brt %	Ab %	Hem %	Qtz %	Gr %	Ms %	Ot+ %	Total	SG
Refractory gold ore	4,981	1,572	0,066	0,016	29,423	0,032	18,707	8,104	20,349	1,286	13,248	2,216	100,000	**2,932**

	ID	Limestone		ID	Refractory gold ore		ID	Massive sulfide ore			hardness
Calcite	**Cal %**	83,609	Pyrite	**Py %**	4,981	Chalcantite	**Chal %**	0,024		Py	6,5
Quartz	**Qtz %**	11,901	Arsenopyrite	**Apy %**	1,572	Brochantite	**Bro %**	1,957		Cal	3
Pyrite	**Py %**	0,108	Tetrahedrite	**Ttrh %**	0,066	Chalcocite	**Cc %**	5,572		Qtz	7
Chalcopyrite	**Ccp %**	0,040	Sphalerite	**Sp %**	0,016	Tetrahedrite	**Ttrh %**	0,099		Dol	3,5
Albite	**Ab %**	1,406	Dolomite	**Dol %**	29,423	Arsenopyrite	**Apy %**	0,628		Albite	7
Phlogopite	**Phl %**	2,542	Barite	**Brt %**	0,032	Galena	**Gn %**	0,521		Phl	2,5
	Total	99,607	Albite	**Ab %**	18,707	Stannite	**Stnn %**	0,125		Cc	2,5
	SG	**2,705**	Hematite	**Hem %**	8,104	Sphalerite	**Sp %**	0,151			
			Quartz	**Qtz %**	20,349	Chalcopyrite	**Ccp %**	1,146			
	Hardness	3,34	Graphite	**Gr %**	1,286	Pyrite	**Py %**	60,098			
			Muscovite	**Ms %**	13,248	Quarz	**Qtz %**	28,602			
			Others	**Ot+ %**	2,216	Calcite	**Cal %**	1,258			
				Total	100,000		**Total**	100,180			
				SG	**2,932**		**SG**	**3,972**			
					4,418655			6,047794			

Appendix 23. RGO optical microscope pictures

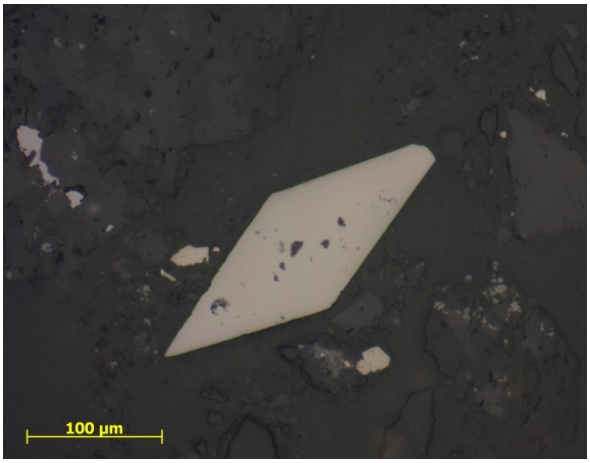

A

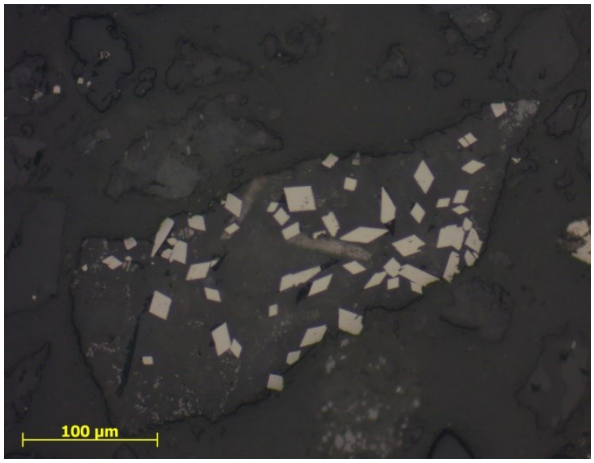

B

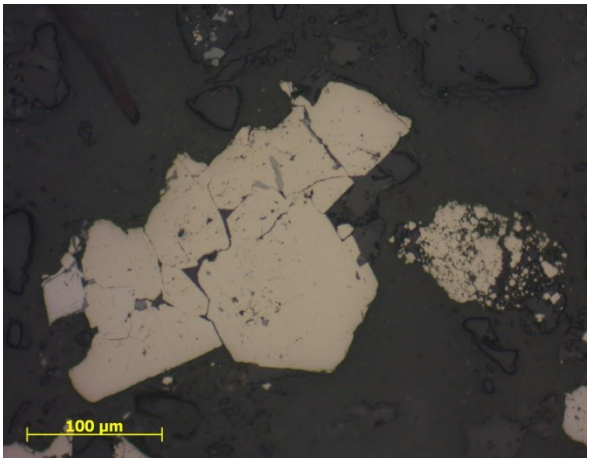

C

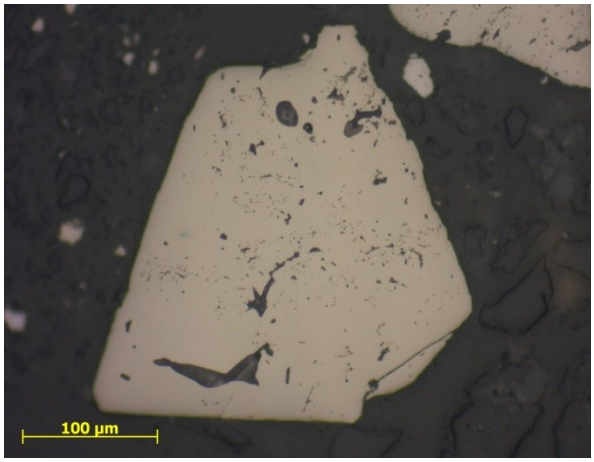

D

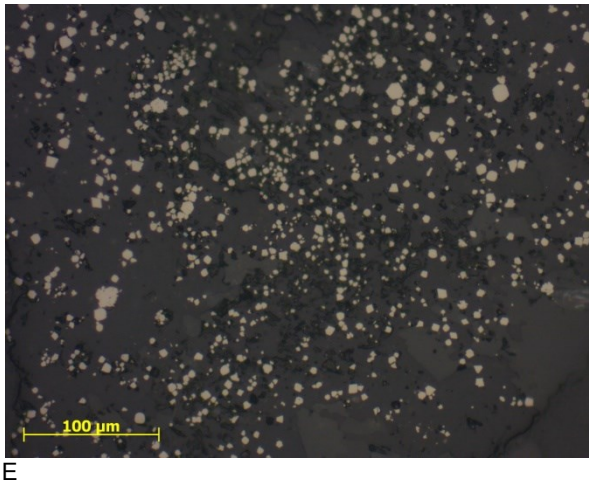

E

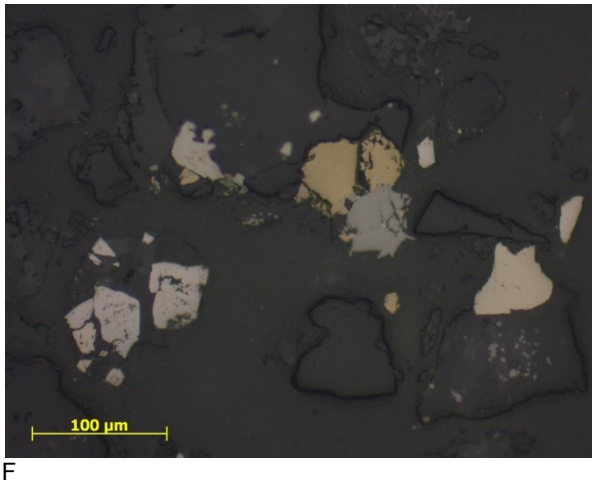

F

Appendix 24. MSO optical microscope pictures

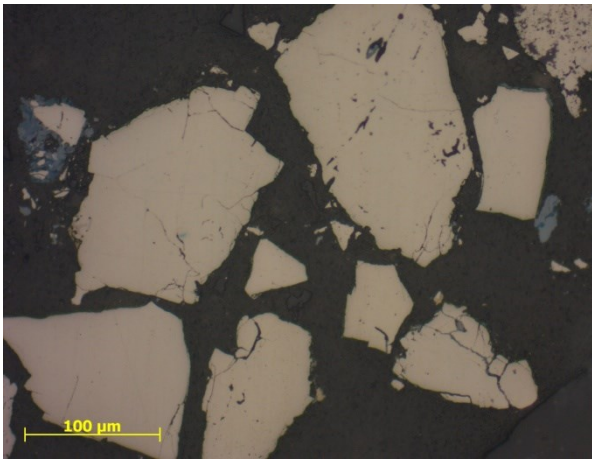

A

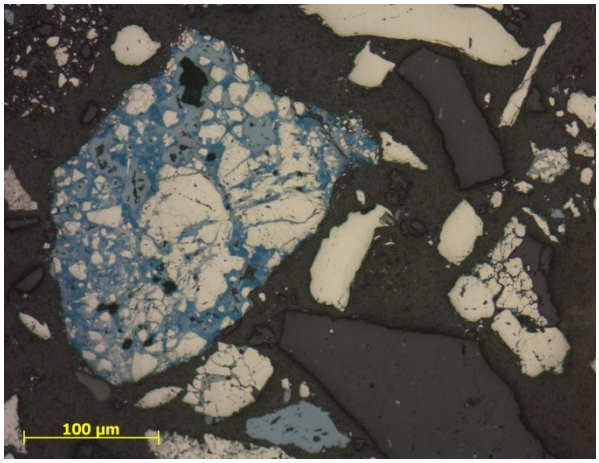

B

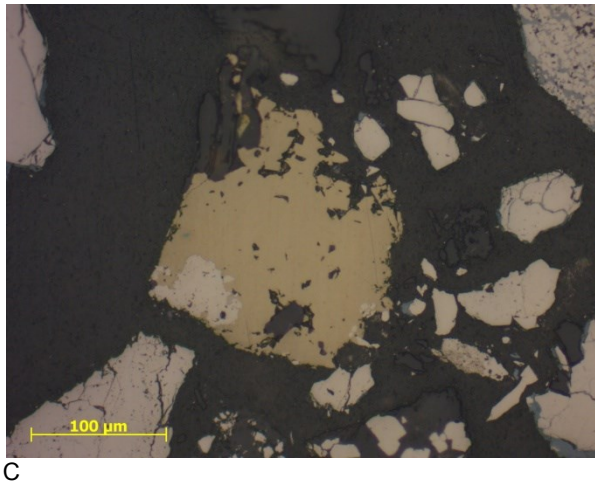

C

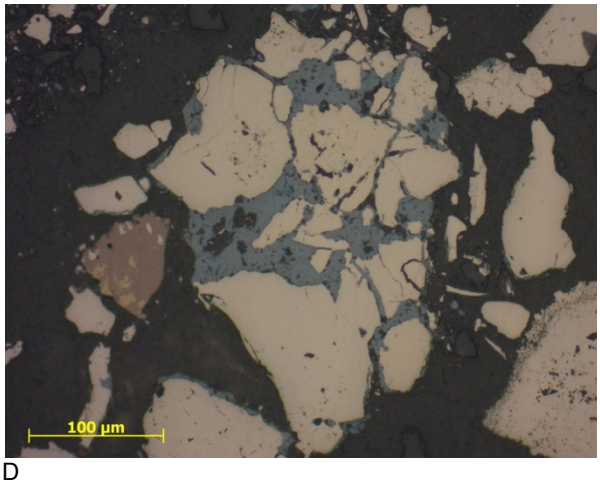

D

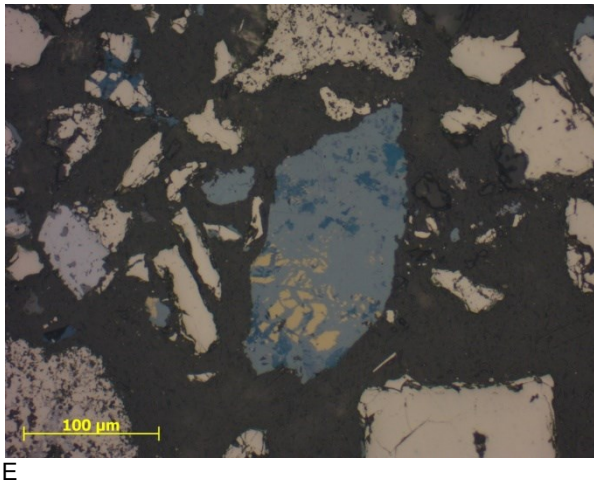

E

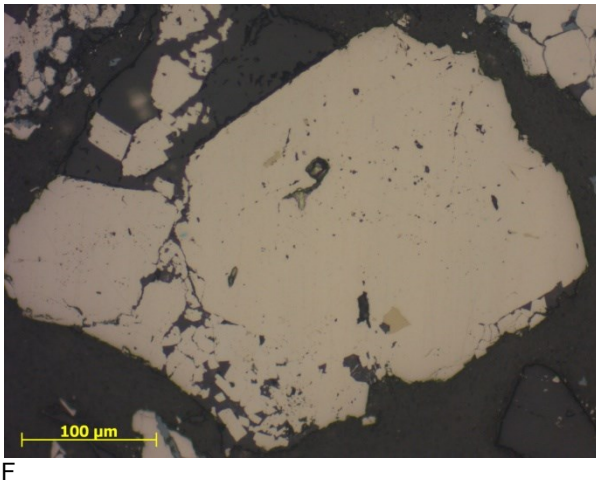

F

Appendix 25. Limestone optical microscope pictures

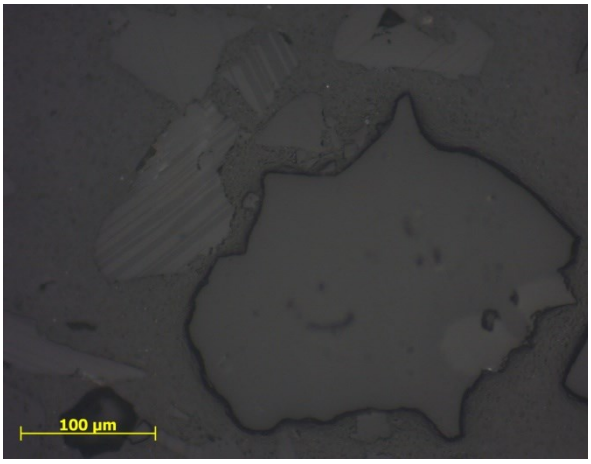

A

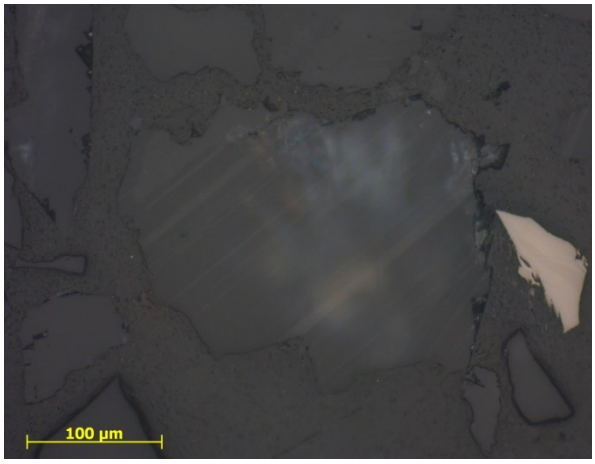

B

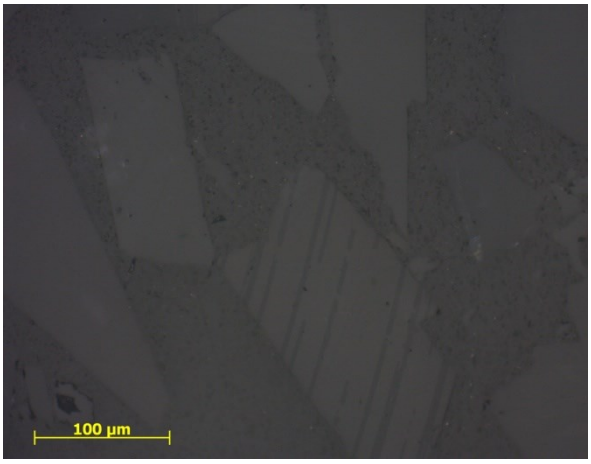

C

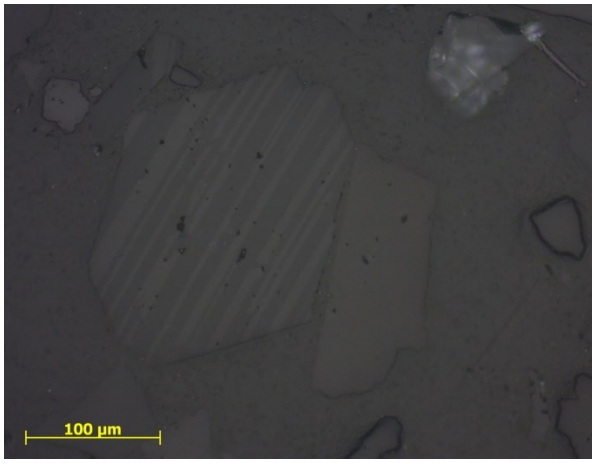

D

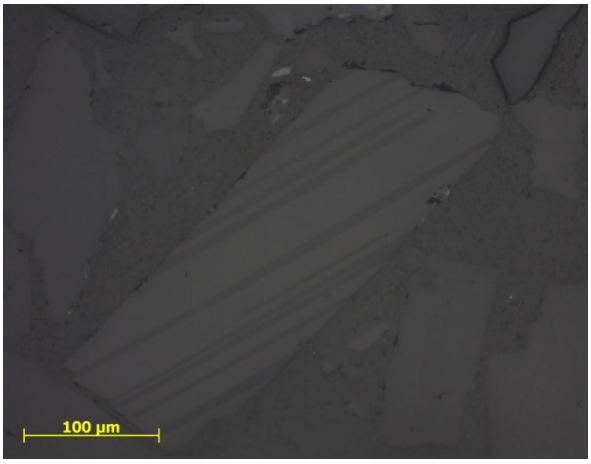

E

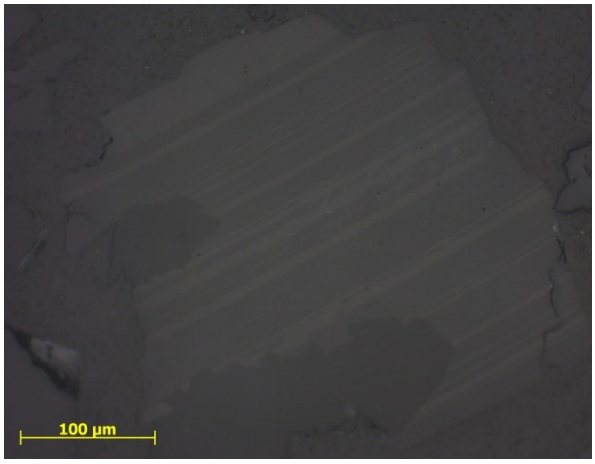

F